ALFRED-WEGENER-INSTITUT
HELMHOLTZ-ZENTRUM FÜR POLAR- UND MEERESFORSCHUNG

772
2023

Berichte
zur Polar- und Meeresforschung

Reports on Polar and Marine Research

Russian-German Cooperation: Expeditions to Siberia in 2021

Edited by

Anne Morgenstern, Birgit Heim, Luidmila A. Pestryakova, Dmitry Yu. Bolshiyanov, Mikhail N. Grigoriev, Dmitry Ayunov, Antonia Dill, and Iuliia Jünger

HELMHOLTZ

Die Berichte zur Polar- und Meeresforschung werden vom Alfred-Wegener-Institut, Helmholtz-Zentrum für Polar- und Meeresforschung (AWI) in Bremerhaven, Deutschland, in Fortsetzung der vormaligen Berichte zur Polarforschung herausgegeben. Sie erscheinen in unregelmäßiger Abfolge.

Die Berichte zur Polar- und Meeresforschung enthalten Darstellungen und Ergebnisse der vom AWI selbst oder mit seiner Unterstützung durchgeführten Forschungsarbeiten in den Polargebieten und in den Meeren.

Die Publikationen umfassen Expeditionsberichte der vom AWI betriebenen Schiffe, Flugzeuge und Stationen, Forschungsergebnisse (inkl. Dissertationen) des Instituts und des Archivs für deutsche Polarforschung, sowie Abstracts und Proceedings von nationalen und internationalen Tagungen und Workshops des AWI.

Die Beiträge geben nicht notwendigerweise die Auffassung des AWI wider.

Herausgeber
Dr. Horst Bornemann

Redaktionelle Bearbeitung und Layout
Susan Amir Sawadkuhi

Alfred-Wegener-Institut
Helmholtz-Zentrum für Polar- und Meeresforschung
Am Handelshafen 12
27570 Bremerhaven
Germany

www.awi.de
www.awi.de/reports

Der Erstautor bzw. herausgebende Autor eines Bandes der Berichte zur Polar- und Meeresforschung versichert, dass er über alle Rechte am Werk verfügt und überträgt sämtliche Rechte auch im Namen seiner Koautoren an das AWI. Ein einfaches Nutzungsrecht verbleibt, wenn nicht anders angegeben, beim Autor (bei den Autoren). Das AWI beansprucht die Publikation der eingereichten Manuskripte über sein Repositorium ePIC (electronic Publication Information Center, s. Innenseite am Rückdeckel) mit optionalem print-on-demand.

The Reports on Polar and Marine Research are issued by the Alfred Wegener Institute, Helmholtz Centre for Polar and Marine Research (AWI) in Bremerhaven, Germany, succeeding the former Reports on Polar Research. They are published at irregular intervals.

The Reports on Polar and Marine Research contain presentations and results of research activities in polar regions and in the seas either carried out by the AWI or with its support.

Publications comprise expedition reports of the ships, aircrafts, and stations operated by the AWI, research results (incl. dissertations) of the Institute and the Archiv für deutsche Polarforschung, as well as abstracts and proceedings of national and international conferences and workshops of the AWI.

The papers contained in the Reports do not necessarily reflect the opinion of the AWI.

Editor
Dr. Horst Bornemann

Editorial editing and layout
Susan Amir Sawadkuhi

Alfred-Wegener-Institut
Helmholtz-Zentrum für Polar- und Meeresforschung
Am Handelshafen 12
27570 Bremerhaven
Germany

www.awi.de
www.awi.de/en/reports

The first or editing author of an issue of Reports on Polar and Marine Research ensures that he possesses all rights of the opus, and transfers all rights to the AWI, including those associated with the co-authors. The non-exclusive right of use (einfaches Nutzungsrecht) remains with the author unless stated otherwise. The AWI reserves the right to publish the submitted articles in its repository ePIC (electronic Publication Information Center, see inside page of verso) with the option to "print-on-demand".

Titel: Start zum multispektralen Aufnehmen der Vegetation im Einzugsgebiet des Sees Ulu (Ostjakutien) im August 2021 (Foto: Stefan Kruse, AWI)

Cover: Liftoff for a multispectral survey of the vegetation in the catchment of Lake Ulu (East Yakutia) in August 2021 (Photo: Stefan Kruse, AWI)

Russian-German Cooperation: Expeditions to Siberia in 2021

Edited by
Anne Morgenstern, Birgit Heim, Luidmila A. Pestryakova, Dmitry Yu. Bolshiyanov, Mikhail N. Grigoriev, Dmitry Ayunov, Antonia Dill, and Iuliia Jünger

Please cite or link this publication using the identifiers

https://hdl.handle.net/10013/epic.ca415238-2471-4215-809e-da91add52585

https://doi.org/10.57738/BzPM_0772_2023

ISSN 1866-3192

Expeditions to Siberia in 2021

Expedition LENA to Research Station Samoylov Island and the Lena Delta
04.05.–23.09.2021
Expedition Yakutia 01.08.–06.09.2021

Chief scientists

Andrey Belimov (ARRIAM), Julia Boike (AWI), Dmitry Bolshiyanov (AARI), Mikhail Grigoriev (MPI, IPGG), Ulrike Herzschuh (AWI), Andrei Kartoziia (IPGG), Lyudmila Lebedeva (MPI), Luidmila Pestryakova (NEFU)

Contents

Chapter 1

Introduction

Anne Morgenstern [1], Birgit Heim [1], Luidmila A. Pestryakova [2], Dmitry Yu. Bolshiyanov [3], Mikhail N. Grigoriev [4,5], Dmitry E. Ayunov [4]

[1] Alfred Wegener Institute Helmholtz Centre for Polar and Marine Research, Potsdam, Germany

[2] Federal State Autonomous Educational Institution of Higher Education "M. K. Ammosov North-Eastern Federal University", Yakutsk, Russian Federation

[3] Arctic and Antarctic Research Institute, St. Petersburg, Russian Federation

[4] Melnikov Permafrost Institute, Siberian Branch, Russian Academy of Sciences, Yakutsk, Russian Federation

[5] Trofimuk Institute for Petroleum-Gas Geology and Geophysics, Siberian Branch, Russian Academy of Sciences, Novosibirsk, Russian Federation

Overview

This report provides an overview of the study locations, scientific objectives and field activities of the joint Russian-German expeditions to Siberia conducted in 2021. The expeditions cover investigations on the biology, geology, geomorphology, coastal dynamics, ecology and reconstructions of the paleoenviroment. Focus regions of this year's expedition were the Lena River Delta and Samoylov Island, and locations close to Yakutsk (Maya, Tyungyulyu) to the eastern extent of the Central Yakutian Lowland (Churapcha) and in Eastern Yakutia in the Verkhoyansk mountain range (Lake Ulu). (Figure1.0.1).

Co-operative Russian-German geoscientific research in Siberia included annual expeditions to Yakutia and the Siberian Arctic since 1993. An expedition to the Lena River Delta in 1998 within the framework of the Russian-German Cooperation SYSTEM LAPTEV SEA, supported by the research ministries of both countries was the first in the series of the annual joint Russian-German "LENA Expeditions". This first expedition laid the foundation for the establishment of a permafrost observatory on Samoylov Island in the central Lena Delta and the operation of a research station, which has been serving as a scientific and logistical base for the LENA expeditions. Permafrost conditions, micrometeorology, trace gas exchange, biology, and many other parameters are monitored at long-term measurement sites on the island. The new Research Station Samoylov Island (Figure 1.0.2) has been operated by the Trofimuk Institute for Petroleum Geology and Geophysics, Siberian Branch, Russian Academy of Sciences (IPGG SB RAS) since 2013, and provides a logistics-staging base, laboratories for field work and accommodation for the scientists, technicians and students. The LENA expeditions have been jointly organized by the Arctic and Antarctic Research Institute (AARI), the Alfred Wegener Institute Helmholtz Centre for Polar and Marine Research (AWI) and the Melnikov Permafrost Institute, Siberian Branch, Russian Academy of Sciences (MPI SB RAS). In 2022 the joint Lena expeditions were discontinued in connection with the cooperation stop of German research institution with Russian state institutions.

For many years, the Northeastern Federal University Yakutsk (NEFU) has been collaborating with the AWI to investigate lake systems and vegetation dynamics in Siberia. Expeditions based on field camps in remote areas of Siberia and the Russian Far East aimed at understanding processes and environmental trajectories in this vast boreal and Northern treeline biomes. Given the fast warming of the Arctic but the very sparse coverage of paleolimnological, genetic, and publicly available environmental and tree-level data in eastern Siberia, the Russian-German scientific teams gained sample material data from remote

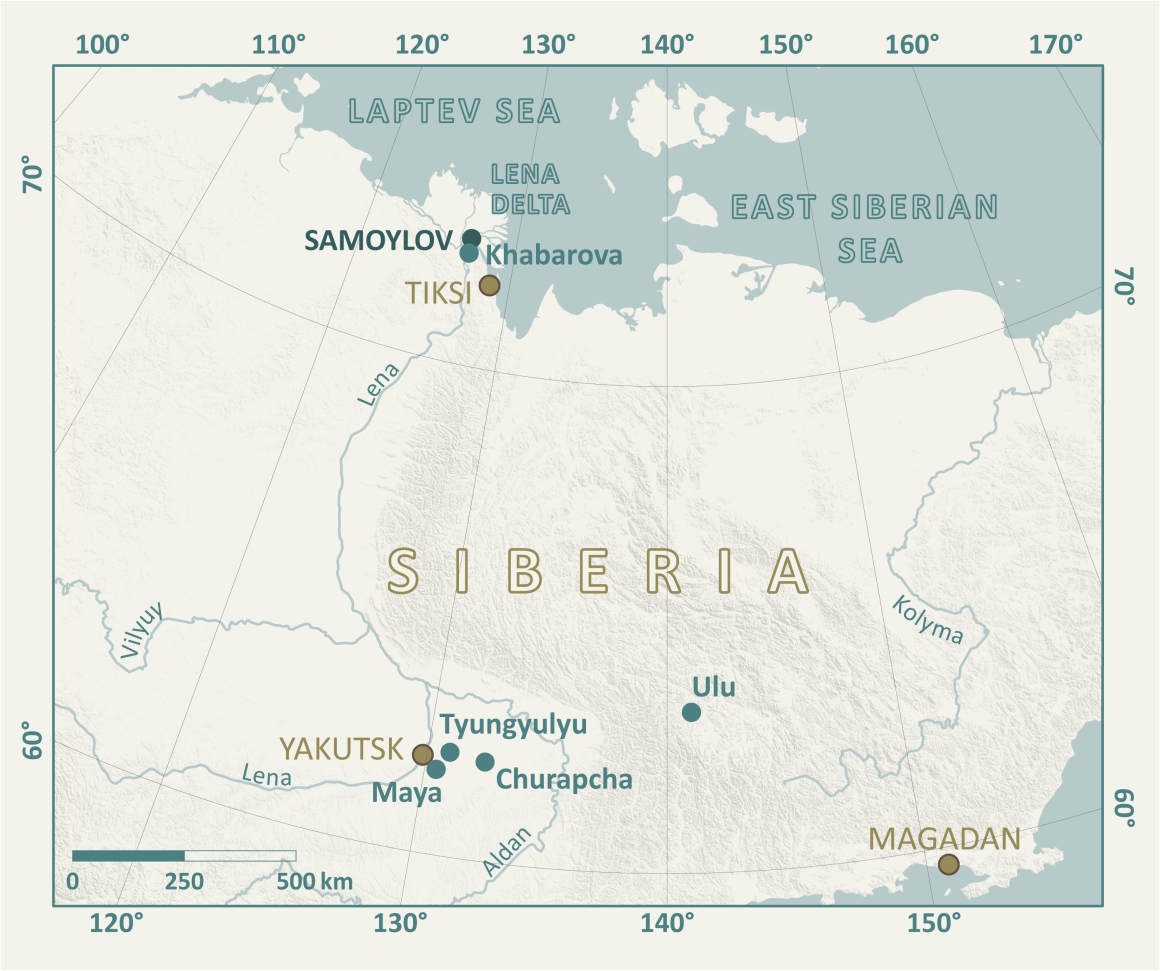

Figure 1.0.1: *Field sites of Russian-German expeditions to Siberia in 2021*

lakes, i.e. sediment cores, field measurements, e.g. sub-bottom profiling, forest structure data from aerial imagery, and vegetation material, e.g. tree-rings and material for DNA analyses.

Expedition Lena 2021 (RU-Land_2021_Lena) – Participants and itinerary

The LENA 2021 expedition was coordinated by Prof. Dr. Guido Grosse (Alfred Wegener Institute Helmholtz Centre for Polar and Marine Research – AWI, Potsdam), Prof. Dr. Dmitry Yu. Bolshiyanov (Arctic and Antarctic Research Institute – AARI, St. Petersburg), Dr. Mikhail N. Grigoriev (Melnikov Permafrost Institute, Siberian Branch, Russian Academy of Sciences – MPI SB RAS, Yakutsk) and Prof. Dr. Igor Yeltsov (Trofimuk Institute of Petroleum-Gas Geology and Geophysics – IPGG, Novosibirsk) and led by Sergei A. Pravkin (AARI) and Julia Boike (AWI).

In addition to research on Samoylov Island, field sites included other locations within the Lena River Delta and adjacent to it, e.g. Kurungnakh, Sardakh and Muostakh islands, as well as to Khabarova meteo station. Field work was conducted in several groups during the period May–September.

Figure 1.0.2: *Logos of the Expedition LENA 2021 and Research Station Samoylov Island*

Figure 1.0.3: *Group photo of the Lena 2021 geophysics and geobotany team*

Figure 1.0.4: *Group photo of the Lena 2021 participants in August (first part)*

Figure 1.0.5: *Group photo of the Lena 2021 participants in August (second part)*

Expedition Yakutia 2021 (RU-Land_2021_Yakutia) – Participants and itinerary

The Yakutia 2021 expedition that took place in August 2021 was led and coordinated by Prof. Dr. Ulrike Herzschuh (Alfred Wegener Institute Helmholtz Centre for Polar and Marine Research – AWI, Potsdam), and Prof. Dr. Luidmila A. Pestryakova (Federal State Autonomous Educational Institution of Higher Education "M. K. Ammosov North-Eastern Federal University", Yakutsk, Russian Federation – NEFU, Yakutsk).

Dr. Boris Biskaborn led the coring campaigns on Lake Ulu in the Verkhoyansk mountain range and on Lake Saysary within the urban area of Yakutsk, combined with parametrical sub-bottom profiling. The "Coring team" consisted of three German and four Russian team members in the field. For the first time, the new steerable UWITEC drilling double platform with its HYBRID 90 mm piston coring system was operated, with successfully retrieving long cores in Lake Ulu. In Lake Saysary, the traditional Niederreiter 60 mm piston coring system mounted on a tripod platform was employed and successfully retrieved long cores.

Prof. Dr. Ulrike Herzschuh, Dr. Evgenii Zakharov, and Dr. Lena Ushnitskaya were leading the "Lake team" that was responsible for the sampling in lakes (sediment short cores, sediment surface samples, water samples) in the Yakutian lowland (Maya, Tyungyulyu, Churapcha) and in the Verkhoyansk mountain range (Lake Ulu). The "Lake team" with four German and four Russian team members was successful in sampling a wide range of lake types in different settings and environments, from thermokarst lake types in the lowlands to glacial lakes in the mountain region.

In parallel, Dr. Stefan Kruse (AWI), Dr. Alexei Kolmogorov (NEFU) and their "Vegetation team" measured and sampled the vegetation plots in the lake catchments, including installation of dendrometers on the trees, and ground temperature and soil moisture sensors in soil pits, to establish long-term monitoring. Rhizospheres and soils were systematically sampled by the team and the vegetation plots were overflown by drones carrying multispectral camera and drone lidar sensors for large area acquisitions. Dr. Stefan Kruse and Dr. Robert Jackisch (Technical University of Berlin TUB) together with Dr. Alexei Kolmogorov were responsible for the drone data acquisitions. Dr. Elisabeth Dietze (AWI), wildfire and fire biomarker expert, was joining the expedition team at all the permafrost lowland locations (Maya, Tyungyulyu and Churapcha) to do the soil sampling. The "Vegetation team" consisted of eight German and two Russian team members.

Overall, the Yakutia 2021 expedition took four weeks for the majority of the 25 Russian-German field team members. All teams together ("Coring team", "Lake team", "Vegetation team") started with a large tent camp at Lake Ulu close to the road to Magadan at around 1000 m a.s.l. in the Verkhoyansk mountain region. A wildfire moderate in areal extent in the vicinity of Lake Ulu had just stopped, but wildfire smoke from the Aldan region strongly impacted the atmosphere also during some days in this mountain region. Fourteen lakes and nineteen vegetation plots (up to over 2000 m a.s.l.) were overflown by drones and sampled, loggers installed. The Coring team successfully retrieved long cores in the south-eastern, and also in the western part from Lake Ulu and then moved to Yakutsk for the Lake Saysary drilling. In parallel, the "Lake team" and the "Vegetation team" organized together the tent camps in Churapcha, Tyungyulyu and Maya to

assess thermokarst lakes and boreal forest plots with a ca. 100 km-wide radius. Close to the Aldan River, excessive large area fires had burned until early August 2022 and this region was in addition visited for lake and vegetation sampling, and burned areas were specifically investigated.

Figure 1.0.6: *Logo of Yakutia Expedition AWI & NEFU 2021*

Figure 1.0.7: *Group photo of the Yakutia Expedition AWI & NEFU 2021*

Participants of all expeditions and their affiliations are listed in the appendix (Table A.1.1 – Table A.1.5). In addition, the appendix lists collected samples and measurements made in 2021. This report consists of

contributions from the expedition participants. The authors of the contributions are responsible for content and correctness.

Data management

The data collected during the expeditions to Siberia in 2021 will be published by the respective scientific principal investigators (PIs) of the specific data collections on the PANGAEA data repository (`www.pangaea.de`). Data from chapter 2 are archived under the campaign label RU-Land_2021_Lena. Data from chapter 3 are archived under the campaign label RU-Land_2021_Yakutia. Both expeditions were supported by the Helmholtz Research Programme "Changing Earth – Sustaining our Future" Topic 5 (Landscapes of the future), Subtopic 3 (Determining natural functions and sensitivities of the Earth surface system). The AWI in cooperation with the research station on Samoylov Island has been an important hub for permafrost temperature measurements and the integration of data into international data base repositories, such as the Global Terrestrial Network for Permafrost (GTN-P; `http://gtnp.arcticportal.org/`).

Acknowledgements

The expeditions to Siberia in 2021 depended on essential support of the Russian and German organizing institutions, funding agencies, authorities and individuals. In particular, we would like to express our appreciation to the staff of the Research Station Samoylov Island, the Lena Delta Reserve, the Tiksi Hydrobase, the Arctica GeoCenter, and the North-Eastern Federal University Yakutsk (NEFU).

Chapter 2

Expedition Lena 2021 (RU-Land_2021_Lena)

Edited by Anne Morgenstern

2.1 Continuation of meteorological and soil-hydrological observation and restart of greenhouse gas flux observation

Lutz Beckebanze [1,@], Niko Bornemann [2], Christian Wille [3,], Julia Boike [2,*], Charlotta Mirbach [1], Lars Kutzbach [1,*], Torsten Sachs [3,*]*

[1] Institute of Soil Science, Universität Hamburg, Hamburg, Germany

[2] Alfred Wegener Institute Helmholtz Centre for Polar and Marine Research, Potsdam, Germany

[3] Helmholtz-Zentrum Potsdam – GFZ German Research Center for Geosciences, Potsdam, Germany

[*] not in the field

[@] Corresponding author: lutz.beckebanze@uni-hamburg.de

Fieldwork period and location

04.09.2021 – 23.09.2021 (Samoylov, Kurungnakh, and Sardakh; Lena River Delta)

Objectives

Within the Lena River Delta, measurements of meteorological and soil-hydrological observations as well as greenhouse gas observations are conducted on three different islands: Kurungnakh (subsidence and hydrological observations), Sardakh (ground temperature observation at the bore hole) and Samoylov. The Island of Samoylov with its research station functions as a main hub for meteorological, soil-hydrological, and greenhouse gas flux observations. Since 2018, the greenhouse gas flux observations are located in the **Sa**moylov **L**ong-**T**erm **O**bservatory (SALTO), a field lab in the shape of an igloo next to a new 10 meter tall observation tower. All observations run as long-term observations to get insights into ongoing changes in the permafrost landscape and atmospheric conditions.

The ongoing Covid-19 pandemic caused the cancellation of all expeditions from Germany to the Lena River Delta in 2020. Therefore, all loggers and instruments of the long-term observations could not be maintained or replaced between September 2019 and September 2021. Fortunately, our Russian partners helped us with downloading and rescuing some data in 2020 and throughout the summer of 2021.

Therefore, the objective for this expedition was the continuation of all long-term observations. Especially the long-term observatory for greenhouse gas fluxes did not deliver data anymore and needed a complete replacement of all instruments (except of the 3D-anemometer). Also the long-term meteorological station on Samoylov Island experienced a power shortage in August 2021 and was not in operation anymore.

Fieldwork summary

Greenhouse gas and energy flux observation at SALTO (SaEddy2018)

The eddy covariance measurement tower for greenhouse gas and energy fluxes (SaEddy2018) was not running anymore due to multiple measurement instrument failures throughout 2020 and 2021. Therefore, we replaced all eddy covariance measurement instruments and loggers with newly calibrated instruments and send the disassembled instruments back to Germany for calibration and maintenance. Only the 3D-anemometer (CSAT by Campbell Scientific) was still functioning and running. Additionally, we installed a new logger with a better performance (CR6 by Campbell Scientific) in the field lab to log all eddy covariance instruments at a measurement rate of 20 Hz with one logger. At the end of the expedition, the eddy covariance tower with all its instruments was in full operation again and the igloo was prepared for the winter.

Meteorological (SaMet2002) and soil station (SaSoil2002) on Samoylov Island

The meteorological and soil station on Samoylov Island was installed in 2002. It functions as a climate reference station for all ongoing measurements on Samoylov Island. In August 2021, a shortage caused a power cut at the station. The cause was found quickly and the station was running again shortly after the beginning of the fieldwork. Throughout the next weeks, the short- and longwave radiation sensors as well as temperature and humidity sensors were replaced by newly calibrated instruments.

Bore Holes on Samoylov and Sardakh
The data from ground temperature at the bore holes on Samoylov (SaHole2006, 27 meters, and SaHole2018, 67 meters) and Sardakh (SdHole2009, 100 meters) were downloaded in the field and the batteries were charged. The cancelled expedition in 2020 in combination with missing storage capacity caused a one-year data loss at SaHole2018. On Sardakh the bore hole was equipped with a new data logger and a solar panel, to extend possible maintenance free periods.

Additional maintenance and measurements of long-term observations
Temperature and water level sensors in multiple lakes on Samoylov Island were recovered and data was downloaded. However, a few sensors could not be found again causing in a data loss.
At the meteorological station SaMet2017 (at the 10 meter tower next to the igloo), all temperature and humidity sensors as well as short- and longwave radiation sensors were replaced with newly calibrated instruments. The active layer depth observation in a 150-point grid for the CALM network (circum arctic active layer monitoring) was continued and measured twice, at the beginning and at the end of the expedition.
The measurement of subsidence on Samoylov Island and Kurugnakh (started in 2013) was continued.
At the snow (SaSnow2012) and soil station (SaSoil2012) close to the 10m tower, all sensors for short- and longwave radiation were replaced by newly calibrated sensors. Additionally, the membranes for snow depth measurements were replaced.

Preliminary results

The observations of active layer in the 150-point grid showed a mean active layer of 62.6 and 62.1 cm on September 6th and September 20th, respectively. A maximum active layer depth of 83 cm was observed on September 20th. The time series of air temperature in 2 meters height at the SaMet2017 station is shown in Figure 2.1.1. It shows a minimum temperature of -45.2°C on January 27th, 2021 and a maximum temperature of +28.9°C on July 21st, 2021. If the April expedition of 2020 would have taken place, the expedition participants would have experienced high temperature variations of up to +2.2°C on April 9th and down to -31.6°C on April 16th, 2020.

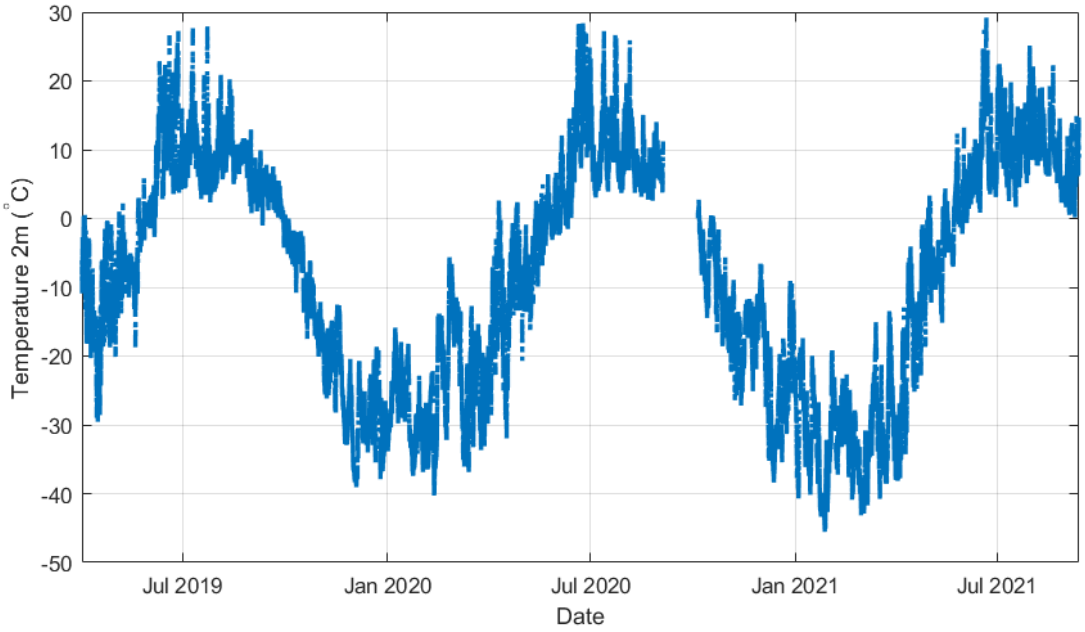

Figure 2.1.1: *Temperature time series between September 2019 and September 2021 in 2 meters height at the Eddy Covariance tower (SaMet2017)*

2.2 Lena River Water Monitoring at the Research Station Samoylov Island and in the central Lena River catchment in 2021

Bennet Juhls [1,@,], Lyudmila Lebedeva [2], Antje Eulenburg [1,*], Anne Morgenstern [1], Sofia Antonova [1,*], Paul Overduin [1,*], Sergey Volkov [3], Ekaterina Abramova [3,4]*

[1] Alfred Wegener Institute Helmholtz Center for Polar and Marine Research, Potsdam, Germany

[2] Melnikov Permafrost Institute, Siberian Branch, Russian Academy of Sciences Yakutsk, Russia

[3] Research Station Samoylov Island, Trofimuk Institute for Petroleum-Gas Geology and Geophysics, Siberian Branch, Russian Academy of Sciences, Novosibirsk, Russia

[4] Lena Delta Nature Reserve, Tiksi, Sakha Republic, Russia

[*] not in the field

[@] Corresponding author: bennet.juhls@awi.de

Fieldwork period and location

From 01.01.2021 to 31.12.2021 (Research Station Samoylov Island, see Figure 2.2.1). Field work was conducted by Sergey Volkov (entire period), Ekaterina Abramova (April-September), Anne Morgenstern (August-September).

From March to July, 2021 (*Lena River at Tabaga, Shestakovka River at Khamyrdagystakh and occasional sampling points on the Aldan and Olekma rivers, see Figure 2.2.1*)

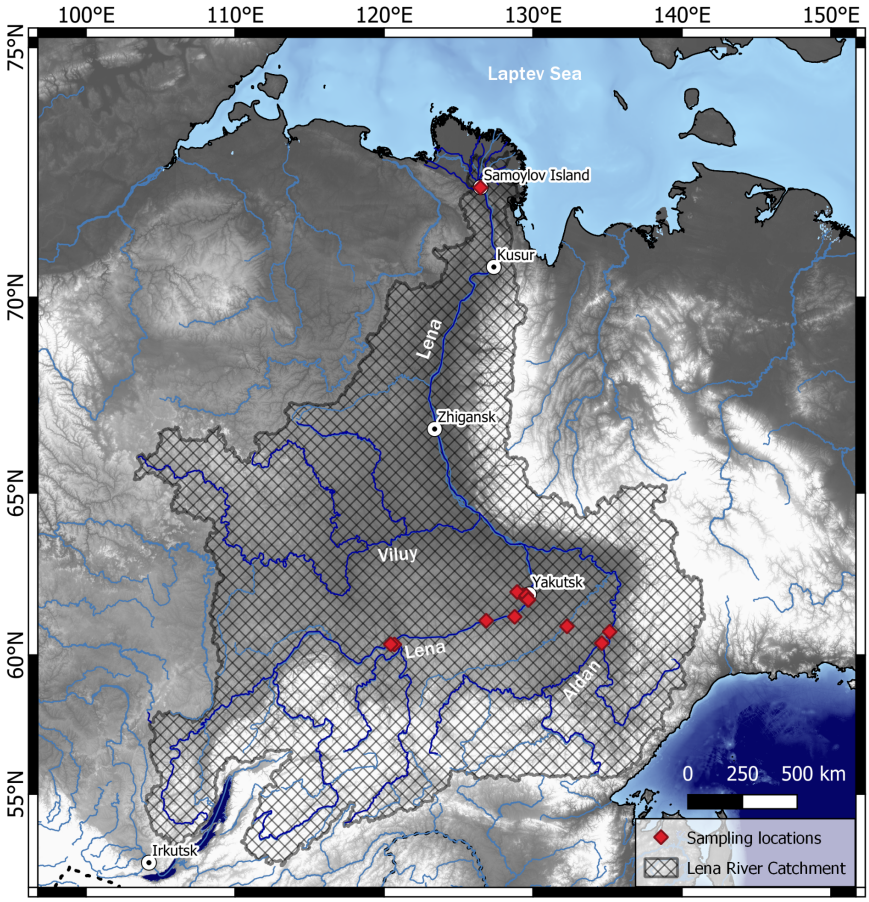

Figure 2.2.1: *Map of the Lena River catchment and the sampling locations (red dots)*

Objectives

Numerous studies expect an increase of carbon export by rivers to the Arctic Ocean due to rapidly changing climate in the Arctic (Camill 2005, Freeman et al. 2001, Frey et al. 2005). One possible source of carbon export is thawing permafrost, which mobilizes previously frozen dissolved organic matter (DOM). The Lena River delivers about one fifth of all river water to the Arctic Ocean (Holmes et al. 2012) and is the main source of DOM in the Laptev Sea shelf (Thibodeau et al. 2014). The discharge of the Lena River and the DOM concentration vary greatly by season. Scarce measurements of DOC and the coloured fraction of DOM (CDOM) (< 8 samples/year) have been used previously to estimate fluxes to the Arctic Ocean for the whole year based on correlation between DOM and discharge (Stedmon et al. 2011). The use of such correlations can result in systematic biases and potentially large errors. Longer-term and higher-frequency sampling would establish a baseline of fluxes, generate data to investigate causes of seasonal and shorter timescale variability and improve our understanding of future impacts of climate, landscape and hydrological change on land-to-ocean transfer. With this monitoring program, we seek to extend the existing 1.5 yr record for another year with daily to biweekly sampling of the Lena River at the Research Station Samoylov Island. The sampling program includes regular collection of samples for measurements of several water parameters, such as temperature, conductivity, dissolved organic carbon (DOC), spectral CDOM absorption $(aCDOM(\lambda))$, dissolved and total nutrients and stable isotopes. The sampling interval has been variable, between 1 and 11 days, with an average of 2.7 days. After successful sampling from spring 2018 until spring 2019 (data: Juhls et al. 2020a) Lena River surface water monitoring near the Samoylov Island Research Station) resulted in an initial partition of Lena River sources with an end-member model (Juhls et al. 2020b), the sampling program continued through 2020 and is ongoing, with slight changes to the sampling protocols and further sample series for additional parameters.
In order to better understand geographical differences in the biogeochemistry of the Lena River and to improve the discrimination of organic matter sources, sampling at various locations within the catchment is needed. During 2020 and 2021, the sampling of the Lena River near Yakutsk as well as sampling of tributaries of the Lena River was introduced (Figure 2.2.1), using the same protocols as the Samoylov sampling.

Fieldwork summary

1. Samoylov sampling

   Sampling originally began on 20.04.2018, carried out by staff from the Research Station Samoylov Island following sampling instructions that included a description of the sampling procedure, a protocol for recording each sampling event and a manual for sample filtration, preservation and storage.

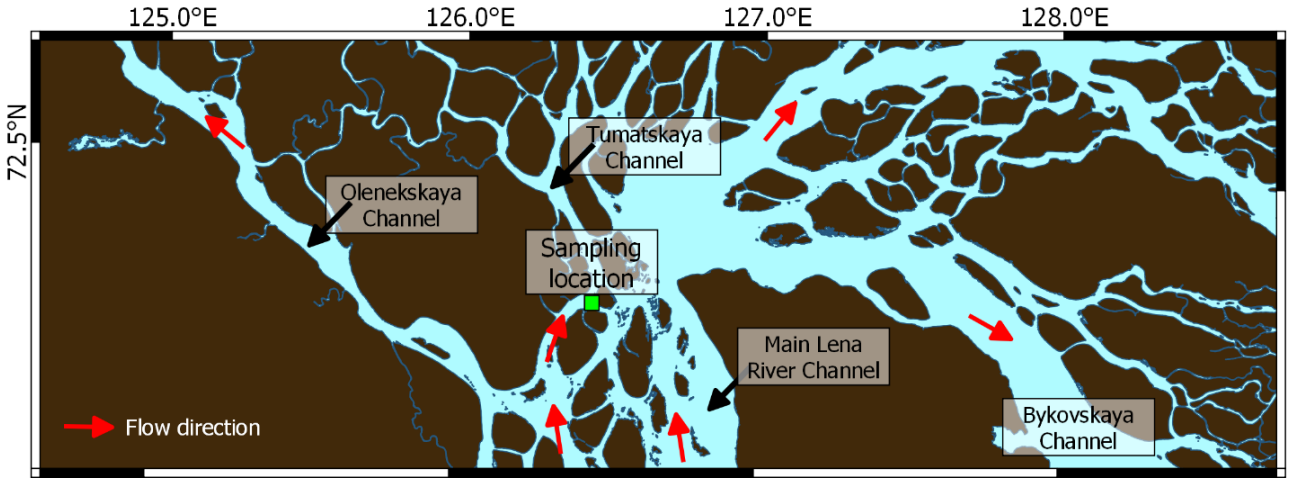

Figure 2.2.2: *Overview map of the part of the Lena River Delta displaying the sampling location, different Lena River channels, and flow directions*

   If weather or ice conditions allow, samples are usually taken from the center of the Olenekskaya Channel (Figure 2.2.2) from a boat or from the river ice. Otherwise, samples are taken from the

shoreline, which is usually restricted to short periods in spring and fall when ice break-up and freezing make access to the river dangerous. Note, that the flow direction of the channel that is sampled is following the Tumatskaya Channel throughout the spring flood and changing towards the Olenekskaya Channel with decreasing discharge.

Samples for a core set of parameters (Table A.2.1) have been collected throughout the monitoring program. In addition to the cited publications, this sampling program has been described in the annual field reports on the Russian-German research activities in Siberia (Biskaborn et al. 2021a; Fuchs et al. 2021a; Kruse et al. 2019b). A sampling interval was introduced that varies over the year in a standardized fashion. The intervals were defined as follows: 10th May to 15th June: every day; 15th June to 1st November: every two days; 1st November to 10th May: once per week. Changes in sampling interval can vary depending on variability in discharge, on the availability of sampling materials and on station staffing.

Until the end of the 2021 field season, a total number of 441 samples had been taken within this monitoring effort since its start (Table A.2.2 and Figure 2.2.3).

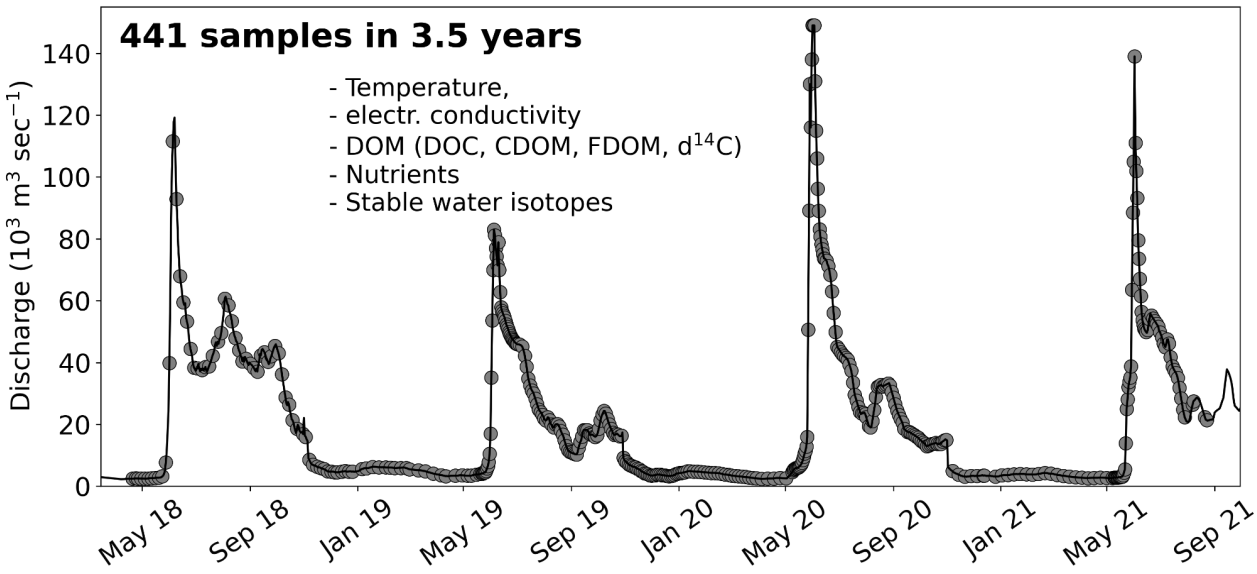

Figure 2.2.3: *Sampling dates (grey circles) on the hydrograph of the Lena River (black line)*

Sampling, processing, analysis log 2021:

- 2021-02-22: CDOM measurements of samples #288–#363 (see Table A.2.3) by Bennet Juhls and Martha Lütjen in GFZ Potsdam using 1 cm cuvette, 1 cycle.
- 2021-03-29: DOC measurements of samples 288–363 by Antje Eulenburg in AWI Potsdam.
- 2021-06-11: EC measurement in AWI Potsdam (by Antje Eulenburg). Rest sample #288–#327 (unfiltered, frozen) thawed on 10.06.2021, subsetted, filtered and preserved (by Antje Eulenburg, Bennet Juhls, Paul Overduin).
- 2021-06-14: EC measurement in AWI Potsdam (by Antje Eulenburg). Rest sample #328–#362 (unfiltered, frozen) thawed on 11.06.2021, subsetted, filtered and preserved (by Antje Eulenburg, Bennet Juhls, Paul Overduin).
- EC for sample #202 to #362 was measured on the frozen unfiltered Rest sample as well as on the CDOM sample. The rest sample was thawed at room at 4°C for 48h before EC measurement.
- Anions and cations for samples #202 to #362 were measured on the unfiltered frozen rest samples. Samples were thawed, filtered and acidified before analysis. Additionally, anions and cations for samples #202 to #286 were analysed on CDOM samples.

- d14C samples were analyzed in MICADAS laboratory in AWI Bremerhaven, however, results showed contamination that was explained by corrosion issues within the MICADAS lab.
- Nutrients (dissolved and total) samples #202 to #362 were transported to Tina Sanders at Hereon Geesthacht and will be analysed there.

2. Central Lena River catchment sampling

   Additionally to the sampling on Samoylov Island, samples in the central Lena River catchment were taken (Figure 2.2.1). The sampling location and intervals depend on local capacities and field trips (Table A.2.3). For most of the samples, samples were filtered and conserved some time after sampling (see Table A.2.3). Other than that, the same materials and protocols were used as in 1).

   Main sampling locations were Tabaga (60 km from Yakutsk) in the beginning of summer 2020 and during different periods in 2021 with varying sampling intervals (10-30 days). Another sampling location was established on the small Shestakovka River basin that is located 20 km from Yakutsk. Samples from the Shestakovka River were taken with daily intervals during the spring flood and in 10-20 days intervals during the low-flow season. Additionally, single samples were taken from other large and small tributaries of the Lena River such as Aldan, Olekma, Amga, Sinyaya, Buotoma rivers.

   Sampling, processing, analysis log 2021:

   - 2021-02-22: CDOM measurements of samples LA-LE (see Table A.2.3) by Bennet Juhls and Martha Lütjen in GFZ Potsdam using 1 cm cuvette, 1 cycle.
   - 2021-03-29: DOC measurements of samples LA-LE by Antje Eulenburg in AWI Potsdam. Samples were not acidified according to pH measurements.
   - 2021-06-11: EC measurement in AWI Potsdam (by Antje Eulenburg). Rest sample LA-LE (unfiltered, frozen) thawed on 10.06.2021, subsetted, filtered and preserved (by Antje Eulenburg, Bennet Juhls, Paul Overduin).
   - 2021-06-14: EC measurement in AWI Potsdam (by Antje Eulenburg). Rest sample LA-LE (unfiltered, frozen) thawed on 11.06.2021, subsetted, filtered and preserved (by Antje Eulenburg, Bennet Juhls, Paul Overduin).
   - EC for sample LA-LE was measured on the frozen unfiltered Rest sample as well as on the CDOM sample. The rest sample was thawed at room at 4°C for 48h before EC measurement.
   - Anions and cations for samples LA-LE were measured on the unfiltered frozen rest samples. Samples were thawed, filtered and acidified before analysis.
   - Nutrients (dissolved and total) samples LA-LE were transported to Tina Sanders at Hereon Geesthacht and will be analysed there.

Preliminary results

A list of samples collected to date is given in Table A.2.2 (Samoylov sampling) and Table A.2.3 (Central catchment sampling).

2.3 An experimental approach to evaluate the driving force for short-term response of methane release from polygonal tundra

Svetlana Yu. Evgrafova [1,@], Valerii K. Kadutskii [1]

[1] V.N. Sukachev Institute of Forest FRC KSC Russian Academy of Sciences, Siberian Branch, Krasnoyarsk, Russia

[@] Corresponding author: esj@yandex.ru

Fieldwork period and location

From 07.08.2021 to 28.08.2021 (on Samoylov Island)

Objectives

Recent studies (Douglas et al. 2020; Neumann et al. 2019) predicted that in the high latitudes of the Earth in the future there will be warmer and wetter summers, and an increase of precipitation and their temperature will affect the thermal processes in the soil and, as a result, for methane emissions.

In this study, we want to measure the potential emissions of methane to the atmosphere from the terrestrial landscapes of the Arctic, as ecosystem that have already proven high methanogenic potential, but which are limited by cold habitat conditions. As the main factor under study, we propose to take an increase in precipitation, since rain is an important transport of heat into the soil.

We propose an experimental approach to evaluate several hypotheses: (i) what period, amount and timing of precipitation should be the driving force for short-term or long-term (over the growing season) impacts on Arctic ecosystems? (ii) what are the main factors / conditions causing this effect? (iii) how wide is the range of responses of microbiocenoses of the methane cycle to increased precipitation under current conditions and projected changes?

Methods and fieldwork summary

During fieldwork in August 2021 we started “raining” experiment to evaluate an influence of increasing amount of precipitation on active layer thickness and methane release from soil (Table 2.3-1).

From August, 10 to August, 25, every day, 5 mm per m² of ambient temperature water poured on plot (0.5 x 0.5 m) of ice-wedge polygon center (Figure 2.3.1). The experiment included 4 plots. The active layer thickness measured with permafrost probe during the whole period of watering. In parallel, there were two control sites nearby where active layer thickness measured as well. In each control site, the active layer thickness measured in 6 replicates, for 5 times during the August.

Gas release from experimental plots measured by chamber technique in 2 minutes after watering. Gas samples collected into gas-tight syringes to measure at the Institute of Forest, Krasnoyarsk.

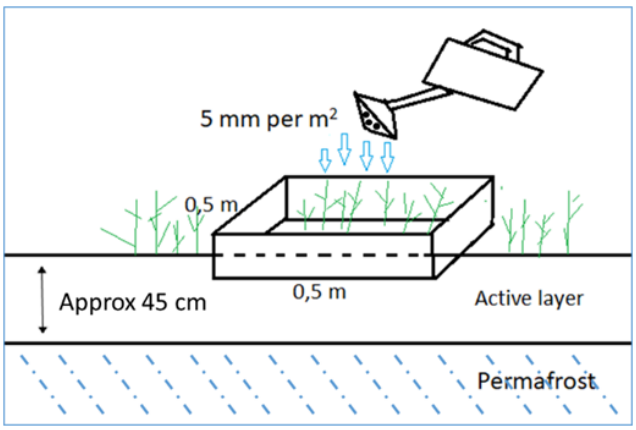

Figure 2.3.1: *An experiment design*

Preliminary results

Watering of ice-wedge polygon plots during 15 days increased active layer thickness by 6.3 ± 2.2 cm. Active layer thickness increasing during this period at control plots was 5.2 ± 0.8 and 4.5 ± 2.6 cm (Figure 2.3.2). Difference between plots with increased precipitation and "normal amount" of precipitation consisted 28% and 17%, respectively. Thus, we observed short-term impact of precipitation increasing on Arctic ecosystem.

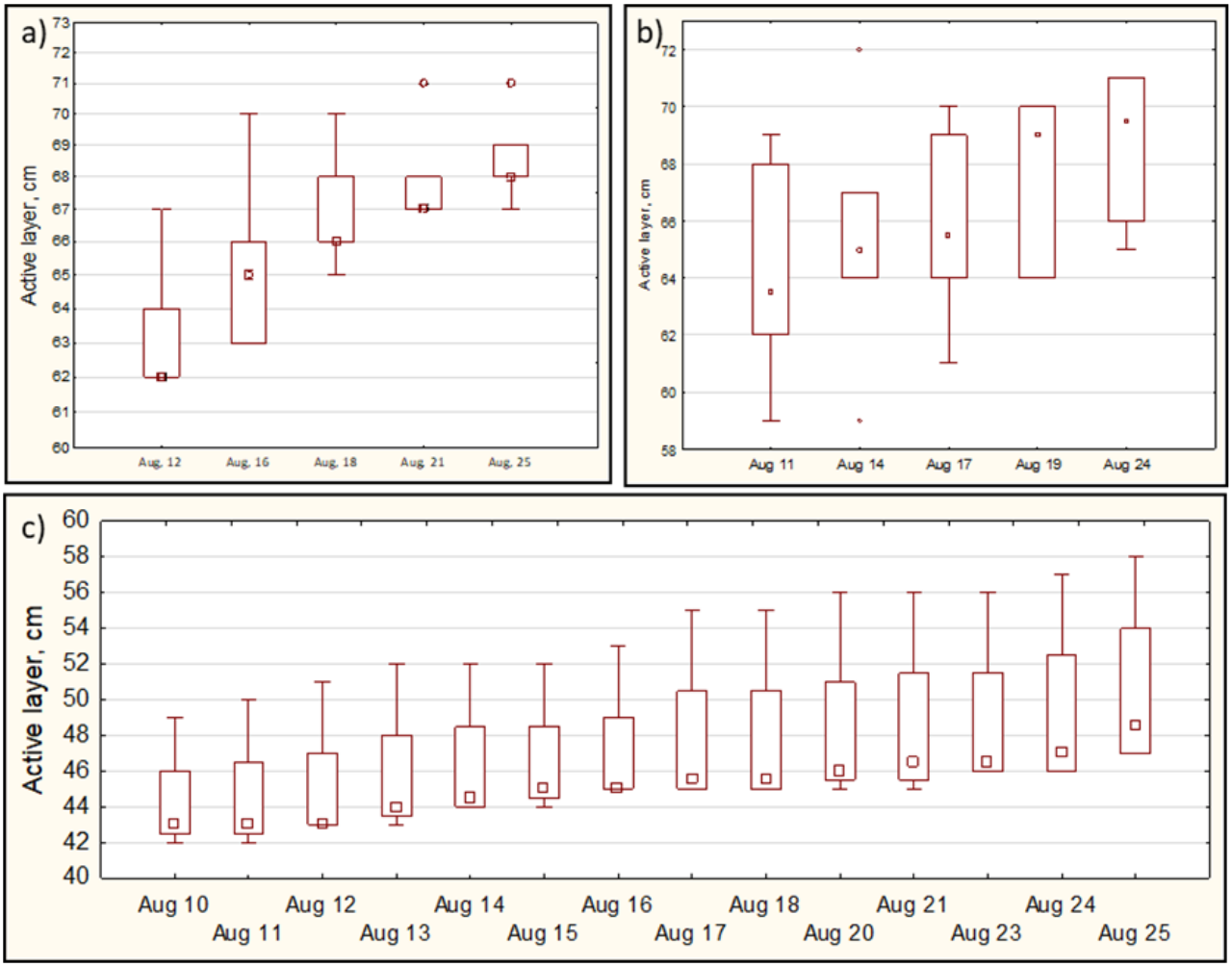

Figure 2.3.2: *Active layer thickness dynamic at control plots (a, b) and at experimental plot (c)*

Gas measuring showed that the main amount of CH_4 released soil in two first minutes after watering. There was no reliable difference in CH_4 efflux between experimental and control plots, except experimental plot #2 where CH_4 flux was 2 times higher in comparison with other plots (experimental and control).

Table 2.3-1: Experimental and control sites

Sample	Date	Latitude	Longitude	Notes
Experimental plots	10.08.2021	N 72.370306	E 126.482167	4 plots
Control plots	11.08.2021	N 72.366556	E 126.493194	12 plots

Acknowledgements

The Russian Science Foundation, project #21-17-00163, supported the work.

2.4 Pilot project: Migratory birds connect polar ecosystems worldwide: quantifying links, transport effects, and consequences of a changing world *(PolarConnection)*

Simeon Lisovski [1,@]

[1] Alfred Wegener Institute Helmholtz Centre for Polar and Marine Research, Potsdam, Germany

[@] Corresponding author: simeon.lisovski@awi.de

Fieldwork period and location

From 07.07.2021 to 16.07.2021 (on Samoylov Island and Kurungnakh Island)

Objectives

The main objective of the 2021 pilot fieldwork was to get a good estimate of breeding bird numbers and diversity on Samolyov as well as adjacent Islands. In the project PolarConnection, I aime to quantify the connections migratory birds establish between polar regions and the rest of the world and how these connections might influence polar ecosystems and their function in our rapidly changing world. The Lena Delta and notably Samoylov Island will play a central role in the empirical research of the project. The Lena Delta is a known hotspot for migratory birds, both in terms of numbers and species richness. Furthermore, the Dealt is unique in its location at the top end of several so-called migratory flyways. Thus, I expected find species that spend thenon-breeding season in America, Australia, East-, Central- and West Asia all the way to Afrika (and Arctic terns are known to fly south to the Antarctic coastline). The billions of individuals migrating to the Arctic each year, transport nutrients, energy, bacteria, pathogens, and pollutants into their breeding grounds. While this is likely driving and stabilizing ecosystem function (predator prey interactions, herbivory, nutrient cycles), new viruses and increasing amounts of toxins and pollutants brought in from other parts of the world might also negatively affect the arctic ecosystems. In addition, climate warming and concomitant phenological shifts and changes in vegetation structure are known to alter species assemblages that will likely change the global connections of migratory birds and likely also their function in polar environments. In the Lena Delta and with regards to the migratory animals and their global function, we may have the unique opportunity to disentangle climate change effects from other direct human impacts across the globe, since all individuals face the same changes in the Arctic but come from vastly different locations that experience equally different human impacts (e.g., habitat destruction, pollution, rate of emerging infectious diseases).

Methods and fieldwork summary

During the 10 days stay on Samoylov Island, and a short visit to the south-west of Kurungnakh Island, I was mainly monitoring the occurrence of birds and their breeding activities (using direct observations and remote observation with binoculars and scope). In addition, I tried to catch individuals to deploy tiny light weight geolocators that will allow reconstruction of migration paths after recapture in 2022. I used spring clap-nets over nest with eggs and clap traps on perches (wooden poles) to capture individual birds. Captured individuals where banded with a metal ring (with individual id from the Russian Birds Banding Bureau), a color code (specific to the Lena Delta), and morphological measurements were taken (weight, wing length, tarsus length, bill lengths).

Preliminary results

I recorded 30 bird species on Samoylov Island from which 21 species where actively breeding during the field expedition period (Table A.2.4).

Note, that some if the species that were seen on the island but not with a nest or chicks, might have bred or tried to breed on the island but finished or failed by the time of my visit.

During my short visit on Kurungnakh Island (N 72.326670°, E 126.037161°), (Figure 2.4.1) on 13.07.2021, I have recorded 12 species with clear signs of breeding in 8 species (Table A.2.5).

Figure 2.4.1: *Landing point (circle) and observation area (rectangle) on Kurungnakh Island*

Catching birds on Samoylov Islands was difficult since almost all breeders were finished incubating their eggs. At that time, chicks hide in the vegetation and adults escape from humans. I found two nests with an incubating adult that I could catch (Ringed plover, Sharp-tailed sandpiper) and managed to catch two Temminck's sandpiper (Figure 2.4.2) using a spring trap on a pole that these individuals frequently used as a perch. I attached a light-level geolocator on a leg-flag of the Ringed plover and the Sharp-tailed sandpiper.

Figure 2.4.2: *1-2 day old chicks from a Little stint (Calidris minutus) on the left, and a captured and ringed Temminck's sandpiper (Calidris temminckii) on the right. The color flag combination of sky blue (upper leg) and black (tarsus) has been established within international color schemes and is unique for the Lena Delta*

In conclusion, I was successful in the assessment of species diversity and abundance of migratory birds on Samoylov Island. The situation on the island is most suitable to tackle the objectives of the PolarConnection project. However, to successfully catch enough individuals and to take samples straight after the arrival of the birds, fieldwork needs to be conducted in mid-May to mid-June.

Acknowledgements

I would like to thank Anne Morgenstern and Sofia Antonova for their continuing support in organizing the fieldtrip and getting all necessary permits from the respective authorities. I would also like to thank the Lena Delta Reserve staff for their support and notably Katya Abramova for her assistance and for sharing valuable information on breeding birds on Samoylov Island. Finally, I would like to thank the staff of the Samoylov Research Station for their support.

2.5 TEM observations on Samoylov Island

Vladimir V. Potapov [1,2,@], Anna A. Zaplavnova [1,2,], Andrei A. Kartoziia [1,2,3], Petr A. Dergach [1,2]*

[1] A. A. Trofimuk Institute of Petroleum Geology and Geophysics, Siberian Branch, Russian Academy of Sciences , Novosibirsk, Russia

[2] Novosibirsk State University, Novosibirsk, Russia

[3] V. S. Sobolev Institute of Geology and Mineralogy, Siberian Branch of the Russian Academy of Sciences, Novosibirsk, Russia

[*] not in the field

[@] Corresponding author: PotapovVV@ipgg.sbras.ru

Fieldwork period and location

From 10.07.2021 to 29.07.2021 (on Samoylov Island)

Objectives

The main research goal was to determine the thickness of permafrost on the island Samoylov using the TEM (transient electromagnetic sounding) method. According to the MTS data, permafrost thickness was roughly estimated as 400–1000 m.

Methods and fieldwork summary

TEM measurements were carried out for 6 days and included 2 profiles. The first profile crosses Samoylov Island from the southwest to the northeast. The second profile is located on the southern bank of the Olenekskaya channel near Samoylov Island. It strikes from north to south.

The measurements were carried out using a 200 x 200 m generator loop, a 20 x 20 m measuring loop with a 100 m spacing from the centre of the generator loops, both sides from the centre and a coaxial loop. The layout of the loops is diagonal, with a distance between the generator loops centres 300 m, and between the centres of the measuring loops - 100 m. As a result, were made 27 TEM measurement points. The profiles location is shown in (Figure 2.5.1).

Most TEM signals have a duration from 40 μs to 4-5 ms. These limitations on the signal duration make it possible to achieve the required sounding depth for solving the problem stated in the primary research goal. Primary processing was carried out in specialized software for FastSnap equipment (Sharlov 2017). During processing, field data is filtered, averaged and transformed into a format suitable for geophysical interpretation. This software package has all the necessary procedures for obtaining the final TEM signals and includes: summing signals from all pulses, stitching data from different records, normalizing data to the current and moment of the generator and measuring complex, filtering, interpolation, etc. The preprocessing technique is described in the monograph of software developers (Pospeev 2018).

Figure 2.5.1: *Profiles and points scheme for measurements by the TEM method on the Samoylov Island: the southern profile is the first, the northern profile is the second*

Preliminary results

As a result of preliminary processing, the final signals of transient and their transformation into curves of apparent resistance were obtained. (Figure 2.5.2) shows a typical apparent resistivity curve.

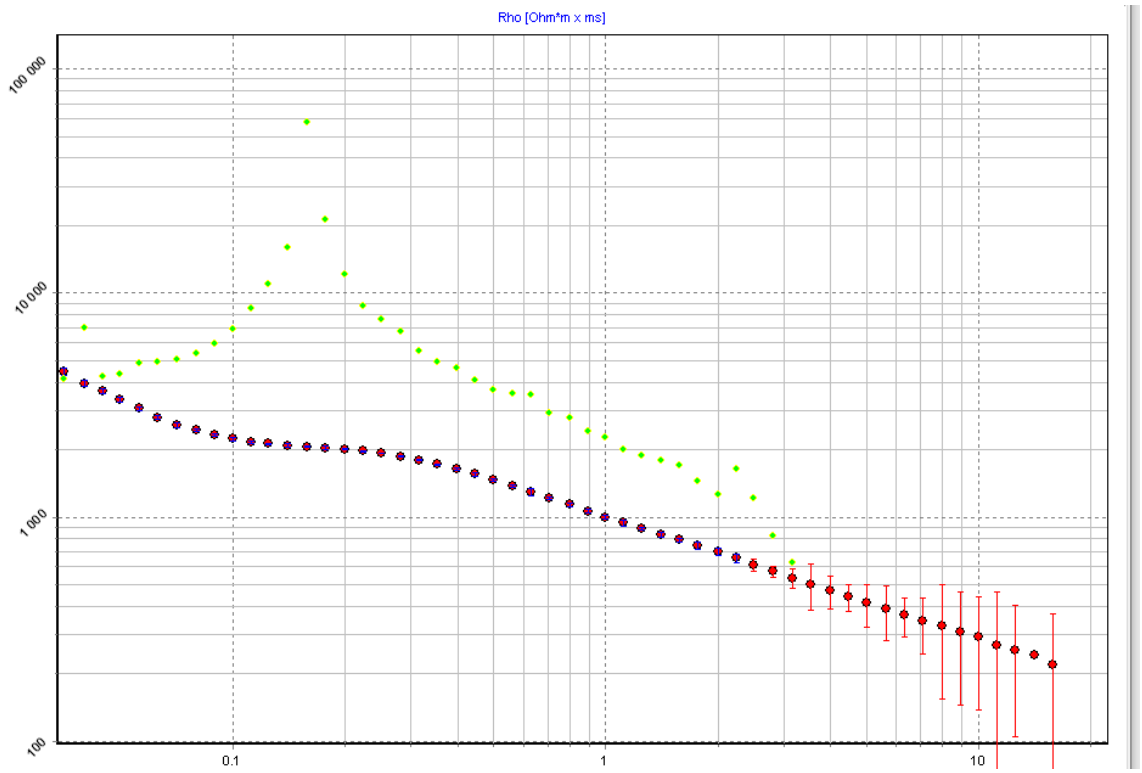

Figure 2.5.2: *The curve of apparent resistance at station 36 without significant influence of reduced polarization*

As shown in (Figure 2.5.2), the curves have the following form: the beginning of all curves characterizes by very high resistances of a few kOhm, with a further decrease to several hundred Ohms.
The next step was primary data inversion. The inversion was carried out by employees of the Laboratory of Geoelectrics of the Institute of Geological and Geological Problems of the Siberian Branch of the Russian Academy of Sciences under the Antonov E. Y. direction.
(Figure 2.5.3) below shows a preliminary profile geoelectric section along with the first profile.

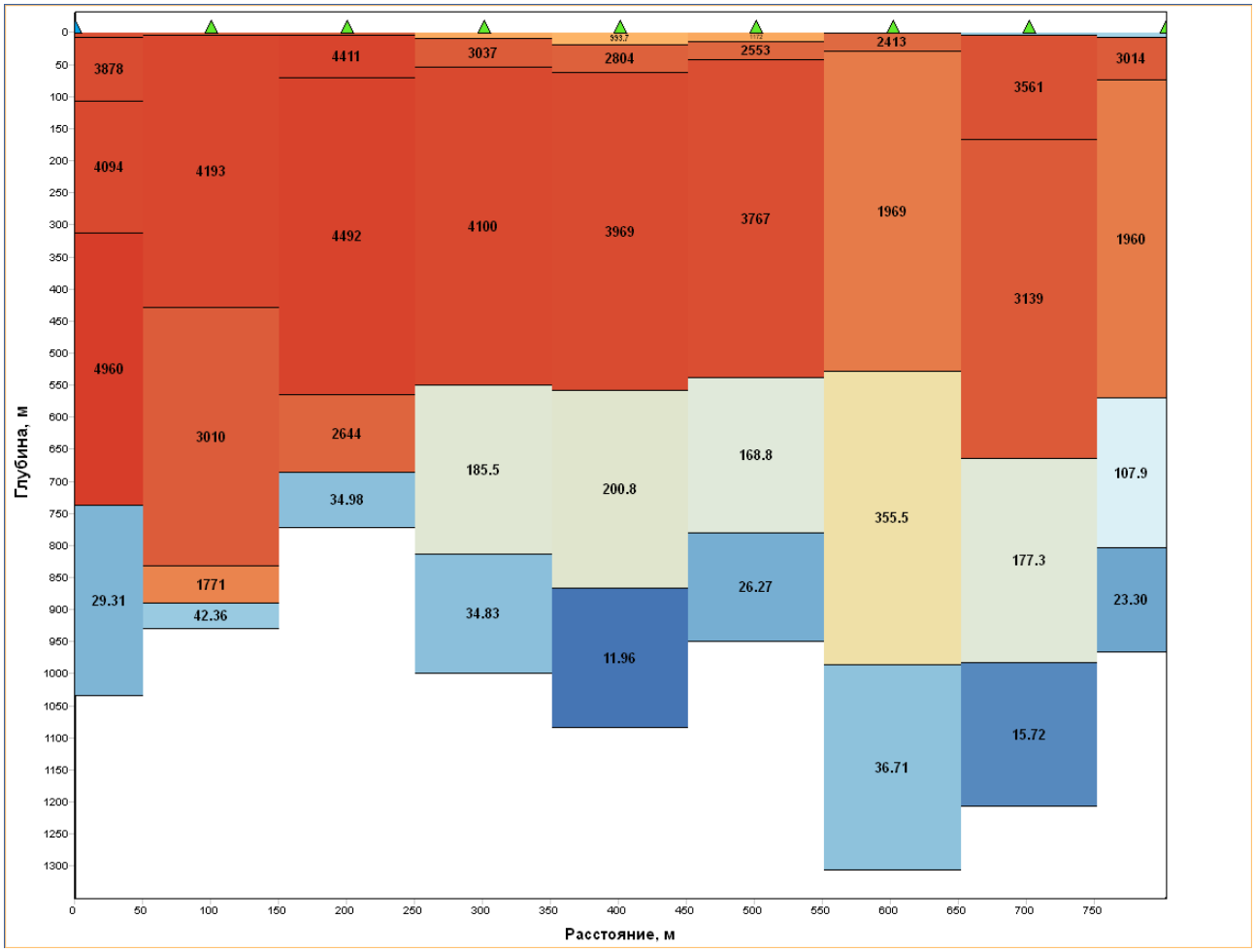

Figure 2.5.3: *Preliminary geoelectric section of the first profile, the profile strike is south north*

The analysis of the resulting sections shown, that the thickness of permafrost is about 700 meters. It is presented in both sections.

2.6 Seismological observations in Samoylov Island area of the Lena Delta

Petr A. Dergach [1,2,@], Svyatoslav N. Ponasenko [1,2], Lyubov Y. Eponeshnikova [1,2,], Gleb Y. Zobnin [1,2,*], Vladimir V. Potapov [1,2], Andrei A. Kartoziia [1,2,3], Wolfram H. Geissler [4,*], Stepan A. Gukov [5,*], Sergey V. Shibaev [5,*], Rustam M. Tuktarov [5,*]*

[1] A. A. Trofimuk Institute of Petroleum-Gas Geology and Geophysics, Siberian Branch, Russian Academy of Sciences, Novosibirsk, Russia

[2] Novosibirsk State University, Novosibirsk, Russia

[3] V. S. Sobolev Institute of Geology and Mineralogy, Siberian Branch of the Russian Academy of Sciences, Novosibirsk, Russia

[4] Alfred Wegener Institute Helmholtz Centre for Polar and Marine Research, Bremerhaven, Germany

[5] Yakutsk Branch Federal Research Centre Geophysical Survey, Russian Academy of Sciences, Yakutsk, Russia

[*] not in the field

[@] Corresponding author: DergachPA@ipgg.sbras.ru

Fieldwork period and location

From 10.07.2021 to 29.07.2021 (on Samoylov Island, America-Khaya, Kharaulakh Ridge)

Objectives

The main objective of this work is the creation of a detailed seismotectonic model of the Samoilov area and the northern part of Kharaulakh ridge. This will be useful in the study of the geodynamic situation in the whole region. Delta Lena region is one of the few examples of the transition between oceanic and continental rifting. Here is the end of the seismic active zone, which begins in the Okhotsk Sea and marks the boundary between the Eurasian and North American lithospheric plates. As part of the research, a detailed study of the local seismicity in the region, arising from the interaction of fault systems in the southern part of the Laptev Sea and the northern part of the Kharaulakh ridge, is being carried out. This will help answer the question about the relationship of modern seismicity with active faults on the surface, previously identified during structural-geological studies and analysis of satellite images (Imaev et al. 2018), as well as build an updated fault-block model of the earth's crust. The research is, in a way, a continuation of the Russian-German research carried out within the framework of the SIOLA project in 2016-2020 (Geissler et al. 2021), and will focus on a more detailed study of the northern part of the Kharaulakh ridge. This will allow obtaining more reliable information about hypocenters and mechanisms of local earthquakes, as well as building a velocity model of the study area by seismic tomography. A distinctive feature of the research is the integration of the results with the results of magnetotelluric sounding (Potapov et al. 2021) and near-field transient electromagnetic sounding (NTES).

Methods and fieldwork summary

This year we continued our continuous seismological observations in the Samoilov Island area of The Lena Delta Region. Due to the pandemic situation, in 2020 there are only four stations were installed. In 2021, we moved two stations to another location and installed four new stations (Figure 2.6.1).

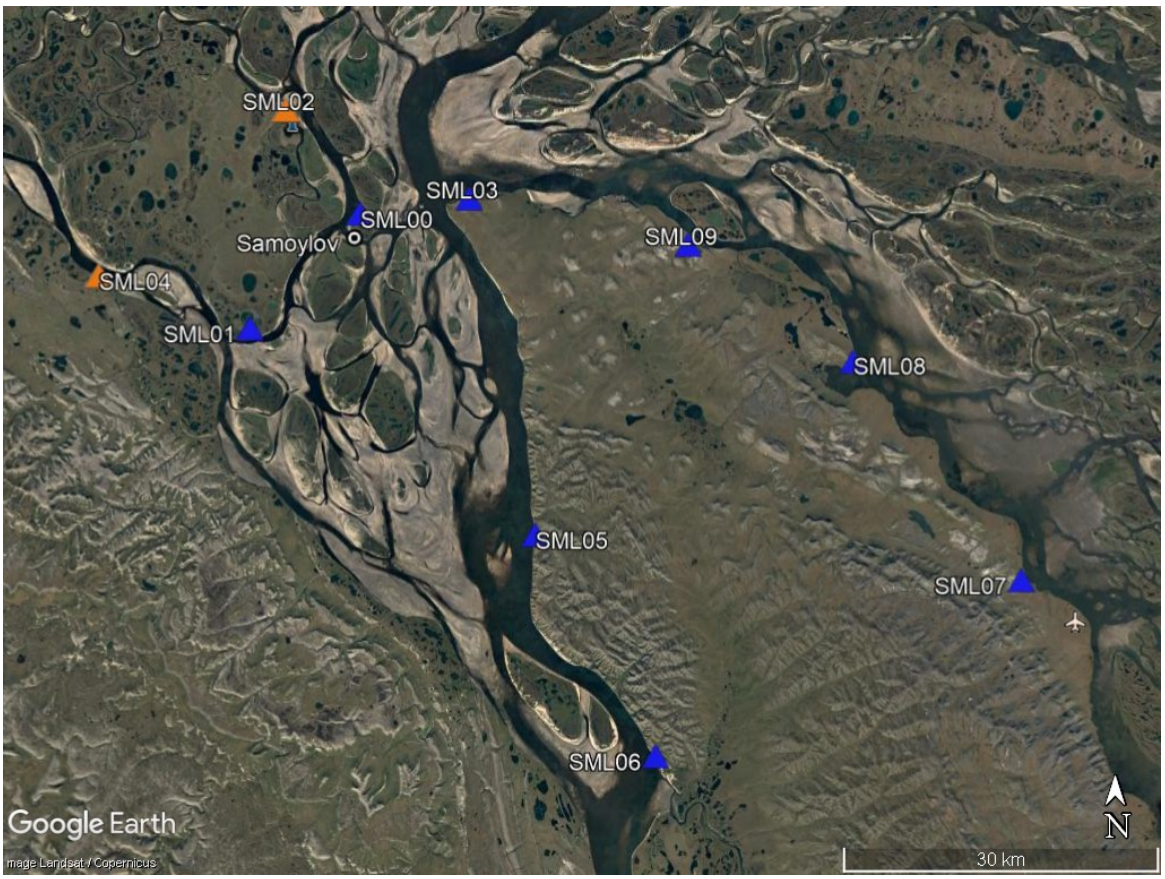

Figure 2.6.1: *Map with observation points of the local seismological network. Blue triangles -– existing stations, orange triangles – dismantled stations*

All stations of our network are equipped with seismic digitizers “SCOUT-3.1”, low-frequency geophones “GS-ONE LF”, and batteries “BAKEN” (350 Ah, 2.6 V). Batteries were connected in series by six units, which provided a total voltage of about 16 V per station. Such a set of equipment provided a continuous recording of signals at two stations for 11 months: from the start of recording in August 2020 to the time of station maintenance in July 2021. A detailed description of seismological equipment technical characteristics is given in (Tables 2.6-1-2.6-2).

The weakness of batteries “BAKEN” is the need to provide a constant flow of air through the tubes brought to the surface. In the past season, air access at two observation points was allegedly blocked by water and snow. Because of this, the stations were shut down in October 2020 and February 2021. When installing the stations in July 2021, we tried to change the way the pipes were brought to the surface to eliminate this deficiency.

Table 2.6-1: Digitizer “SCOUT-3.1” main technical parameters

№	**Parameter**	**Value**
1	ADC resolution	24 bit
2	Number of channels	3
3	Amplifier gain	36 dB
4	Sampling frequency	125 Hz
5	Internal memory	32 Gb industrial SD-card
6	Storage temperature	-40˚C to +85˚C
7	Operating temperature	-40˚C to +70˚C

Table 2.6-2: Geophone “GS-ONE LF” main technical parameters

№	**Parameter**	**Value**
1	Natural frequency	5 Hz
2	Sensitivity	100.4 V/m/s
3	Damping factor	0.45
4	Coil resistance	2450 Ω
5	Spurious frequency	160 Hz
6	Operating temperatures	–40°C to +80°C
7	Tilt angle when coil hit end stop	30° for vertical, 8° for horizontal

To provide continuous data recording to SD-card (32 Gb) with a duration of a year or more, the digitizer “SCOUT-3.1” implements the ability to archive raw data.
The raw data quality control is already finished. All records are acceptable for processing quality. The example of the local earthquake raw record is shown in (Figure 2.6.2).

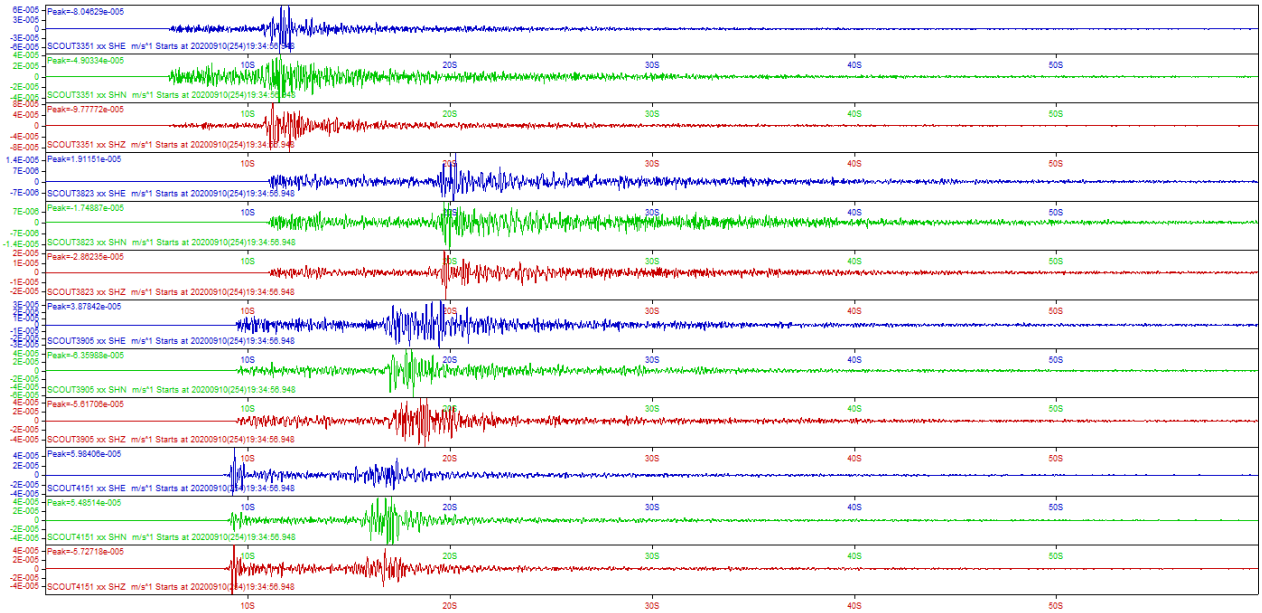

Figure 2.6.2: *Example of the local earthquake raw record*

Preliminary results

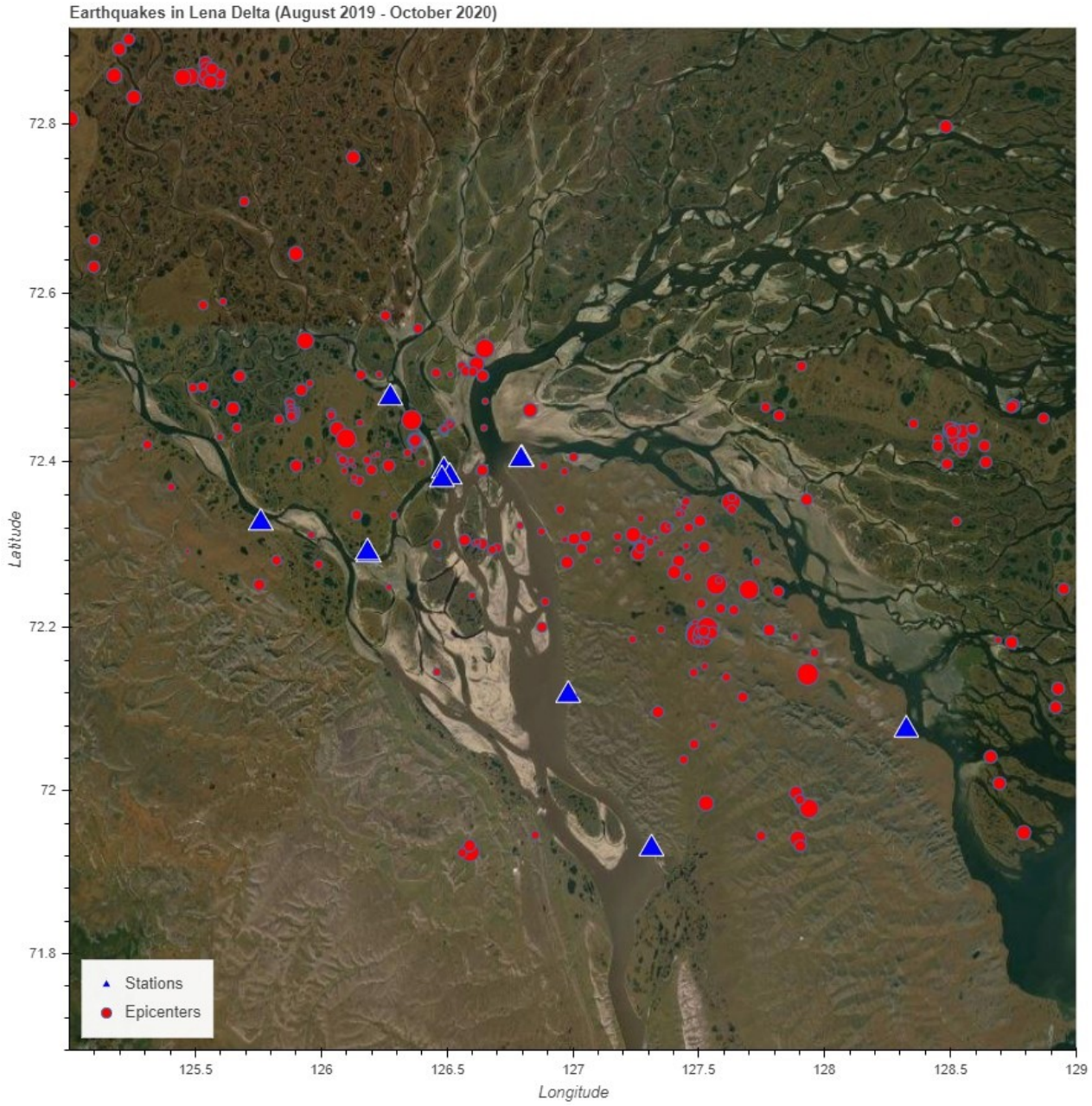

Figure 2.6.3: *The preliminary results of the local earthquakes hypocenter localization around Samoylov Island*

The building of the velocity model of the studied area by seismic tomography followed by hypocenters relocation as well as the determination of strong earthquakes source mechanisms now are in progress.

2.7 Geobotanical observations on Samoylov

Nikolay N. Lashchinskiy [1,2,@]

[1] Central Siberian Botanical Garden, Novosibirsk, Russia

[2] A. A. Trofimuk Institute of Petroleum Geology and Geophysics, Siberian Branch of the Russian Academy of Sciences, Novosibirsk, Russia

[@] Corresponding author: nnl630090@gmail.com

Fieldwork period and location

From 10.07.2021 to 29.07.2021 (on Samoylov Island, America-Khaya, Kharaulakh Ridge)

Objectives

For this year, main focus of the geobotanical research was on floodplain vegetation. The main task was to describe floristic and vegetation diversity of floodplain habitats.

Methods and fieldwork summary

Floodplain vegetation was described on three neighboring islands: Samoylov, Kurungnakh and Sasyl – Ary. Descriptions were made on transects by standard method on sample plots 10 to 10 meters. In addition, herbarium specimens were collected. As whole 63 geobotanical description were made and 78 herbarium specimens collected.

Preliminary results

Floodplain vegetation showed big changes on a gradient from the beach to the first terrace cliff. These changes can be considered as primary plant succession under colonization of fresh newly appeared substrate. The initial point of this succession is a sand beach without any plants and quite often with aeolian microrelief. This stripe along the coast could be up to 15 m widths in mid-August – a time of the lowest water in Lena River.

The next stripe inland from the beach is about 10–15 m width covered by sparse vegetation with pioneer species. Single plants spread from each other are on a distance few times bigger than their own crown projection and not associated into communities. Species composition of this stripe includes pioneer grasses (*Arctophyla fulva, Deschampsia sukatschewii, Poa alpigena* etc.) and other plants, which are typical for the fresh non-colonized substrate (*Cardaminopsis petrea, Sagina nodosa, Tripleurospermum subpolare*).

The next step inland is a stripe with pioneer plant communities. This stripe could be up to 20 m widths. Microrelief here is flat and surface substrate consists of sand and fine silt. Vegetation cover is about 30 to 60%. Depending on moisture, main dominants could be *Arctophyla fulva* and *Eriophorum scheuchzeri* on wet habitats or *Deschampsia sukatschewii*, *Calamagrostis holmii* and *Equisetum arvense* on moist well-drained habitats. Pioneer communities have a quite simple structure. The main dominant species cover from 20 to 50% of the community area. In the case of graminoid-dominated communities graminoids form upper stratum 20-30 cm height and underneath second stratum 10-15 cm height with coverage about 20–30% formed by *Equisetum arvense* and few other species. Plants have a nearly uniform distribution in the community area. Vascular plant diversity is about 12 to 15 species per 100 m^2. Mosses are nearly absent. On this successional stage, the first shrub seedlings of *Salix* species could be found. On most elevated and slightly disturbed habitats in this stripe psammophitic communities formed on moving sand. These habitats have a well-developed microrelief made of small sand dunes. A surface substrate consists of more coarse sand than on flat surfaces in this stripe. There are very few specialized psammiphytes like *Aconogonon ochreatum* but some other plants could be abundant here: *Sanguisorba officinale*, *Tanacetum bipinnatum* and *Festuca rubra*.

Further stage-willow thickets with horsetail – is the most widespread vegetation on the floodplain. It is continuous vegetation with an average coverage from 50 to 70%. A shrub layer is up to 70 cm high and its coverage is about 30%. It consists almost exclusively of *Salix glauca* with a small admixture of *S. alaxensis*, *S. boganidensis* and *S. viminalis*. In the herbaceous layer, main dominant species is *Equisetum arvense*.

The herbaceous layer is spotty with an average coverage of 50 to 70% distributed in between shrubs. Vascular species diversity is up to 20–28 species per 100 m². Mosses cover about 50–70% of the soil surface and presented by pioneer species like *Bryum sp*.
The most elevated parts of the floodplain are occupied by two main community types: willow thickets with rich herbaceous layer and willow thickets with a well-developed moss layer. In both cases, the shrub layer consists mainly or exclusively of *Salix glauca*. In the first case, the shrub layer is 40 to 80 cm height and its coverage is 40 to 50%. Few specimens of *Dushekia fruticosa* could be found here on their very northern limit. The herbaceous layer is dense and diverse. An average height is 20–25 cm and coverage about 70%. Vascular species diversity is up to 28–35 species per 100 m². Many typical tundra species are present here (*Dryas punctata, Arctous alpina, Tofieldia coccinea,* etc.). The moss layer is well-developed, covers up to 60% of the soil surface and consists of few moss and lichen species. The main dominants are *Tomentypnum nitens* and *Hylocomium obtusifolium.*
Another type of willow thickets has a shrub layer a bit lower than in the first case (30 to 50 cm) with coverage of 30 to 40%. The herbaceous layer dominated by *Carex concolor* and sometimes *Eriophorum angustifolium* is not so species-rich – from 18 to 25 vascular plant species per 100 m². In species composition, there are many hygrophilous species (*Pedicularis albolabiata*, *Cardamine pratense*, *Juncus arcticus*, etc.). The most distinctive feature of this community type is the thick moss layer with *Tomentypnum nitens* as the main dominant.
These two types of willow thickets differ by habitats – the first one occurs on elongated slightly elevated ridges and as a narrow fragmented stripe along the first terrace cliff. The second one occupied a flat or slightly concave surface between ridges.
There are few small creeks drain floodplain surface. In the headwater of each creek, there is sedge fen with *Carex concolor* and *Eriophorum angustifolium*.This community type is species-poor (not more than 4-8 vascular plant species per 100 m²), with coverage of 60 to 85% and sometimes standing water. The moss layer is fragmented, consists of swamp species and quit often submerged under the water.
Along the channel of the creek there is a stripe of aquatic vegetation about 5 to 10 m width, formed by *Arctophyla fulva* and *Dupontia pelligera*.
The abovementioned community types describe vegetation diversity on the floodplain. Most of these types could be united into successional series. The main driving force of plant succession is the frequency of floods and the duration of flood events. In addition, floodplain received more hit with water flow from the south. Also, bare sand exposed to sunlight gets more hit than tundra surface covered with thick moss layer acting as a good isolator. All together, this additional hit caused dropping down the upper border of permafrost and development of thick active layer. We measured the deepness of the active layer with a metal stick at the end of August across the floodplain. On the sand beach and in pioneer plant communities according to 100 measurements deepness of the active layer was 96.6 ± 1.5 cm and under the ridges – 98.1 ± 1.2 cm. Only under the willow thickets with well-developed moss cover active layer was 53.3 ± 1.2 cm. These warmer conditions in comparison with zonal situations allow the development of shrubby communities more typical for the southern tundra. These willow thickets can exist for quite a long time stabilized by periodical flood events. Floods carried big amount of mad which precipitate on floodplain surface and pressed down moss development. However, in case of floodplain contact with the first terrace, it heavily influenced by the runoff from the terrace surface. In our case, few creeks open to floodplain from the first terrace. Existing creeks on the floodplain cannot drain this surface effectively because of very weak inclination. In addition, these creeks periodically dam by sand bars near the mouth. Standing water on the floodplain surface caused fen formation and development of the moss layer.
For the test polygon on Samoylov island vegetation map of floodplain was built based on field vegetation survey and UAV images received from Supercam S 250 (Figure 2.7.1). It shows the spatial distribution of all described plant community types. In the northern part of the floodplain there is a clear successional sequence with four steps in the eastern direction from the beach to the creek valley. In the southern part of the floodplain situation is more complex.
Comparison with geomorphology map of the Samoylov Island shows a good concurrence with main geomorphological units.

In the case of scroll-bars, not only geomorphology is important for vegetation development, but also a time of origin. From the very beginning plant succession goes in different ways on different surfaces. Well-drained scroll-bars with deepest active layer accelerate plant succession. When falt surface covered by pioneer communities on scroll-bars willow thickets with horsetail already formed – this is the situation with a second scroll-bar on the map. For now, the most developed successional stage on scroll-bars is willow thickets with the rich herbaceous layer. The same community type developed on the base of the first terrace's slope – the oldest and highest part of the floodplain. Scroll-bars to a certain extent can prevent parts of floodplain in between them from flooding. Short floods and a relatively small amount of precipitated mad in these spots in comparison with flat terrain prevents mosses from burial under the mad and supported development of the thick moss layer.

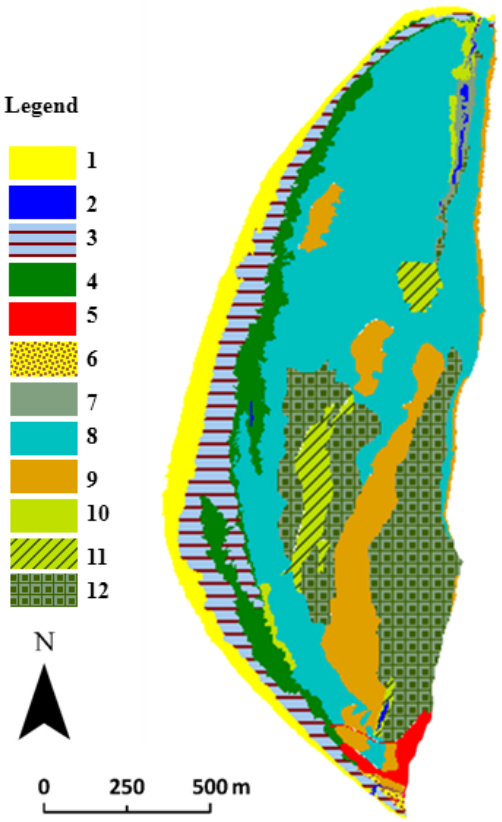

Figure 2.7.1: *Vegetation map of the Samoylov Island floodplain: 1 – sandy beach without plants; 2 – open water; 3 – sandy beach with pioneer plants; 4 – pioneer plant communities; 5 – antropogenic disturbances (roads, buildings, etc.); 6 – psammophitic communities on moving sand; 7 – aquatic vegetation; 8 – willow thickets with horsetail; 9 – willow thickets with rich herbaceous layer; 10 – horsetail communities; 11 – sage fens; 12 – willow thickets with well-developed moss layer*

Vegetation dynamics on the recent floodplain in Lena delta is presented by primary succession driven by flood regime. Four main stages of this succession could be distinguished with quite stable last one presented by willow thickets with horsetail. Besides floods, important factors for the succession development are additional hit transported by river from the south and amount of sand and silt precipitated on the floodplain. In case of the contact between the first terrace and the floodplain, the last one is heavily influenced by the runoff from the terrace. Because of it, succession goes further towards wet tundra with a well-developed moss layer. Spatial vegetation distribution strictly depends on relief formations and could be used as a sensitive indicator for the geomorphological mapping based on satellite or UAV high-resolution images.

2.8 Search for and collection of Arctic legumes and their microsymbionts in the Lena River Delta

Denis S. Karlov [1,@], Irina A. Alekhina [2], Andrey A. Belimov [1]

[1] All-Russia Research Institute for Agricultural Microbiology, Saint Petersburg, Russia

[2] Arctic and Antarctic Research Institute, Saint Petersburg, Russia

[@] Corresponding author: deniskarlov23@gmail.com

Fieldwork period and location

From 13.07.2021 to 14.07.2021 (on Tiksi Bay and Samoylov Island)

Objectives

Global climate change, accompanied by a widespread increase in temperature, is the most pronounced in the polar regions of the Earth. In the Arctic, these processes are accompanied by a gradual increase in the depth of permafrost thawing and the duration of the growing season, which leads to a significant restructuring of the entire Arctic ecosystem. The observed "greening effect" of the tundra leads to the active migration of plant communities to the north, particularly of pasture phytocenoses including legume species. Legumes form symbiosis with nitrogen-fixing nodule bacteria (rhizobia), providing the plants with nitrogen and making them rich in protein. This allows increasing the productivity of Arctic territories, particularly pastures. Plant-rhizobia symbiosis also makes legumes ecologically flexible, resistant to environmental stress and serve as a nutrient source for many organisms. Therefore, the nodule bacteria of the Arctic latitudes area unique gene pool with a significant potential for the formation of highly productive pasture agrocenoses that contribute to an increase in the food supply for farm animals in the Arctic region. In addition, the biodiversity studies of nodule bacteria that form nodules on the roots of Arctic legumes will complement and expand the spectrum of species of these bacteria, create a unique collection of rhizobia as a valuable genetic resource for their use in agriculture and for gaining fundamental insights into plant-microbe interactions and other areas. The proposed study of symbiosis between Arctic legumes and rhizobia will contribute to the evaluation of their agricultural potential for the formation of highly productive pasture phytocenoses and for the restoration of disturbed lands in the Arctic regions of Russia. Several Arctic legume species are endemic and relict. The study of their symbiosis with provide unique fundamental knowledge about adaptation of plants and microorganisms to extreme soil-climate conditions of the Arctic.

The project aims to collect samples of legume plants, particularly endemic and relict species and mostly belonging to genera *Hedysarum, Astragalus* and *Oxytropis*, and soil samples located on the territory of the Lena River delta in order to create a unique collection of symbiotic nodule bacteria.

Methods and fieldwork summary

The search, collection and species identification of legume plants was carried out in cooperation with the botanist Nikolay N. Lashchinskiy (CSBG SB RAS). The plants were collected from various cites of the Lena River delta, Tiksi Bay and Lake Sevastian-Kuele (Table A.2.6). Due to the different growing conditions and phenotypes of legumes, various tools were used to collect root nodules and soils samples: garden shovels, chisels and bushhammer. The nodules and seeds were collected and stored in clean paper envelopes and dried at room temperature. Soil samples were collected in clean plastic bags and stored at +4°C. For all the collected plant species, the root nodules and soil samples were taken. The seeds were collected for most of the plant species. All samples of soils, seeds, and nodules were transported to a laboratory of the All-Russia Research Institute for Agricultural Microbiology (Saint Petersburg). The nodules were calculated and prepared for further isolation of rhizobia.

Preliminary results

In total, 13 species of legume plants belonging to 5 genera (*Astragalus*, *Oxytropis*, *Hedysarum*, *Vicia* and *Lathyrus*) were collected in the period from 14.07.2021 to 14.08.2021 (Table A.2.6). According to available information from the literature, about 20 species of legume plants grow in the studied area of the Lena River

delta (Labutin et al. 1985). So, more than a half plant species were found. For most of the species, two or three populations growing in different areas (Lena River delta, Tiksi Bay and Lake Sevastian-Kuele) were collected.

For the first time, on Samoylov Island, we (together with Dr. Nikolay Lashchinskiy) have found populations of the legume *Lathyrus palustris.* This species was not described previously as an inhabitant of this area according to various sources (oral communication from Dr. Nikolay Lashchinskiy (Labutin et al. 1985). Earlier, a population of *Lathyrus palustris* was found in the village of Tiksi (Nikolin et al. 2017).

Thus, our group collected comprehensive biological material in the form of herbarium, seeds and nodules of arctic legumes, as well as the soil samples where these plants were found. This material will serve as an unique resource for further experiments in laboratory conditions aimed at characterization biodiversity of nodule bacteria and evolution of nitrogen fixing symbiosis.

Acknowledgements

We are very grateful to Dr Nikolay N. Lashchinskiy for his help in collection and identification of the legumes and valuable advices. We thank very much Dr Sergey Pravkin (AARI) for help in collecting and transporting legume seeds. We would like to express our gratitude to the management and coordinators of the Expedition "Lena 2021" for organizing and conducting the expedition. We are grateful to the staff of Samoylov Research Station and particularly to Fedor Selyakhov for providing transport and comfortable living conditions, which positively affected the implementation of research tasks. The work was partially supported by the Russian Science Foundation (grant 20-76-10042).

Figure 2.8.1: *Trip to the lake Sevastian-Kuele and collecting plants Oxytropis nigrescens (left) and Astragalus tugarinovii (right)*

Figure 2.8.2: *Collecting plants Oxytropis adamsiana at the terrace of Samoylov Island*

Figure 2.8.3: *Collecting plants Astragalus frigidus on the slope of the terrace at Tit-Ary Island*

2.9 Microbial communities and molecular composition of permafrost soils as a factor of stabilization of organic matter from Ice Complex of the Lena River Delta

Vyacheslav Polyakov [1,@], Sergey Pravkin [1]

[1] Arctic and Antarctic Research Institute, Saint-Petersburg, Russia

[@] Corresponding author: slavon6985@gmail.com

Fieldwork period and location

From 20.08.2021 to 24.09.2021 on Samoylov Island, Kurungnakh Island, Botulo-Sise Island, Chay-Ari Island, Olenekskaya Channel.

Objectives

This work is the continuation of a long-term study of the molecular composition of humic acids (HAs) in Arctic soils, using the example of alluvial soils of the Lena River Delta. Thus, the aim of this work is to study HAs by ^{13}C–NMR spectroscopy of permafrost soils of the Lena River Delta, buried organic matter, and melted soil-like bodies from the Ice Complex of the delta. Moreover, comprehensive knowledge of the microbial community is needed for studying the fundamental problem of organo-mineral substrate transformation under climatic conditions of Arctic. This is especially relevant in regards to studying the initial soil-forming process of fresh material which is thawed from Ice Complex.

Methods and fieldwork summary

The sampling and classification procedure of soils and soil horizons was carried out according to the standard procedure (WRB classification 2015). In the course of this work, samples were taken from the upper organo-mineral as well as the lower horizons in which suprapermafrost accumulation of organic matter occurred.
The key areas of research are soils from Kurungnah islands (third terrace), Botulo-Sise Island (third terrace) (Figure 2.9.1), Chay-Ari Island (first terrace) and small islands without names on the Olenekskaya Channel (first terrace) (Figure 2.9.2). Samples were taken from the superficial soil horizons, as well as from the lower ones located on the permafrost table. In order to assess the degree of stabilization of organic matter and study the evolutionary selection of HAs molecules within the soil profile.

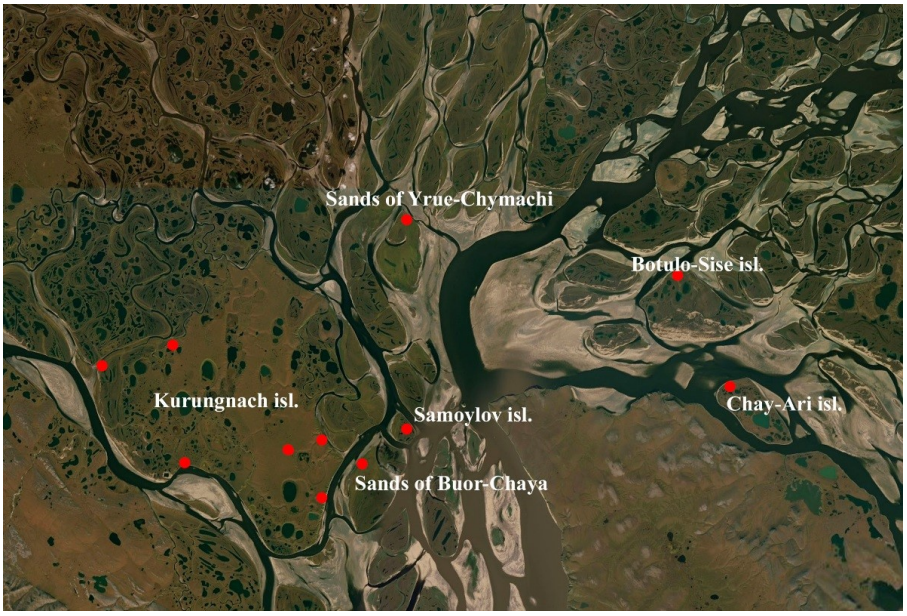

Figure 2.9.1: *Key areas of work. Lena River Delta*

Figure 2.9.2: *The soil-like bodies from Botulo-Sise Island*

Prelimnary results

During the field season, was conducted an initial assessment of the soil cover on the studied islands. The soil cover in most cases is represented by zonal cryogenic soils, the development of which is associated with active cryogenic processes in the region. The soils formed on the first terrace of the Lena River delta are represented by modern alluvial deposits with a relatively thick (up to 20 cm) organomineral horizon, the border of permafros table was more than 1 m.

For the first time, we studied the soil cover of Botulo-Sise Island, which is represented by cryogenic soils; in this area, we sampled soils thawing from the Ice Complex of the Lena River Delta, as well as a variant of zonal soils as a background for the region, and took a soil sample to determine the age of the sediments.

Sampling for metagenomic sequencing included deposits of the Ice complex, zonal soil, soil from the youngest site in the Lena River Delta (Chai-Ary Island), as well as sandy islands involved in periodic flooding.

The sampling procedure for the study of the molecular composition of humic acids was continued, in particular from the Ice complex of Lena Delta, since earlier results from Kurungnakh Island indicate a relatively high content of aromatic fragments in sediments from the Ice complex and their resistance to biodegradation.

Samples were taken for micromorphological analysis of the soil cover to reveal the structural features of organic-mineral particles of cryogenic soil and possible mechanical stabilization of organic matter.

On Samoilovsky Island, soil samples were taken at different distances from the station in order to analyze possible soil contamination by polyaromatic hydrocarbons, which are the result of the work of diesel generators.

Together with Charlotta Mirbach, an analysis of the vegetation and soil cover of the flooded areas of the Lena River Delta was carried out in order to identify the relationship between the vegetation cover and the content of nutrients in the soil. According to the working hypothesis, the soils that develop here have a fairly high level of aeration, this is due to the sandy texture class, in this regard, a favorable conditions for soil microorganisms is formed, under the influence of which the mineralization of organic matter occurs.

Together with Andrey Kartozia (not in the field), an analysis of various variants of polygonal tundra on Samoilovsky Island was carried out in order to identify the main patterns in the transformation of the soil cover depending on time, landscape positions and the degree of development of thermokarst processes.

A primary investigation of soils formed in the zone of coastal erosion along the Lena River, as well as those areas that are formed inside the island as a result of degradation of the Ice complex, has been carried out.

2.10 Observation of thermal erosion on the key sites "Khabarovo", "Kurungnakh" and "Tiksi"

Anna M. Tarbeeva [1,@], Lyudmila S. Lebedeva [2], Vladimir V. Shamov [2,3]

[1] Lomonosov Moscow State University, Moscow, Russia

[2] Melnikov Permafrost Institute, Siberian Branch, Russian Academy of Sciences, Yakutsk, Russia

[3] Pacific Geographical Institute Far-Eastern Branch, Russian Academy of Sciences, Vladivostok, Russia

[@] Corresponding author: amtarbeeva@yandex.ru

Fieldwork period and location

From 08.07.2021 to 11.07.2021 and from 08.09.2021 to 10.09.2021 on Khabarovo; from 12.07.2021 to 13.07.2021 and from 05.09.2021 to 09.09.2021 on Kurungnakh, and from 18.07.2021 to 20.07.2021 and from 03.09.2021 to 04.09.2021 and from 11.09.2021 to 15.09.2021 in Tiksi.

Objectives

Intensive changes in the Arctic climate lead to activation of exogenous processes, changes in the land surface, water and sediment runoff, and pose a threat to engineering structures. One of such processes is thermal erosion – the erosion of the ice-rich permafrost by the combined thermal and mechanical action of the moving water (Ershov 1982; Everdingen 2005). A few decades ago, thermal erosion was very limited in unimpacted tundra landscapes (Sidorchuk et al. 1999), but it is becoming increasingly widespread in the last decades (Boike et al. 2019; Bowden et al. 2008; Godin et al. 2014; Gooseff et al. 2009).

Methods and fieldwork summary

Studies of the dynamics of small thermoerosional landforms in the Lena River Delta area were started in 2019, in the vicinity of the Tiksi – in 2020. The first observations were made using repeated tacheometric surveys and direct measurements with a tape measure. In 2020-2021 we used aerial photography from a DJI Mavic mini quadrocopter. Photogrammetric processing of the overlapping images allows to obtain orthophotomosaics and digital terrain models, that are used for quick and detailed assessment of the landforms dynamics.

The studied thermoerosional forms are located in three key areas (table), that are different in geomorphology, lithology and geocryology. The key site "Khabarovo" is located on the mainland in the Lena River delta area on the spurs of the Kharaulakh ridge near the polar weather station named after Yu. A. Khabarov (Stolb Island Station). The relief of the site is represented by hills (with elevations up to 171 m above sea level). The lower parts of the slopes are composed of silty loams and contain polygonal ice wedges. The key site near the Tiksi is located on the slope of Mount Lyalkina, which also has a loose slope cover with thick (up to 2 m wide) ice wedges. The "Kurungnakh" key site is located in the Lena Delta on the island of the same name. It is composed of Late Pleistocene ice complex underlying by the Early Pleistocene sandy unit (Grigor'ev 1993). The sites "Khabarovo" and "Kurungnakh" are located within the Ust-Lensky Nature Reserve - the area protected from human activity at least over the past 35 years. The gully in the Tiksi village was partially initiated by a winter road laid 50 m above its head.

The investigated thermoerosional landforms can be attributed to two types: rills and gullies (Timofeev 1981). Rills are recently formed small (less than 1-1.5 m deep) thermoerosional landforms that develop rapidly and can be quickly filled with sediment, but can also grow into a gully. Gullies are larger and more stable forms, which have a depth of more than 1-1.5 m, and, as a rule, exist for a longer time.

In 2021, observations of the dynamics of thermoerosional landforms were continued. They covered two periods – the middle of July and early September, which made it possible to track the snowmelt-induced changes and the changes resulting from the summer floods. In total, the surveys of 15 thermoerosional landforms were obtained by the end of the 2021 field season, six of which have repeated observations (Table A.2.7).

In addition to the monitoring of landforms, the measurements of water discharge, water level, suspended and bedload sediments were carried out, and water samples were taken for chemical analyzes. Such a dataset, together with the published data from other observations in this area (weather conditions, active layer dynamic, etc.), allows us to draw preliminary conclusions on the rates, reasons and mechanisms of current thermal erosion development.

Preliminary results

During the field trip in July 2021, we observed the snowmelt process. It was revealed that in mid-July, at the Khabarovo site, snowfields were still preserved in most of the gullies oriented to the east (Left Meteorologichesky, Neskuchny). The snow contained a large amount of silty and sandy particles of aeolian origin, which, as the snow melts, were accumulated onto the ground surface, being an additional source of stream sediments (Figure 2.10.1).

Figure 2.10.1: *Highly polluted snowfield in the Left Meteorological gully in July 2021. (Photo: A. M. Tarbeeva)*

To assess the bedload accumulation, both projected from snowfields and transported during floods from rills and gullies, 4 trap mats were installed in the Meteorologichesky Creek valley in July 2021. The data from the trap mats were obtained in September and reflect the results of the flood event on August 26–27, 2021. It was revealed that the sediments deposition occurred on two of the four mats. The third mat was washed away, and the fourth one, installed on the site of a snowfield high above the channel, remained clean.
The maximum thickness of sediment accumulation (up to 7 cm) was observed below the inflow of the watercourse from the Arbuznaya rill (Figure 2.10.2).

(a) *July 2021* (b) *September 2021*

Figure 2.10.2: *A mat for trapping accumulated sediments, installed in the valley of the Meteorologiechsky stream near the mouth of the Arbuznaya rill: a) clean during installation (in July 2021) and b) buried under sediments after the summer flood event (September 2021). (Photo: A. M. Tarbeeva)*

The aerial photographs obtained from a quadcopter were being processed. According to the preliminary comparisons of the images, significant dynamics of thermoerosional landforms was observed on Gully No 4 at Kurungnah key site, as well as on the Tiksi Gully.

From July to September 2021, the head of Gully No 4 on Kurungnakh Island has retreated upstream by 14 m, and the sides have retreated by 10 m due to thaw slumping (Figure 2.10.3).

For the two summer months, the head of the Tiksi Gully has moved upstream by 5.6 m. The width of the gully has increased from 11 to 14 m, and the head of the left tributary has advanced by 3.8 m (Figure 2.10.4).

The edges of the gullies in Khabarovo did not experience significant changes, despite the flood that took place at the end of August 2021. At the same time, erosion of the channel and accumulation of sediments in the bottom of the Meteorologichesky Creek were noted. Apparently, during the flood, soil blocks that had fallen into the bottom of the gully earlier were eroded. The two new rills appeared in the summer of 2021 – Arbuznaya rill and Rill No 2.

The high intensity of the gullies dynamics is also confirmed by the data on the concentration of suspended sediments in the watercourses in the gullies. The maximum values of turbidity (550–670 mg/l) were observed in the gullies on Kurungnakh and near Tiksi. They are 2 orders of magnitude higher than the turbidity values in the ravines at the Khabarovo site (1-5 mg/l).

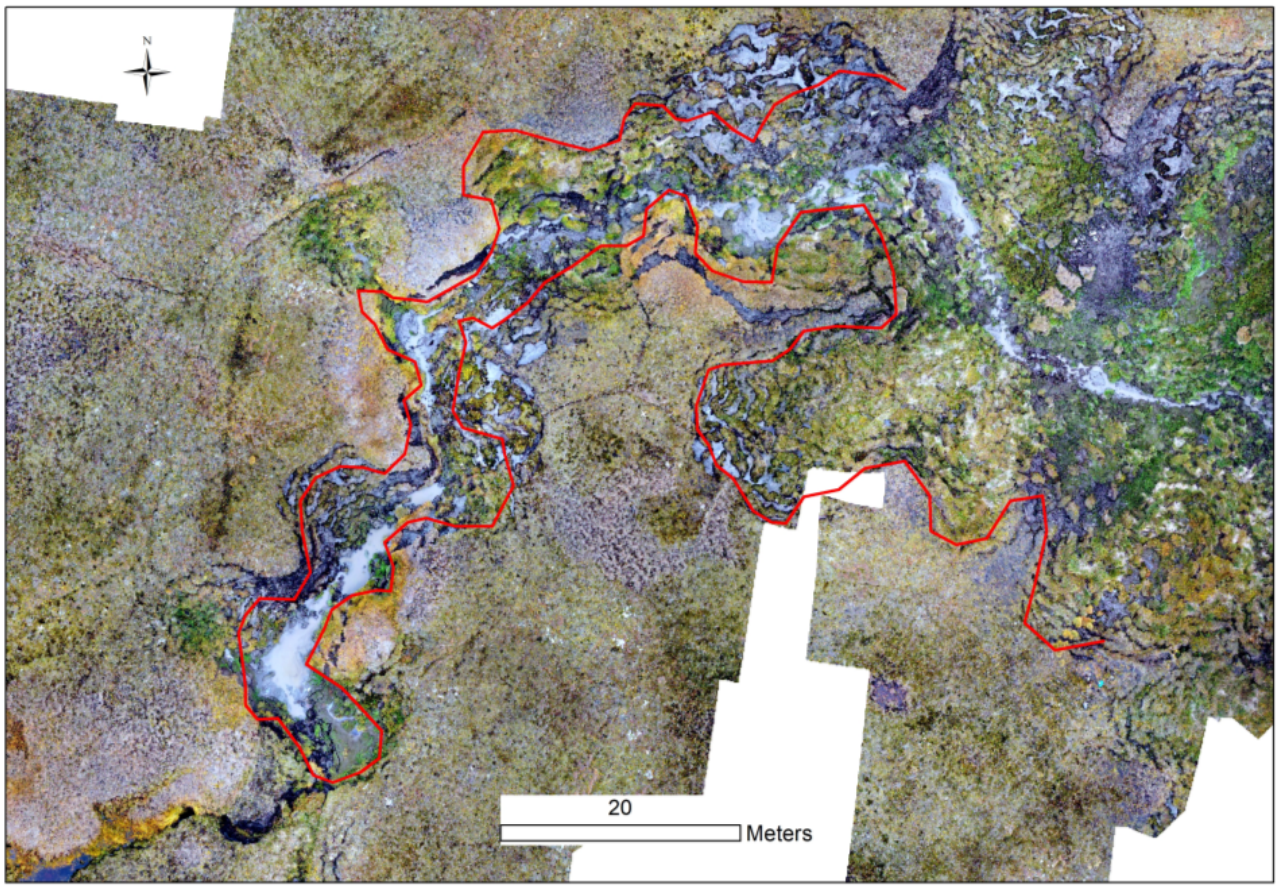

Figure 2.10.3: *Dynamics of the Gully No 4 on Kurungnakh Island for the summer period: the picture was taken on 07.09.2021, the red line shows the edge of the gully on 13.07.2021*

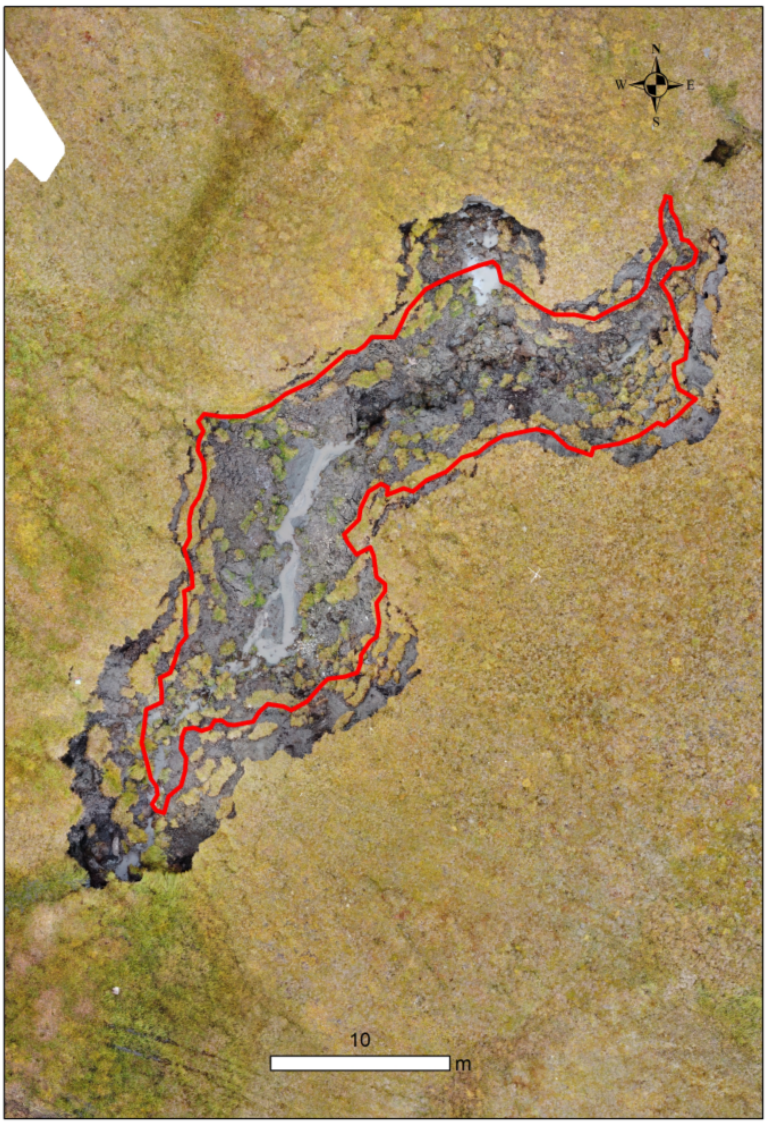

Figure 2.10.4: *Dynamics of the Tiksi Gully over the summer period: the image was taken on 03.09.2021, the red line marks the edge of the gully on 18.07.2021*

The detailed processing of the obtained data, comparison them with the monitoring data of the active layer, meteorological parameters ground and surface water levels, as well as further relevant observations would expand and clarify the preliminary conclusions.

Acknowledgments

The fieldwork carried out was supported by the RFBR: projects No. 20-05-00840 (A. M. Tarbeeva), No. 20-35-70027 (L. S. Lebedeva, V. V. Shamov). The methodological studies were carried out within the framework of State Task No. 121051100166-4 Moscow State University and State Task No. AAAAA 20-120111690008-9 IMZ SB RAS.

2.11 Chemical composition of tundra creeks on the key sites "Khabarovo", "Kurungnakh" and "Tiksi"

Lyudmila S. Lebedeva [1,@], Vladimir V. Shamov [1,3], Anna M. Tarbeeva [2]

[1] Melnikov Permafrost Institute, Siberian Branch, Russian Academy of Sciences, Yakutsk, Russia

[2] Lomonosov Moscow State University, Moscow, Russia

[3] Pacific Geographical Institute Far-Eastern Branch, Russian Academy of Sciences, Vladivostok, Russia

[@] Corresponding author: lyudmilaslebedeva@gmail.com

Fieldwork period and location

From 08.07.2021 to 11.07.2021 and from 08.09.2021 to 10.09.2021 on Khabarovo; from 12.07.2021 to 13.07.2021 and from 05.09.2021 to 09.09.2021 on Kurungnakh, and from 18.07.2021 to 20.07.2021 and from 03.09.2021 to 04.09.2021 and from 11.09.2021 to 15.09.2021 in Tiksi.

Objectives

The chemical composition of small rivers in continuous permafrost is controlled by their interaction with the deposits of the active layer (AL) and the permafrost top. An increase in the AL thickness and the degradation of permafrost under the influence of climate change can significantly transform the chemical composition of ground and surface waters of the permafrost zone. Small rivers of the Russian Arctic are poorly studied due to the logistical difficulties of direct field measurements. The aim of the study is to identify river sources and characterize the runoff formation at the small streams in Arctic tundra in the low Lena River basin, Eastern Siberia using water chemical composition of different water storages in the watersheds. In 2021, new hydrochemical and hydrometeorological data were collected during the summer field campaigns at Samoylov research station in the Lena River Delta.

Methods and fieldwork summary

We made two filed campaigns in 2022 – beginning of July (after the river and sea ice melt) and September (before start of ground freezing). Working plan for the field trips included:

1. Installation of loggers for water level, ground temperature and moisture monitoring and time-lapse cameras
2. Monitoring of the water level, temperature and electrical conductivity at water tracks and creeks
3. Manual measurements of the water discharge
4. Sampling of ground ice and water from water tracks, creeks, surface and suprapermafrost ground water of the active layer for hydrochemical and isotopic analysis
5. Hydrochemical surveys along the water tracks and creeks using portable multimeters (water temperature, pH and electrical conductivity)

Water samples were analysed at the Melnikov Permafrost Institute using titration and capillary electrophoresis methods (analysts L. Y. Boitsova and O. V. Shepeleva).

Preliminary results

In 2021 we took 84 samples for chemical and isotope analysis from creeks, water courses in thermoerosional gullies, ground ice, snow, groundwater seepages and suprapermafrost water of the active layer. We analysed them for concentration of major ions and some trace elements. Here we present chemical data of 124 water samples from both 2020 and 2021 field campaigns.

Total dissolved solids (TDS) of sampled water varies in very wide range – from 8 mg/l in snow to 2255 mg/l in groundwater seepages. Three creeks at the "Khabarovo" key site have TDS from 80 mg/l in July to 400–1112 mg/l in the middle of September indicating significant increase of dissolved solids along with active

layer deepening through the warm season. TDS of the small intermittent tributaries of the creeks at the "Khabarovo" key site vary from 60 to 737 mg/l. Seepages of groundwater have high TDS – 760-2255 mg/l. Ground ice sampled in thermoerosional gullies in Kurungnakh and near Tiksi have relatively low TDS values from 20 to 98 mg/l. TDS values of water courses in thermoerosional gullies in Kurungnakh vary from 30 to 490 mg/l, in Tiksi -– from 311 to 490 mg/l.

In weakly mineralized samples with TDS < 300 mg/l, hydrocarbonate-ion predominates in water (Figure 2.11.1 and Figure 2.11.2). With an increase in TDS, water is saturated with calcium bicarbonate, which begins to precipitate in the form of calcite and fraction of hydrocarbonate-ions decreases. Under normal conditions (at a temperature of +20-25 °C and a neutral reaction of the water), the precipitation of calcite occurs with a mineralization of about 500–600 mg/l. In the study area, the water saturation with calcium bicarbonate occurs at lower TDS, and, apparently, is associated with low temperature. A further increase in TDS occurs along with increase in the concentration of magnesium and calcium sulfates, as well as magnesium chlorides, which is apparently associated with their cryogenic leaching. In samples with TDS > 800 mg/l, these freely soluble salts become predominant.

This general dependence of ions fraction on TDS is interrupted by other patterns in different water types. There is almost linear dependence of hydrocarbonate on TDS for different water types but Seismicheskii creek, gullies in Tiksi and groundwater seepages break this dependence (Figure 2.11.3) because they have too low concentrations of hydrocarbonate. The probable reason is interaction of the mentioned water types with rocks enriched with other salts.

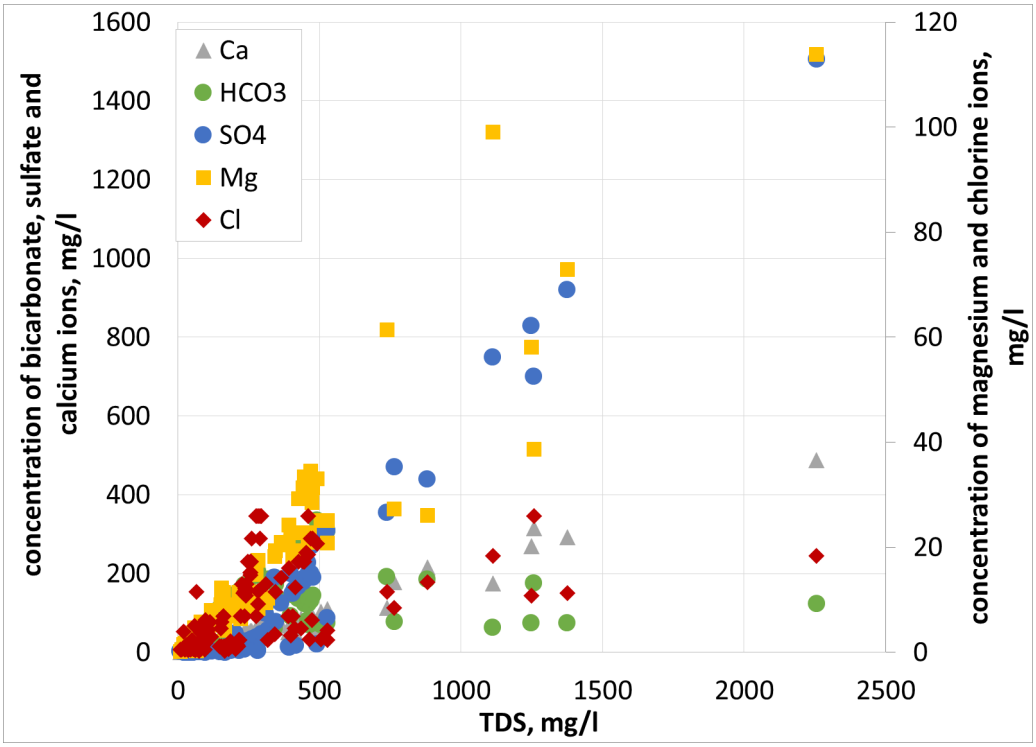

Figure 2.11.1: *Dependence of major ions concentration on TDS for full range of TDS*

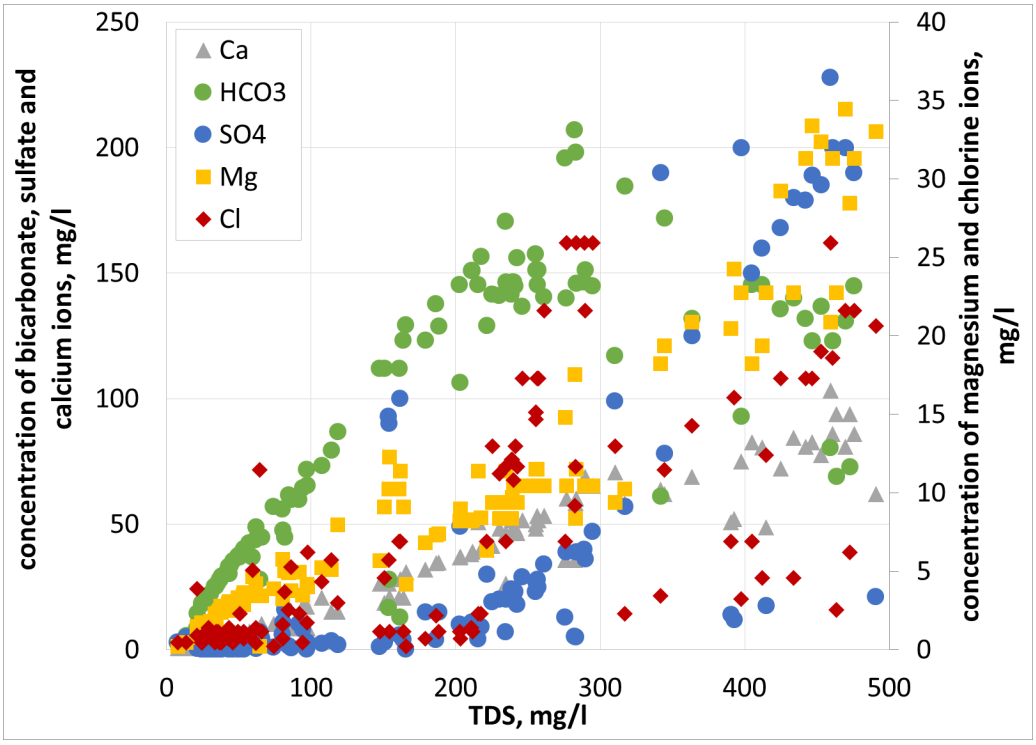

Figure 2.11.2: *Dependence of major ions concentration on TDS for TDS < 500 mg/l*

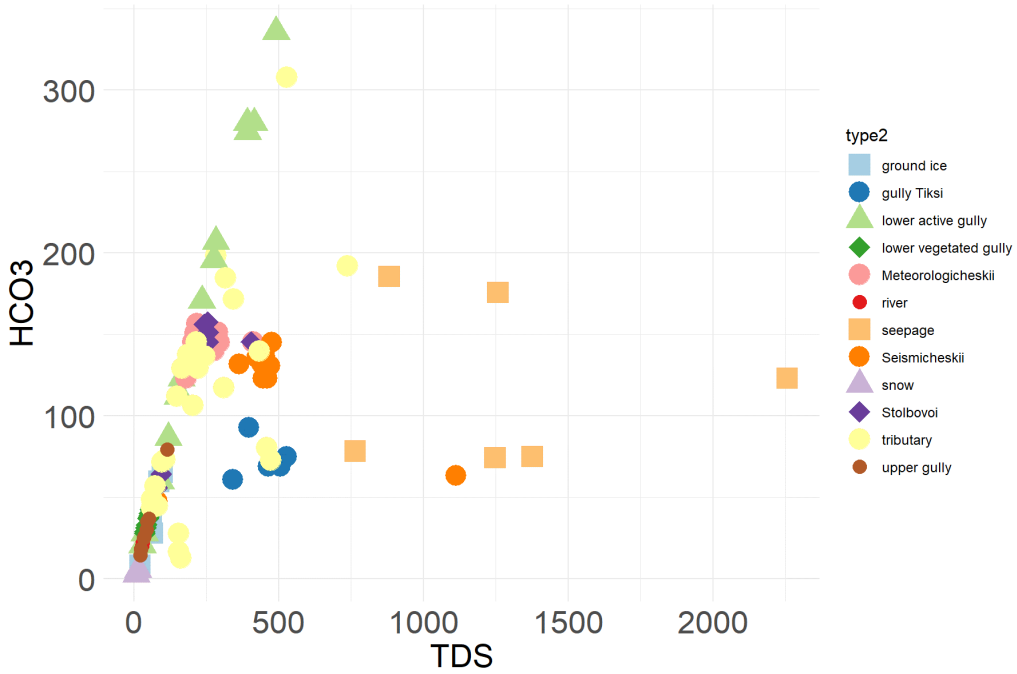

Figure 2.11.3: *Dependence of bicarbonate concentration on TDS for different water types, mg/l*

(Figure 2.11.4) shows concentration of major ions in samples from Meteorologicheskii, Seismiccheskii and Stolbovoi creeks at “Khabarovo” key site. In July, when snowfields are still melting, water has low TDS, hydrocarbonate and calcium dominate in chemical composition. Later in the season in dry periods fraction of sulfates is increasing. Sulfates and magnesium prevail in water of Seismicheski creek in August and September because its watershed has high fraction of bare rock and water freely interact with bedrock while

Meteorologicheskii and Stolbovoi watersheds are vegetated and water interact with bedrock only sparsely, in creek channels and thermoerosional gullies.
Characteristic concentrations of major ions in numerous tributaries of three creeks (Figure 2.11.5) suggests that many of them are formed by atmospheric precipitation and do not interact with bedrock. Such tributaries have low TDS with dominance of calcium and hydrocarbonate ions. Relatively high concentrations of sodium (> 1 mg/l) in weakly mineralized waters of the tributaries indicate that ground ice of the active layer is also one of their water sources. Others have higher TDS that suggests their interaction with bedrock that occurs at active gullies, rills or because of mixing with groundwater. Interesting, that different tributaries with similar TDS values have different fraction of major ions that could suggest different water sources. Tributaries with high fraction of sulfate and magnesium probably have groundwater contribution from groundwater seepages. Tributaries with similar TDS but high fraction of calcium and hydrocarbonate usually relates to thermoerosional gullies. Three tributaries with relatively low TDS (150–160 mg/l) have high fraction of sulfate and low fraction of hydrocarbonate flow in the active rills. Seepages of groundwater at the base of the slopes have the highest TDS (up to 2255 mg/l) and high fraction of sulfate, calcium and magnesium (Figure 2.11.6).

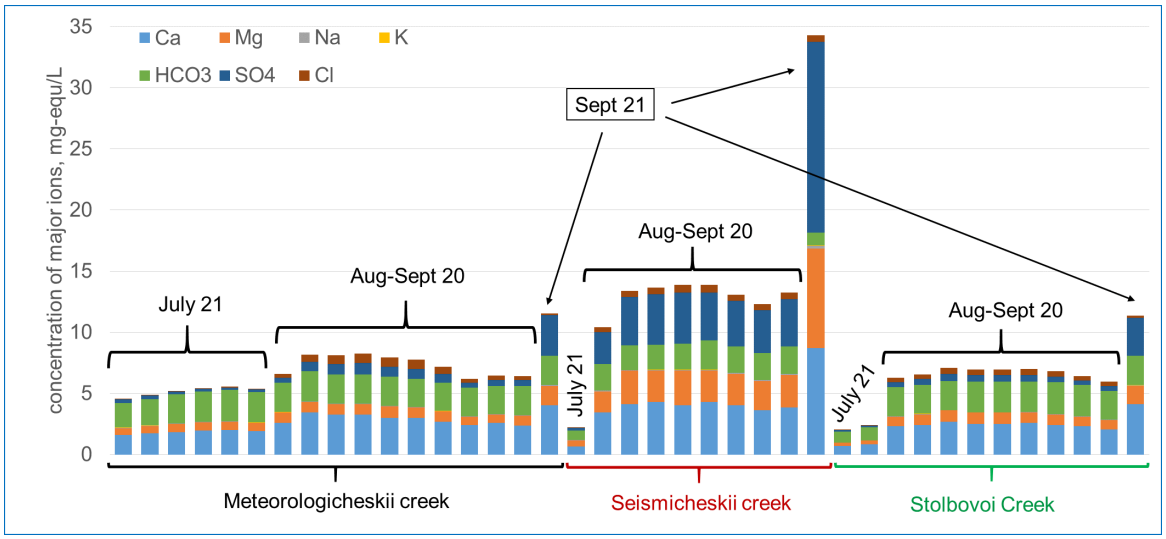

Figure 2.11.4: *Concentration of major ions in samples from creeks at "Khabarovo" key site, mg-equ/l*

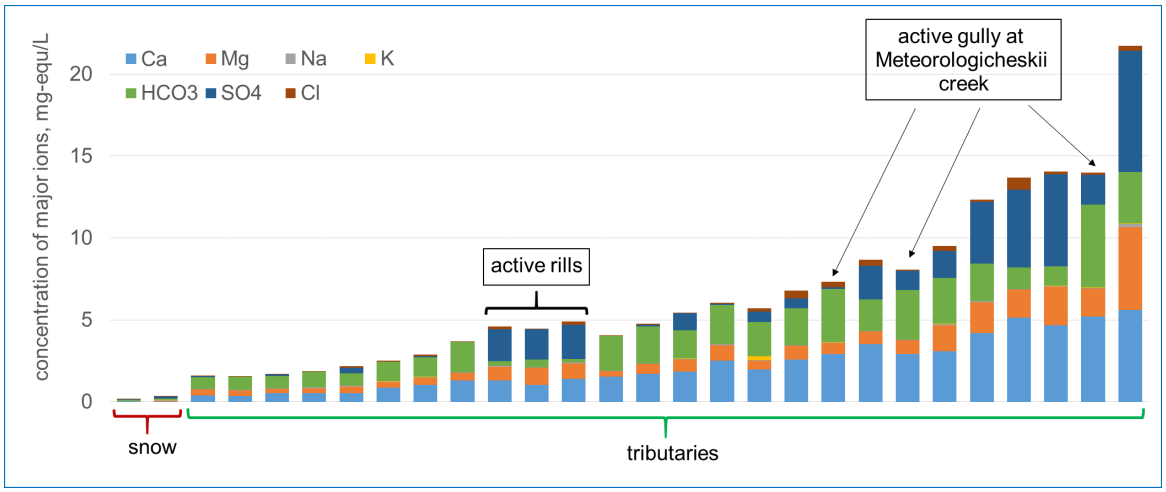

Figure 2.11.5: *Concentration of major ions in samples from snow and tributaries (including watercourses in gullies and rills) at "Khabarovo" key site, mg-equ/l*

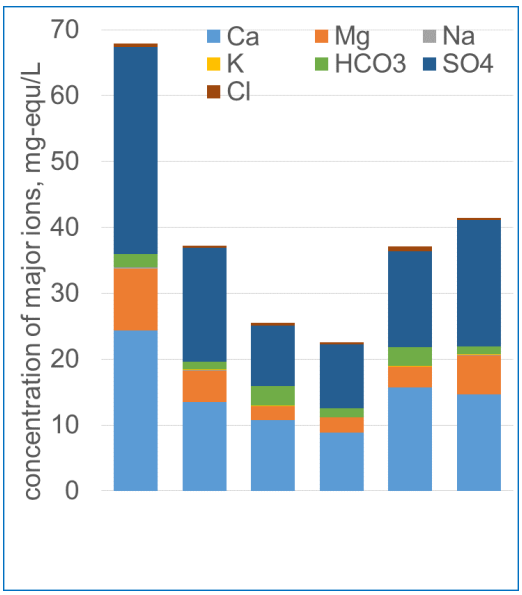

Figure 2.11.6: *Concentration of major ions in samples from groundwater seepages at "Khabarovo" key site, mg-equ/l*

Chemical composition of watercourses in active and vegetated gullies at "Tiski" and "Kurungnakh" key site differs from which other (Figure 2.11.7). In "Kurungnakh" key site water from the upper part of all gullies and lower part of vegetated gullies have very low TDS (20–114 mg/l) that is similar to atmospheric precipitation. Watercourses in lower part of the active gullies (with two exceptions) have high TDS between 90 and 490 mg/l. Hydrocarbonate, calcium and magnesium dominate chemical composition. Many of them have high concentration of sodium (2–15 mg/l) and low concentration of sulfates.
Water in gully near Tiksi has similar chemical composition in upper and lower part of the gully. It has relatively high TDS (340–530 mg/l), high fraction of sulfates and calcium, low fraction of hydrocarbonate.

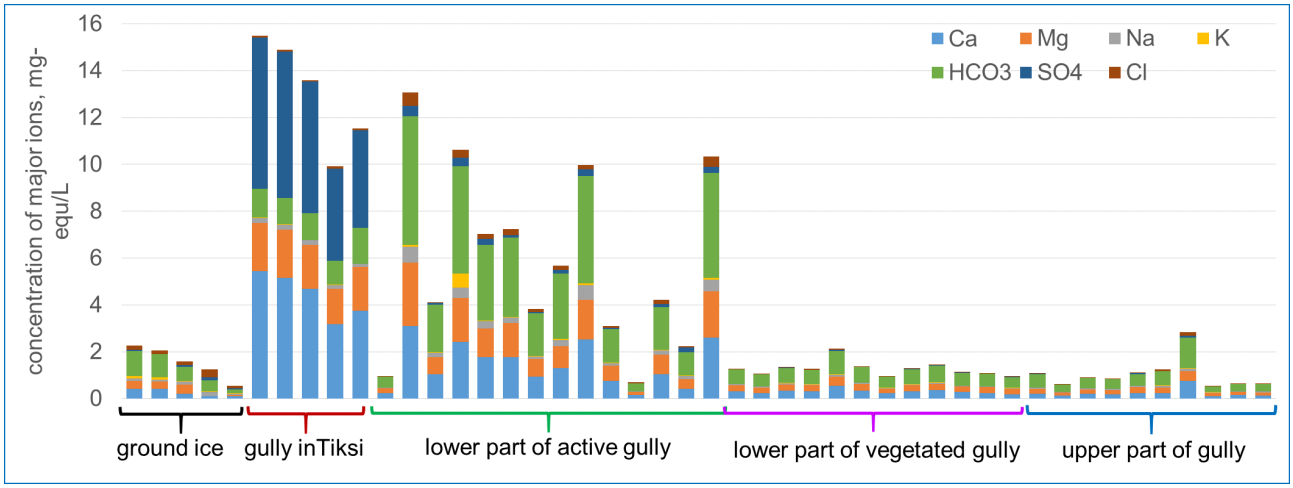

Figure 2.11.7: *Concentration of major ions in samples of ground ice and water in gullies in "Kurungnakh" and "Tiksi" key sites, mg-equ/l*

(Figure 2.11.8) shows dependence of sodium concentration on TDS for different studied water types. There are three lines of Na-TDS relationship: one is for lower parts of the active gullies in Kurungnakh, another one is for groundwater seepages in "Khabarovo" key site and the middle line is for gully in near Tiksi.

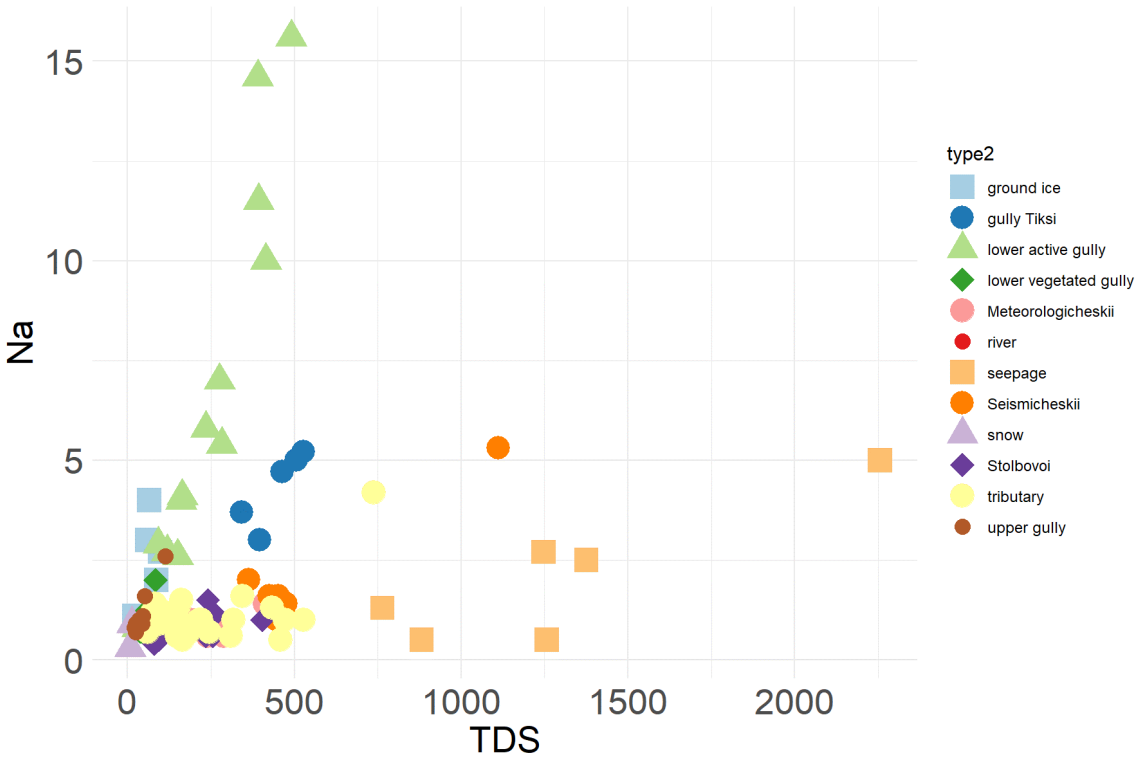

Figure 2.11.8: *Dependence of sodium concentration on TDS for different water types, mg/l*

Acknowledgements

TThe fieldwork was supported by the RFBR: projects No. 20-35-70027 (L. S. Lebedeva, V. V. Shamov) and No. 20-05-00840 (A. M. Tarbeeva). The methodological studies were carried out within the framework of State Task No. 121051100166-4 Moscow State University and State Task No. AAAAA 20-120111690008-9 IMZ SB RAS.

Chapter 3

Expedition to Central Yakutia: modern and past vegetation, lake and fire regimes (RU-Land_2021_Yakutia)

Edited by Birgit Heim, Elisabeth Dietze, Boris Biskaborn, Stefan Kruse, Mareike Wieczorek, Timon Miesner, Luidmila Pestryakova, Ulrike Herzschuh

3.1 Introduction

Birgit Heim [1], Mareike Wieczorek [1], Stefan Kruse [1], Boris K. Biskaborn [1], Elisabeth Dietze [1,2], Ramesh Glückler [1], Izabella Baisheva [1,4], Timon Miesner [1], Alexey Kolmogorov [4], Evgeny Zakharov [4], Lena Ushnitskaya [4], Luidmila Pestryakova [4], Ulrike Herzschuh [1,3]

[1] Alfred Wegener Institute Helmholtz Centre for Polar and Marine Research, Potsdam, Germany

[2] University of Göttingen, Göttingen, Germany

[3] University of Potsdam, Potsdam, Germany

[4] Federal State Autonomous Educational Institution of Higher Education "M. K. Ammosov North-Eastern Federal University", Yakutsk, Russian Federation

Overview

Investigations on field-work derived data on high-latitude vegetation and lakes will support the understanding of climate change, environmental change and enhanced human activities and their impact on Northern ecosystems. Complementary, paleoclimate archives, such as lake sediment cores, and subsequent analyses, will allow us to assess past states of subarctic and boreal systems to predict their future states and ecosystem functionalities.

We report here on the expedition "RU-Land_2021_Yakutia", planned in Russian-German cooperation (Alfred Wegener Institute Helmholtz Center for Polar and Marine Research (AWI), Research Unit Potsdam, Germany & the North-Eastern Federal University (NEFU), Yakutsk, Russia) to continue in summer 2021 a series of detailed studies on high latitude landscape-ecology (vegetation and lakes) and paleolimnology across Eastern Siberia. The environmental monitoring plan envisioned a long-term monitoring transect to be established for at least the next ten years, leading from mixed evergreen-summergreen needle-leaf forests of Western Yakutia (built on past expeditions to the Lake Khamra region in 2018 (RU-Land_2018_Yakutia, Kruse et al. 2019c), 2019 (RU-Land_2019_Nyurba, Fuchs et al. 2021b), and 2020 (RU-Land_2020_Khamra, Biskaborn et al. 2021b) with Principal Investigators (PIs) Herzschuh, Kruse, Dietze) to the treeline biome in northeast Siberia and tundra regions north of the treeline (with past expeditions to Chukotka and the Kolyma region in 2012 (RU-Land_2012_Kytalyk_Kolyma, Schirrmeister et al. 2016), 2016 (RU-Land_2016_Keperveem, Overduin et al. 2017), and 2018 (RU-Land_2018_Chukotka, Kruse et al. 2019a) with PIs Kruse, Herzschuh, Stoof-Leichsenring, Wieczorek). These Russian-German expedition activities were put on hold and stopped in 2022 by the German side due to the ongoing war that the Russian president Putin had started against Ukraine.

In summer 2021, the team of the AWI-NEFU expedition "RU-Land_2021_Yakutia" could intensively examine and sample lakes, vegetation, fire impacts, and environmental properties along a more than 700 km long transect across the Eastern Central Yakutian lowland (between the rivers Lena and Aldan) up to the Verkhoyansk mountain region (Figure 3.1.1). In the intramontane Oymyakon basin region of the Verkhoyansk mountain range, the first campsite was set up at Lake Ulu and was named **"Lake Ulu Camp"** (Figure 3.1.2). Unique to the Oymyakon region is its extreme continentality with lowest temperatures in winter months due to the Siberian High (high atmospheric pressure cell during winter months centred poleward), accentuated in winter further by strong topographic temperature inversions. Here, closest to the location of the cold pole of the Earth, the *lake coring team* successfully retrieved sediment long cores in Lake Ulu for paleoclimate and paleoecology investigations (Chapter 3.2, Figure 3.2.4). In parallel, the *lake team* (Chapter 3.3, Figure 3.3.1) sampled lakes in a wide range of catchment types and the *vegetation team* (Chapter 3.4, Figure 3.4.1) installed vegetation plots across a wide range of Verkhoyansk mountain larch forest habitats, including a fresh fire event.

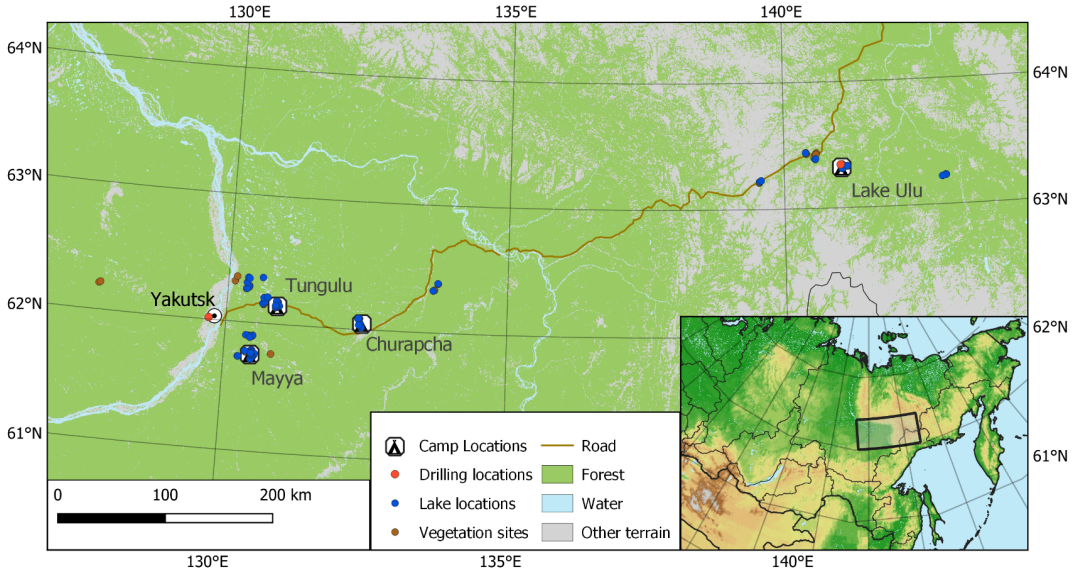

Figure 3.1.1: *The "RU-Land_2021_Yakutia" expedition sites showing the sampled lakes and vegetation plots (blue and brown circles, respectively), two lake drilling locations (red circles): i) Lake Ulu (Verkhoyansk mountain range) ii) Lake Sasary in the city Yakutsk, and the four expedition camp locations: The first expedition camp "Lake Ulu" located in the East in the Oymyakon region of the Verkhoyansk mountain range at around 1000 m elevation. In the Central Yakutian Lowland three successive expedition camp sites were located close to the settlements "Churapcha", "Tyungyulyu" ("Tungulu" in Yakutian) and "Mayya"*

In the second half of the expedition, the *lake coring team* retrieved lake sediment cores from the anthropogenically influenced Lake Saysary located in the urban area of the **city Yakutsk** (Chapter 3.2, Figure 3.2.5). In parallel, the *lake* and the *vegetation teams* assessed and sampled lakes and vegetation cover (forest plots) in different bio-ecological regions of the Eastern Central Yakutian lowland. Field camps were installed first at **Churapcha**, then to the west at **Tyungyulyu** and in the last part of the expedition at the long-term permafrost monitoring site Yukich close to the settlement **Mayya** (Figure 3.1.1, Figure 3.1.2). The Central Yakutian lowlands are characterised by unique ground-ice rich permafrost-landscape types with a multitude of thermokarst landscape forms and thaw lakes in all stages of development and different impacts of anthropogenic land use (Crate et al. 2017). In the Yakutian Lowlands, the *lake team* could assess the wide range of these thermokarst lake types, differently influenced by anthropogenic land use. In parallel, the *vegetation team* inventoried summergreen to mixed with evergreen forest stands with a wide range of different disturbance histories (wildfire, wind throw, land-use, insect infection).
At each site visited, lakes and vegetation plots, the teams conducted detailed surveys and sampling. In the lakes, water was sampled for a wide range of analyses (anorganic and organic chemistry, fauna and flora, environmental DNA), lake surface sediments and sediment short cores were retrieved, vegetation surveys for dominant vegetation types and soil sampling was conducted around each lake. In parallel, at numerous vegetation plots, the *vegetation team* installed soil and tree loggers to set up long term monitoring. The *vegetation team* mapped vegetation at each plot according to a standardised scheme, including the ground vegetation cover, and soil pits that were excavated for soil profile description and sampling. Forest structure properties and tree and shrub species were inventoried (sampling adapted from (Kruse et al. 2016) and described in (Shevtsova et al. 2020) and (Miesner et al. 2022)). In addition, at each plot, plant material was collected from tree individuals for dendrochronological analysis (as described in (Wieczorek et al. 2017a), (Wieczorek et al. 2017b)), modern genetics and biomass per tree type and plot.

In addition, in the field, the land cover and lakes were mapped with unmanned aerial vehicle (UAV) based LIDAR and multispectral camera acquisitions covering large areas in highest detail. After the expedition, all samples (water, vegetation, tree discs, lake sediment cores, surface sediments, soil samples) were transported to AWI Potsdam for further processing and analyses in the laboratories.

Figure 3.1.2: *Field camp at a height of 1000 m elevation at Lake Ulu, in the Verkhoyansk mountain region: "camp Lake Ulu" (left) and at "camp Mayya", one of the three field camps in the boreal Central Yakutian Lowland (right). (Photos: Timon Miesner)*

Acknowledgements

This expedition has been funded by the Alfred-Wegener-Institute Helmholtz Centre for Polar and Marine Research (AWI). Further, we acknowledge funding for our equipment for the project "Potsdamer InnoLab für Arktisforschung" no. F221-08-AWI/001/002 from the Brandenburg Ministry for Science, Research and Culture (MWFK). We sincerely thank Aleksey Pestryakov Bearguard and Lena Ushnitkaya from Yakutsk who have been with us on expedition for their tremendous camp and food logistics for such a large expedition team. We thank Volkmar Aßmann and Jan Kahl for their continuous and strong support for logistics before and during the expedition.

3.2 Parametric sub-bottom profiling and sediment core retrieval at Lake Ulu and Lake Saysary, Eastern Siberia

Boris K. Biskaborn [1], Jan Kahl [1], Igor Syrovatskiy [3], Philip Meister [1,2], Lena Ushnitskaya [3], Paraskovya Davydova [3], Aleksey Pestryakov [3], Luidmila A. Pestryakova [3,]*

[1] Alfred Wegener Institute Helmholtz Center for Polar and Marine Research, Potsdam, Germany

[2] University of Potsdam, Potsdam, Germany

[3] Federal State Autonomous Educational Institution of Higher Education "M. K. Ammosov North-Eastern Federal University of Yakutsk, Yakutsk, Russia

[*] not in the field

[@] Corresponding author: Boris.Biskaborn@awi.de

Fieldwork period and location

From 01.08.2021 (start in Potsdam/Germany) and 05.08.2021 (start field work onsite) at Lake Ulu until 19.08.2021; from 20.08.2021 to 24.08.2021 we worked at Lake Saysary in Yakutsk and arrived back in Potsdam at 27.08.2021.

Objectives

Modern warming of the ground in the last decades is amplified in Russia (Biskaborn et al. 2019b). However, environmental features in Siberia are spatially highly variable (Biskaborn et al. 2021d, 2019a; Herzschuh et al. 2013). At the same time, we observe a sparse coverage of paleolimnological data in Russia (Kaufman et al. 2020) demonstrating the high value of lake sediment cores in this region. Therefore, research focus within our research group "Polar Terrestrial Environmental Systems" at AWI has been targeting palaeoenvironmental reconstructions to understand relationships between climate change, vegetation migrations, biodiversity shifts, and lake trajectories in the extreme cold and continental settings of Siberia. The Oymyakon region in the Verkhoyansk mountain range is a key-region to study extreme annual temperature differences as it is known as the coldest place in the northern hemisphere. The city of Yakutsk is one of the biggest cities in the high north and thus the central city areas should be an ideal place to study intense human impact on boreal arctic ecosystems (such as in Biskaborn et al. 2021c). To gain data on key-interactions in both, extreme continental (Lake Ulu) and urban influenced settings (Lake Saysary), our research is based on (sediment core) time series of environmental change and to establish proxies documenting climate, vegetation, ecosystem composition and sedimentology.

Methods and Fieldwork summary

We used trucks to reach **Lake Ulu** from Yakutsk. Our field work comprised geophysical, palaeolimnological and limnogeological methods that were conducted in a similar way at each site. First, we performed parametrical sub-bottom profiling using an SES-2000 compact device from INNOMAR mounted to a steerable drilling platform on the water with predominantly 8, 10, and 12 kHz. Water samples were retrieved with a Ruttner type water sampler. Surface sediments for geochemical and biological (bioindicators and aDNA) analyses were sampled across the lake with a HYDRO-BIOS sediment grabber to study algae, zooplankton and other benthic organisms.

Parametric sub-bottom profiling data were processed and assessed directly after geophysical surveys to determine bathymetry and potential drilling locations for long and continuous records of sediment layers (Figure 3.2.1, Figure 3.2.2 and Figure 3.2.3). We retrieved short sediment cores using a 90 mm UWITEC gravity corer. Long cores were retrieved with a UWITEC HYBRID 90 mm piston coring system operated from a double-A-platform on water (Figure 3.2.4).This new system was successfully used for the first time under real field conditions. We established four stable anchor positions and lowered a base plate with funnel down to the lake floor connected with two steering ropes mounted at the platform. Coring action was guided by the ropes to operate through the funnel in the same hole. The piston was fixed at the funnel and thus relative to the lake floor (and not to the platform). This method was adjusted according to drilling locations

and objectives, please see the results chapter. Coring was supported by various motors to operate the funnel, the coring chambers and the hammering unit. We also used the 'old' Niederreiter 60 mm piston coring system mounted on a tripod platform on **Lake Saysary** (Figure 3.2.5). All cores were subsequently stored in PVC plastic tubes in dark and cold using thermoboxes. We collected water samples, which were analysed for pH, temperature, and conductivity in the field, and will be analysed for anions and cations in laboratories of AWI in Potsdam.
We measured water Electrical Conductivity and temperature along the water column depth profiles across the lake using a SEA&SUN CTD 48M instrument.

Preliminary results

Lake Ulu
Results of 56 tracks of parametric sub-bottom profiling are shown in (Figure 3.2.2). The deepest part was detected at 43 m in the south-eastern basin of Lake Ulu at sampling site EN21117 (Figure 3.2.1). The profiles showed a rather variable morphology and variation of the sediment infill in the basin (Figure 3.2.3). However, we could locate a suitable drilling location with ca. 10–11 m of continuous horizontal sediment layers and plan for coring. We retrieved long cores at 2 sites in lake Ulu, of which the first site at 17.3–17.4 m water depth consists of three parallel cores EN21101, EN21102, and EN21103, with total lengths of 10, 7, and 11 m, respectively (Figure 3.2.1. The bottom part of the cores suggested sandy layers with gravel and thus indicated that the lake sedimentation part of the basin infill was penetrated. To get undisturbed high resoluted Holocene material, we chose another long-coring site EN21128 in the western part of the lake basin (Figure 3.2.1. We were able to retrieve a very well preserved 174 cm core with intact surface at 21 m water depth. For this we applied the Usinger technique combined with the Niederreiter platform technique and the SES results. After setting the platform at anchors, we used the water depth monitored by SES-2000 echosounding to lower down the funnel 30 cm above ground without touching it and carefully operated the Usinger 2 m system with using weights to let the first ca 1 m penetrate through the layers before starting careful hammering. This way the surface layers are well preserved and we can recommend this technique (in stable weather conditions or from ice).
We retrieved three vertical water profiles through the water column measured 10 vertical CTD sections (Table A.3.1). Preliminary hydrochemical results of in-situ measured surface waters reveal average conductivity and pH of 73.4 μS/cm and 7.61, respectively.

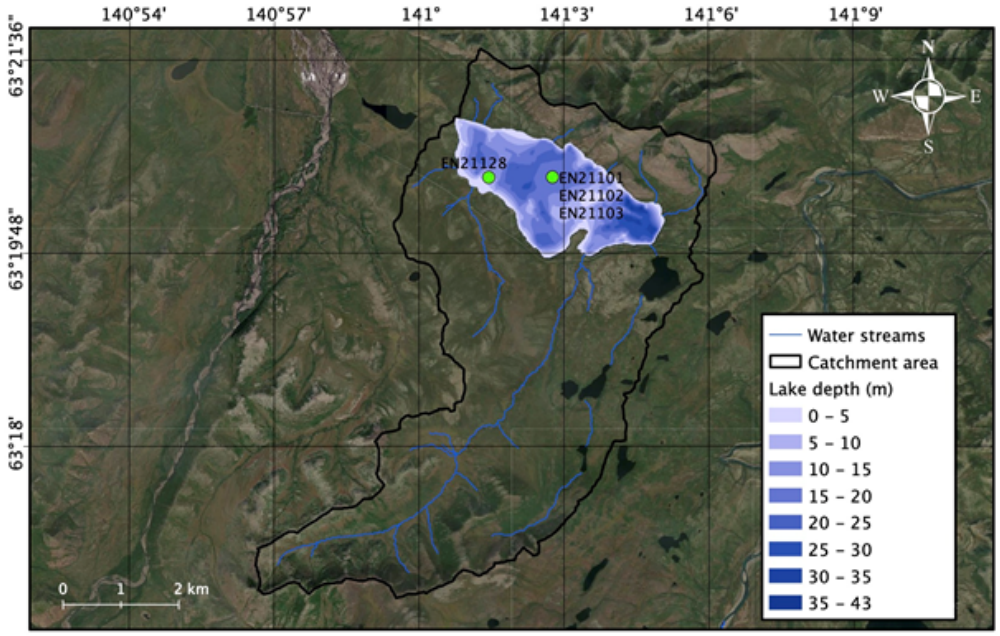

Figure 3.2.1: *Water depth reconstructed from SES-2000 data at lake Ulu. Catchment with rivers/streams and main long coring locations indicated on the map*

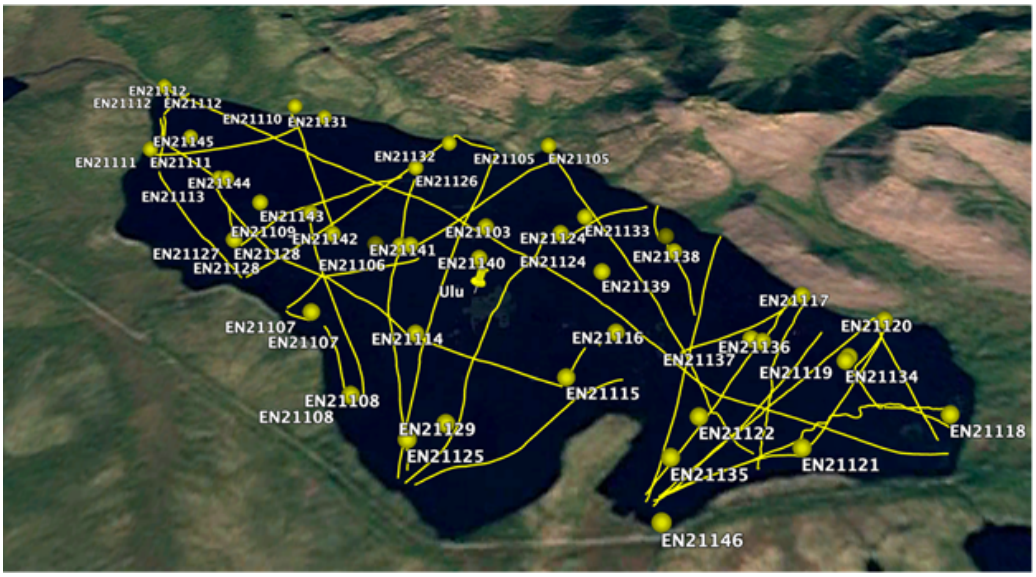

Figure 3.2.2: *Google Earth derived map of lake Ulu with the locations of all sampling locations (compare with Table sampling site) and transects performed with running the SES-2000 parametric sub-bottom profiler. Data from transects were used to generate the water depth map (Figure 3.2.1, scale and northing from this figure apply here also)*

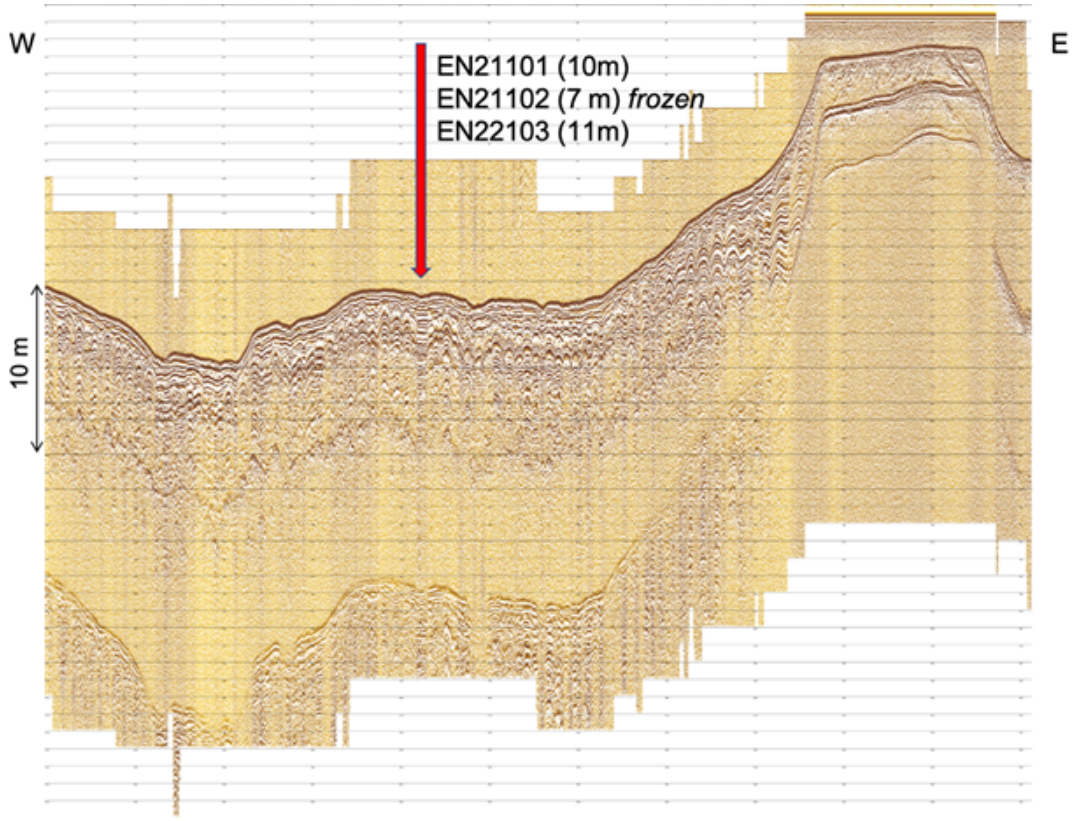

Figure 3.2.3: *Sub-bottom profile from sediments in Lake Ulu, performed with SES-2000 parametric compact*

Lake Saysary

At **Lake Saysary** we only were allowed to power any vessel, i.e. boats and the platform with paddles but not with motor, inspite of strong wind. It took us a considerable amount of time and energy to perform parametric

sub-bottom profiling and to bring the platform over the desired drilling location. We retrieved two long cores EN21160 and EN21161 at 4.5 and 5 m water depth, respectively. Each of the cores reached 2.6 m length before drilling was stopped by hard ground (stones). We also retrieved a vertical water profile at the same site and a short sediment core using the UWITEC gravity corer (before drilling). Water chemistry results of **Lake Saysary** revealed average Electrical conductivity and pH of 909.8 μS/cm and 7.96, respectively.

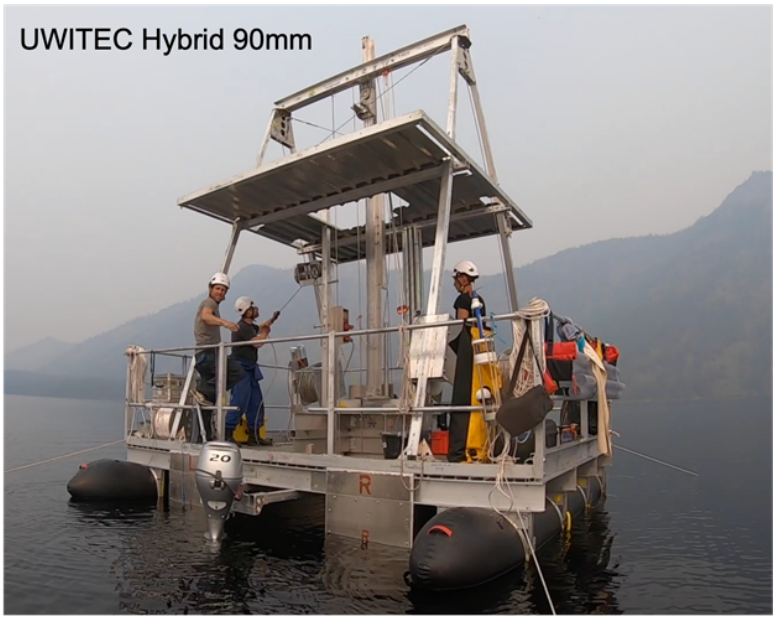

Figure 3.2.4: *The expedition drilling team operating the new UWITEC HYBRID 90 mm piston coring system with double-A-tower mounted on the platform at anchor on lake Ulu at site EN21103. (Photo: Philip Meister (AWI))*

Figure 3.2.5: *Coring on lake Saysary to retrieve anthropogenic influenced lake sediment core time series, with the Yakutsk city in the background. (Photo: Jan Kahl (AWI))*

Acknowledgements

We thank Volkmar Aßmann for logistical support and Bernhard Diekmann and Udo Rothe for great help with testing the new drilling rig in Potsdam as preparation for this expedition.

3.3 Setting up a baseline for the Yakutian-Chukotkan Monitoring transect: Lake inventories including water chemistry, lake sediment coring and UAV-surveys

Ramesh Glückler[1], Izabella Baisheva[1,3], Amelie Stieg[1], Iris Eder[1], Birgit Heim[1], Mareike Wieczorek[1,], Aital Egorov[3], Evgenii Zakharov[3], Kathleen R. Stoof-Leichsenring[1,*], Lena Ushnitskaya[3], Luidmila Pestryakova[3,*], Ulrike Herzschuh[1,2]*

[1] Alfred Wegener Institute Helmholtz Center for Polar and Marine Research, Potsdam, Germany

[2] University of Potsdam, Potsdam, Germany

[3] Federal State Autonomous Educational Institution of Higher Education "M.K. Ammosov North-Eastern Federal University", Yakutsk, Russian Federation

[*] not in the field

[@] Corresponding author: ramesh.glueckler@awi.de, izabella.baisheva@awi.de

Fieldwork period and location

Between 06.08.2021 and 02.09.2021, a total of 66 lakes in Central Yakutia and Eastern Yakutia were assessed and sampled and data obtained with a large variety of different methods and for a wide range of sampling purposes. Of those 66 lakes, 14 lakes (not counting Lake Ulu) are located in mountainous terrain, in the Verkhoyansk mountain range, Oymyakonsky intramontane basin (average elevation around 1100 m a.s.l.) at the eastern end of the expedition route in the Yakutian Oymyakonsky and Tomonsky Districts. The other 52 investigated lakes are located west of the mountain range in the Central Yakutian Lowland (average elevation around 200 m a.s.l.), a ground-ice rich permafrost lowland landscape that is experiencing rapidly changing environmental conditions such as permafrost degradation (Boike et al. 2016; Crate et al. 2017) intensifying wildfire regimes (Walker et al. 2019), and intense Yakutian land use (Crate et al. 2017). This lake dataset representative for the Eastern Central Yakutian Lowland includes seven lakes in the Churapchinsky District and two lakes located towards the River Aldan within a freshly burned forest in the Tattinsky District assessed from the 'Camp Churapcha', 17 lakes assessed from the 'Camp Tyungyulyu', and 28 lakes assessed from the 'Camp Mayya' all located in the Megino-Kangalassky District. The variable lake settings encountered during this expedition allow for a comparison between remote and heavily anthropogenically influenced systems, lakes at low and high elevation, as well as a range of different thermokarst lake development stages.

Objectives

In the Verkhoyansk mountain range and the Central Yakutian Lowland permafrost landscape, the lakes represent sensitive ecosystems, biodiversity hot spots and reflect the environmental conditions of the surrounding land surface. In the Verkhoyansk mountains, the lakes are covered for most part of the year with lake ice and mostly represent oligotrophic glacial lake systems remote from human activities with the exception of fishing and hunting. In addition, these lakes represent the oligotrophic lake type in mountain catchments covered with larch forest (Figure 3.3.3). In contrast, the lowland lakes constitute the shallow, eutrophic lake type set in dense boreal forest, agricultural, or settlement catchments. The Central Yakutian Lowland lakes are mostly thermokarst lakes, originating from thawing of ice-rich permafrost and are in different stages of their development. They constitute the typical and culturally important alas (from yakut 'alaas') landscape of Central Yakutia, with an alas being the latest development stage of these thaw lakes (Bosikov 1991). In Central Yakutia, an alas is a grass-covered depression within a mostly forest-covered region, featuring gentle slopes, and a lake at the deeper part of the basin, and as a typical setting. The traditional use of those alases and alas lakes as freshwater source and for agriculture (hay-making, herding), fishing, recreation, as well as settlement purposes (Crate et al. 2017) constitutes one important reason for exploring thermokarst lakes and their past and potential future trajectories within a rapidly warming climate.

Furthermore, fieldwork at these multiple lake sites aimed at creating a catalogue of data for a variety of research purposes: Unoccupied Aerial Vehicles (UAVs, commonly referred to as drones) based multi-spectral imagery for the characterization of the lake shore and surrounding; water chemistry for the analysis of the

lake water and ecological lake conditions; sediment cores for the reconstruction of long-term environmental, climatic, and fire-related changes; water plants for an inventory of water plant species distributions, among many others. Additionally, sampling protocols were planned to be repeated in future expeditions to those sites in order to monitor changes within lake systems over time. Sites from this expedition should be used within an eastern Siberian transect of research sites, from western Yakutia to Chuktoka, covering the full extent of high-latitude lakes in dense evergreen to mixed to deciduous larch forest towards the treeline formed by *Larix* and beyond to the treeless tundra regions north of the treeline, along a South to North temperature and also a West to East precipitation gradient.

Figure 3.3.1: *Summer 2021, field photo of the 'lake team' responsible for obtaining data from lakes (from left to right): Ulrike Herzschuh (bottom), Aital Egorov, Ramesh Glückler, Izabella Baisheva, Amelie Stieg (bottom), Iris Eder, Evgenii Zakharov. (Photo: Evgenii Zakharov)*

Methods and Fieldwork summary

The field material was collected according to a standardised scheme (Figure 3.3.2), involving sampling of water in different depths, lake surface sediment sampling, lake sediment short core retrieval, and the assessment of the vegetation around the lake and in the close vicinity of the lake, including UAV acquisitions.

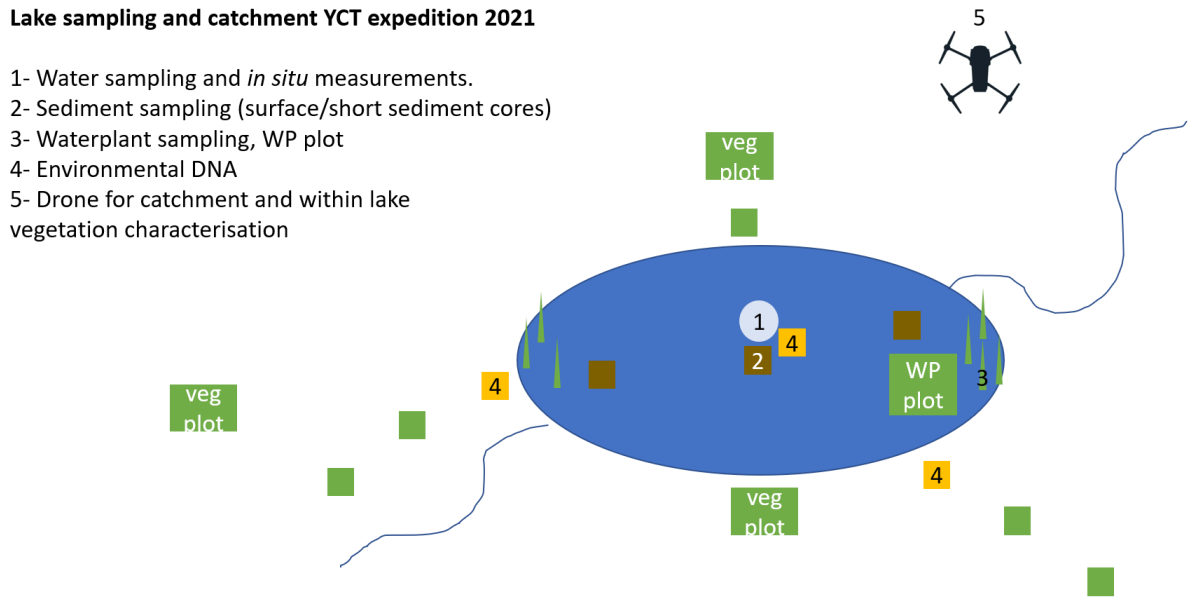

Figure 3.3.2: *Fieldwork scheme for lake inventories on expeditions in Siberia (after Kathleen Stoof-Leichsenring)*

Short sediment cores

At 56 lakes, sediment cores were obtained from the deepest part of the lakes. After estimating the lake's bathymetry with point measurements from a Hondex PS-7 ultrasonic depth sounder, the rubber boat was anchored at the designated coring location. Sediment cores were retrieved using UWITEC gravity corers with PVC tubes. Depending on the lake basin setting, a hammer modification was used to push the tubes deeper into the sediment. Most sediment cores were taken in tubes of 90 mm in diameter, although for some, the 60 mm corer was used. Sediment cores were concealed with caps on the boat and then transported back to the campsite in an upright position, taking care not to disturb the sediment. Depending on lake setting and capacity, multiple sediment cores were taken at each lake, resulting in 126 cores which add up to a total of 54.2 m. On average, the sediment cores are 40 cm in length, but can reach up to around 1.6 m. Each sediment core is named according to the lake ID (EN214XX-X), with an additional indication of the number of each core from an individual lake (-X) and, if applicable, the depth of a core segment (since some of the longer cores had to be separated into two smaller segments for transportation).

From 12 lakes, one sediment core was already subsampled in the field. The sediment was carefully pushed out of the tube in increments of 0.5 or 1.0 cm, sliced off, and separated into different *Whirl-Pak®* bags (58 and 118 ml) for later use in either lead-cesium age dating or proxy analyses. The subsampling scheme varied depending on the sediment core and sometimes included biomarker samples in 40 ml glass bottles. Subsampling tools were cleaned with DNAexitus, water, and, when subsampling for biomarkers, ethanol. All other sediment cores were prepared for safe transport by draining excess water and cutting the PVC tube above the sediment surface, then adding absorbent foam pieces to prevent the sediment from moving inside the tube. After sealing the cores they were ready for transport in a horizontal position (Figure 3.3.3).

Figure 3.3.3: *Left: Fieldwork at lake EN21406, in the Verkhoyansk mountain region. On the left boat: Amelie Stieg and Ulrike Herzschuh, on the right boat: Evgenii Zakharov. Right: Packed short sediment cores in Yakutsk, before shipping to Potsdam. (Photos: Ramesh Glückler)*

Lake surface sediment

From 66 lakes, surface sediment was obtained using a HYDRO-BIOS sediment grabber (Figure 3.3.4). While on the boat, the surface sediment was separated in various vessels for different analyses: a DNA sample (to provide best conditions for sedimentary DNA analyses) into 250 ml Nalgene bottles, biomarker samples were obtained using metal spoons into 250 ml annealed glasses and diatom samples, a backup sample, and an additional larger quantity for the study of benthic organisms were put and stored in *Whirl-Pak®* bags.

Figure 3.3.4: *Izabella Baisheva obtaining surface sediment with the sediment grabber at lake EN21448 in the Central Yakutian Lowland. (Photo: Ramesh Glückler)*

Water samples

Water from 66 lakes was sampled at different depths: surface water (SW) was sampled from the boat (Figure 3.3.5), in case the lake was deep enough, also bottom water (BW) was sampled with an UWITEC water sampler. Physical parameters of the lakes were directly measured using a Multi-340i device for electrical conductivity (EC), and pH directly on the boat for the lakes in the Verkhoyansk mountain range, and for lowland lakes measurements were done at the camp field laboratory (Figure 3.3.5).

The planned analyses of the water samples will target hydrochemical, biological, isotopic and genetic applications. Hydrochemical analysis will be carried out for cations, anions, isotopes, Dissolved Organic Carbon (DOC), and coloured Dissolved Organic Matter (cDOM). Biogeochemical and biological analyses will be carried out for the nutrients, chlorophyll-a (Chl-a), phytoplankton, and zooplankton. Analyses of environmental DNA will be carried out with suspended matter filter material, phytoplankton and zooplankton DNA samples. Each sample was named according to the lake ID, sampling purpose (for which analyses) and with the code for surface water, SW or bottom water, BW (EN21-4XX-parameter-XX).
Water for isotopes was directly sampled from the lake, into 30 ml narrow mouth bottles avoiding any bubbles of air. For anions and cations water was filtered through 0.45 μm pore-size pre-syringe cellulose-acetate filters into 8 ml wide mouth bottles (anions), and 15 ml falcon tubes (cations) and for conservation of cations, 65% HNO_3 was added. Water samples for DOC and cDOM were filtered through 0.7 μm pore-size glass fibre (GF/F) filters. For conservation of DOC samples, 30% HCl was added, cDOM samples were not allowed to be acidified and the filtrate was stored in dark glass bottles and protected from light and heat. Water for nutrients was sampled into 50 ml falcon tubes after rinsing tubes with the lake water. These samples could be frozen during the Central Yakutian Lowland part of the expedition. Chlorophyll (Chl-a) filter preparation required filtering of homogenised (shaken) 1 l of water through 0.7 μm pore-size GFF filter, at the camp laboratory. But most of the lowland lakes contained a lot of particulates, so filters were clogged out after filtering 300 ml of water. The filtering procedure was adapted accordingly: the full sample was homogenised and filtering started with smaller volumes of subsamples. The Chl-a-filters were then folded twice, wrapped into aluminium foil, put into *Whirl-Pak®* bags, and frozen. Phytoplankton and zooplankton sampling was undertaken at the lake, filtering 10 to 40 l of water through special nets and filled in separately in 30 ml wide mouth bottles.
The preparation of samples for the genetic analyses required 250 ml water pumped through a special filter funnel, connected with the adapter on the flask. The sample filters with 0.45 μm pore-size were kept in 8 ml tubes with added QTB buffer (Qiagen equilibrium buffer) for better conservation. Phyto- and zooplankton DNA samples were also conserved with QTB buffer. All genetic samples were frozen.

Figure 3.3.5: *Izabella Baisheva and Iris Eder obtaining water and water plant samples at lake EN21426 (left) and processing them in the camp (right). (Photos: Ramesh Glückler)*

At selected lakes, water samples were taken to analyse δ^{13} C of Dissolved Inorganic Carbon (DIC). For this purpose, prepared glass vials, called *EXETAINER®* vials, were brought from Germany. These *EXETAINER®* were vacuumed, flushed with helium and closed with parafilm in the Isotope-Laboratory at AWI Potsdam. In the camp, 4 ml of the water sample was filled into an *EXETAINER®* vial without air bubbles, using a syringe (Figure 3.3.6). Then 1 ml of H_3PO_4 acid was added to the water sample. In addition to the samples, four vials were filled with H_3PO_4 acid only as a blank to calibrate the samples when measured at the laboratory in Germany. Blanks were prepared at the beginning of the expedition, one halfway through and at the end. Filled *EXETAINER®* were closed with parafilm, stored in styrofoam boxes and stored cool whenever possible.

Figure 3.3.6: *Injecting water sample of lake EN21443 into prepared EXETAINER® vial. (Photo: Amelie Stieg*

Macrophytes

Water plant sampling included several steps. First, assessing the percentage of macrophyte coverage at the lake, then estimating the water depth and the macrophyte plant coverage within a 50 x 50 cm macrophyte plot. Biomass of the 50 x 50 cm plots was harvested and the wet weight measured. Each water plant was also sampled for the herbarium and later dried (Figure 3.3.7). For each herbarium macrophyte samples were prepared for DNA analyses (Figure 3.3.7). Sampling of epiphytes from water plants was undertaken by scraping leaves with a sterile spoon into a *Whirl-Pak®* and conserved with QTB buffer.

Figure 3.3.7: *Water plant herbarium and genetic sample preparation at a camp laboratory. e.g. EN21426-WP1. (Photo: Izabella Baisheva)*

Vegetation plots in the lakeshore area

The projective ground vegetation cover of vegetation plots in the lake shore area was estimated as a percentage within 2 x 2 m plots. The location of the plots was selected directly on site at the lake. Some of the vegetation plots were located directly on the lake shore in the transition to the water, others were chosen near the lakeshore, for example in meadows or in shrub areas close to the lake. The number of plots depended on the different land cover classes, with more plots selected if the vegetation cover was more heterogeneous. The plot size of 2 x 2 m was defined and an overview photo of the plot was taken, the coordinates were recorded and the plot was assigned a corresponding name. If the plot was in the vegetation team's transect, the plot was assigned a corresponding number (EN212XX). Otherwise, the plot was named according to the lake ID (EN214XX). The vegetation cover was estimated for each taxon within the plot. Specimens were collected at least once per taxon during the entire expedition for the preparation of a herbarium and for DNA analyses.

In addition, biomass samples were taken at selected lakes close to a vegetation plot. An area of 50 x 50 cm was defined for the biomass sampling (Figure 3.3.8). A photo of the plot was taken and the vegetation cover was estimated also as a percentage. Then, the biomass of each individual taxon was harvested and the corresponding fresh weight was recorded. In case of a large volume or weight of the sample, a subsample was taken and the proportional weight recorded. The samples were dried with silica after harvesting.

Figure 3.3.8: *Biomass plot 50 x 50 cm at the lake shore area of lake EN21431 (left), soil profile close to the biomass plot at lake EN21431 (right).(Photos: Amelie Stieg)*

Soil profiles in the lakeshore area

Soil profiles were dug at selected lakes within the lakeshore area, mostly located next to the biomass plot (Figure 3.3.8). Before excavating the pit, a DNA surface sample was taken by inserting a soil corer including a Sarstedt tube vertically into the soil. The depth of the active layer was determined using a metal rod. The depth of the profile varied depending on the nature of the subsoil and the number of soil horizons. Attempts were always made to reach the mineral horizon. In some cases, the depth was limited by permafrost. Whenever possible three basic horizons were defined: litter horizon (L), organic horizon (O) and mineral horizon (M). The thickness of each horizon was measured, as well as the temperature and moisture content. The L-horizon was mostly very shallow and therefore often not sampled. From the other horizons, three different types of samples were taken in each case: a cylinder sample (C) taken with a steel cylinder with a specific volume of 100 cm^3, if the cylinder was not completely filled up

the missing volume was noted; a plate sample (P) roughly 2 cm thick originating from the middle of the horizon and a biomarker sample (BM) which was wrapped in aluminium foil directly after sampling. The fresh weight of each sample was determined and the samples were tried to be kept cool whenever possible.

Drone Imagery
Multispectral drone images were acquired to analyse the vegetation along the shore and to record the current shoreline (Figure 3.3.9). The image acquisitions were carried out by using a "DJI Phantom RTK P4 Multispectral" drone in combination with a "D-RTK Station" (antenna). Either a predefined waypoint route along the lake was flown, created with the app "DJI GS Pro", or it was flown manually. In both cases, the images were taken vertically from above (gimbal -90°), the flight height ranged between 50–60 m and the speed was set to be 3–4 m/s. The images were taken every 2 seconds to have enough overlap for later image processing. In the optimal case, two parallel lines were flown with a line distance of 20 m along the shore. Some lakes were very large, so only part of the shoreline was photographed. Due to certain weather conditions (rain, strong wind, low light conditions) a flight was not possible at some lakes. In total, there are drone images for 56 of the lakes and for 47 lakes there are usable images that can be further processed into orthomosaics.

Figure 3.3.9: *Amelie Stieg launches a drone flight at lake EN21401 (left), Ramesh Glückler and Aital Egorov obtaining drone imagery of the lake EN21463 (right). (Photos: Stefan Kruse (left), Izabella Baisheva (right))*

Preliminary results

The lakes in the Verkhoyansk mountain ranges differed from the thermokarst lakes in the Central Yakutian Lowland in their morphometric and hydrophysical properties, related to their different lake genesis and setting (Figure 3.3.10, Table A.3.2).

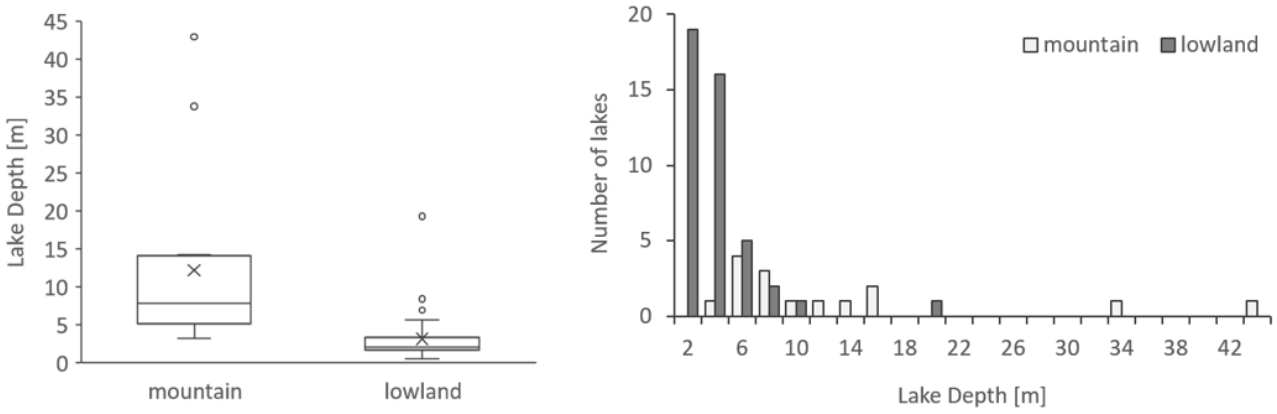

Figure 3.3.10: *Comparison of lake depth between mountain lakes (n=15 including Lake Ulu) and lowland lakes (n=44) (Data Visualisation: Mareike Wieczorek)*

After the transport of all the sampling material to Potsdam, most water analyses were quickly performed in 2021 and sediment surface samples and short cores were partly stored, partly measured and analysed. For the short cores, one sediment core from each lake was cut into two halves under sterile conditions. This allowed us to observe the core's facies, revealing a wide variety of sediment types. Whereas some exhibit fine layering, many cores from lowland lakes resemble dark, organic-rich, peat-like sediments, sometimes pervaded by fine roots. Sediment cores from mountain lakes, on the other hand, seem more likely to feature fine layers and also demonstrate a higher variability in grain size. All 56 opened cores were then photographed and analysed for their elemental composition with an Avaatech XRF (X-ray fluorescence) scanner, creating a large dataset of changes in elemental distributions in each of the lake systems (Figure 3.3.11).

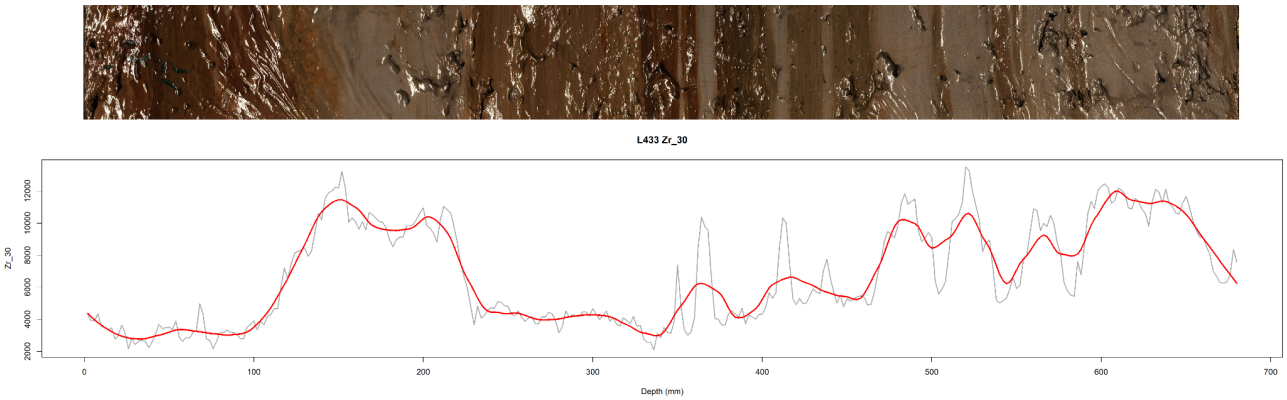

Figure 3.3.11: *Exemplary sediment core linescan (photograph) and parallel preliminary XRF-derived distribution of zirconium (Zr, in counts per second, from measurement at 30 kV) for lake EN21433*

The multispectral drone image data to create high-resolution orthomosaics were processed by Robert Jackisch (TUB) and Luca Farcas (AWI) (Figure 3.3.12 shows an example of lake EN21427). From the orthomosaics, detailed lake perimeters and the lake shoreline can be derived (part of an internship and bachelor thesis project by Jonas Büchner).

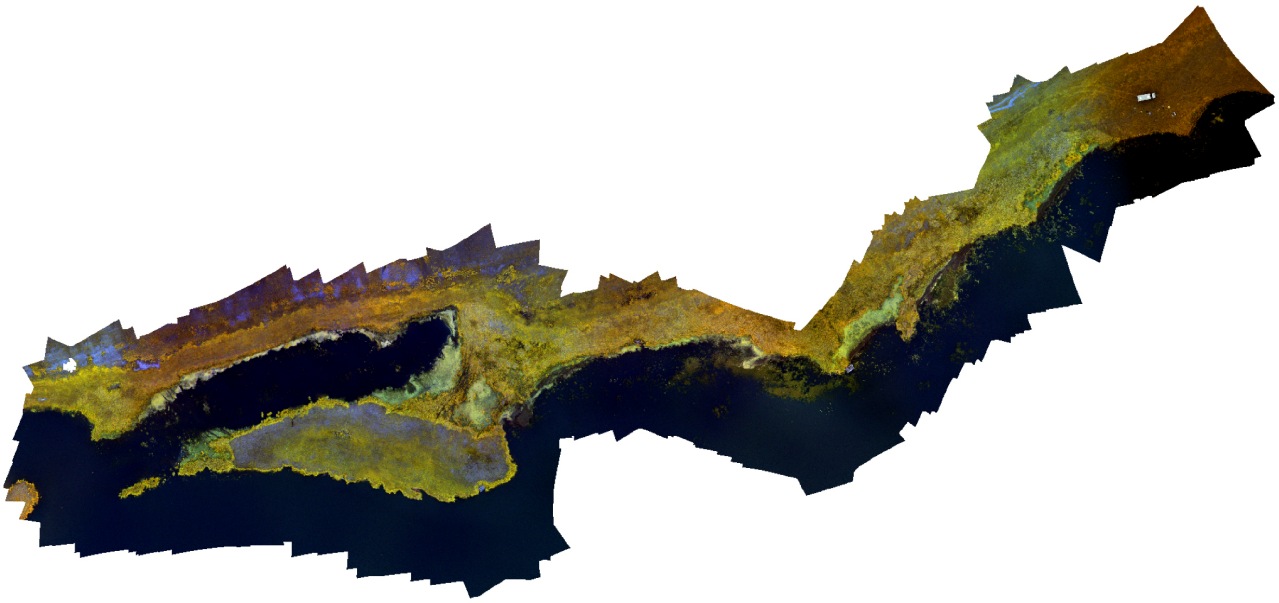

Figure 3.3.12: *Partial RGB orthomosaic of multispectral drone imagery data (shown is lake EN21427). Displayed in Universal Transverse Mercator (UTM) projection on the World Geodetic System Reference Ellipsoid 1984 (WGS84) with geographical coordinates in Decimal Degrees displayed on the latitudinal and latitudinal gridlines*

Also, as part of his internship and bachelor thesis, Jonas Büchner analyses charcoal particles as traces of recent fire activity in the surface sediment samples. So far, samples of 20 individual lakes were examined for charcoal. In these 20 samples, 267 pieces of charcoal were detected (Figure 3.3.13). Further analysis shows that the most frequent charcoal shape (Enache et al. 2007) is elongated (41.6%), followed by angular shapes (19.5%). The rarest are irregular shapes with only six pieces detected among all samples, amounting to a share of (2.3%). The dominance of fragile, elongated particles may hint towards fine fuels which were consumed by low intensity surface fires (Glückler et al. 2021). The highest charcoal concentration was found in lake EN21415 in the Verkhoyansk mountains (26.5 pieces per cm^3) and second highest in lake EN21424, which is located within a recently burned forest east of Churapcha. So far, all other higher charcoal concentrations were also detected in lowland lakes, where more frequent burning would be expected.

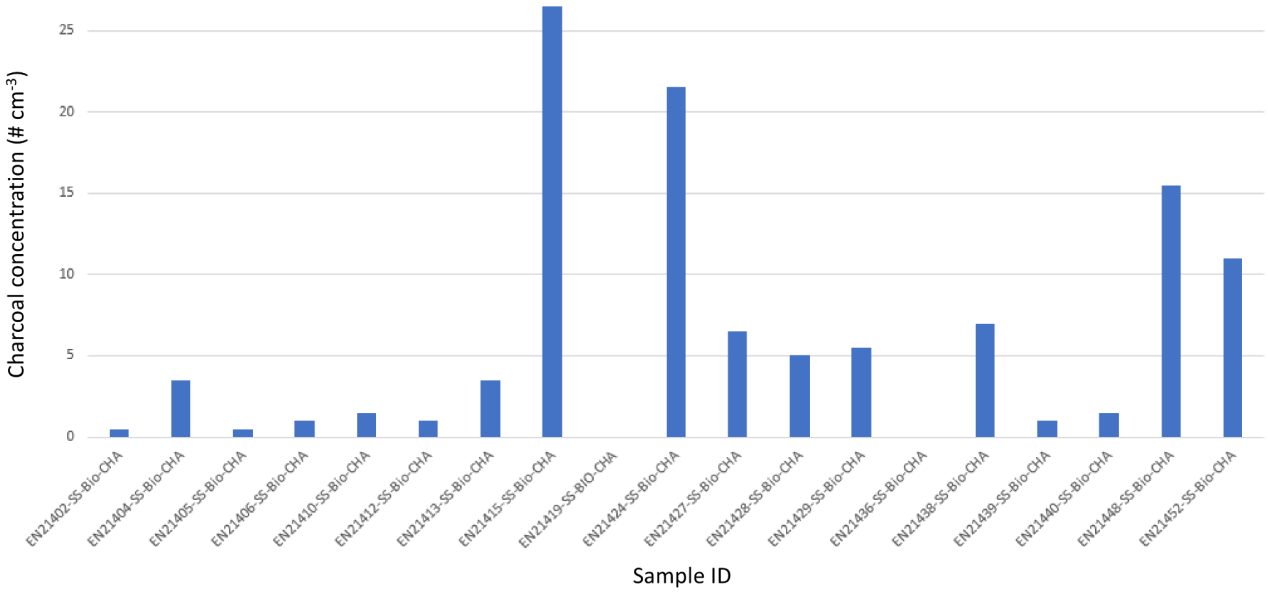

Figure 3.3.13: *Preliminary charcoal concentration from surface sediment samples (part of an internship and bachelor thesis project by Jonas Büchner, Göttingen University). Lake ID is included as part of the sample ID*

3.4 Setting up a baseline for the Yakutian-Chukotkan Monitoring transect: Vegetation plot inventories including vegetation, soil, UAV-surveys and logger installation

Stefan Kruse [1,@], Birgit Heim [1,@], Elisabeth Dietze [1,2,@], Laura Schild [1], Timon Miesner [1,3], Josias Gloy [1], Barbara von Hippel [1], Victor Smirnikov [1], Robert Jackisch [1,3], Alexei Kolmogorov [4], Mareike Wieczorek [1,]*

[1] Alfred Wegener Institute Helmholtz Center for Polar and Marine Research, Potsdam, Germany

[2] now at: University of Göttingen, Göttingen, Germany

[3] Technical University of Berlin, Berlin, Germany

[4] Federal State Autonomous Educational Institution of Higher Education "M. K. Ammosov North-Eastern Federal University", Yakutsk, Russian Federation

[*] not in the field

[@] Corresponding author: birgit.heim@awi.de, edietze@uni-goettingen.de, stefan.kruse@awi.de

Fieldwork period and location

Between 06.08.2021–02.09.2021, a total of 61 vegetation plots were assessed and samples and data obtained with a large variety of different methods and for a wide range of sampling purposes (Table A.3.3). We undertook forest cover and ground vegetation cover inventory as detailed as possible, installed dendrometer sensors on trees for tree growth monitoring, as well as temperature and soil moisture sensors in the forest ground, and, at selected places, we could install time lapse cameras inside the forest plots for environmental monitoring. We also sampled and described the soils and the rhizospheres of the forest plots and the surroundings.

In the first part of the expedition, 19 plots were set up in larch forest and mountain tundra covered mountainous terrain, in the Verkhoyansk mountain range. The selected plots were mostly located up on mountain slopes with different aspects and elevations, on mountain peaks (Figure 3.4.1) and in the wide valleys in the Oymyakon intramontane basin (average elevation around 1100 m a.s.l.).

In the second half of the expedition, the fire and soil specialist Dr. Elisabeth Dietze from AWI could join the expedition and expand on the soil and the geomorphology programme. In this part of the expedition (Figure 3.4.1), 42 vegetation plots were set up in the eastern extent of the Central Yakutian Lowland (average elevation around 200 m a.s.l.), 12 plots were assessed from the 'camp Churapcha' with eight larch forest plots installed in the Churapchinsky District, and four plots further to the East in the Tattinsky District, close to a massive fire event in July 2022 that had burnt an extensively large area. 13 plots were installed in the Western part of the Eastern Central Yakutian lowland with the 'camp Tyungyulyu' as the base, including mixed forest plots close to the River Lena in evergreen dominated forest stands. 17 plots were established in the region of the permafrost long term monitoring station 'Yukechi', assessed from the 'camp Mayya'. These plots in the Western part of the eastern Central Yakutian lowland are all located in the Megino-Kangalassky District.

Always including the sites of the forest plots, large forest areas were mapped in each region, using a suite of optical passive and active sensors: UAV multispectral imagery, UAV lidar, UAV albedo on far-reaching drones.

Objectives

The Siberian larch forest is located in extreme high-latitude environments and grows on permafrost. *Larix* exceeds all other tree species in the ability to grow on cold and frozen soils. Still it is not understood how its geographical distribution and functions are determined by elevation, topography, thermo-hydrological and fire dynamics and what will be future developments under a warming climate. Degradation of the near-surface permafrost, drying of the upper soil layers and higher intensity and frequency of wildfires may severely affect the high latitude *Larix* forest ecosystem and its functionalities. It is an open question as to how *Larix* forests, once established, hinder their replacement by evergreen forests. This self-stabilisation most likely results from the unique interactions between vegetation, fire, permafrost, and climate (Herzschuh 2020, Herzschuh

2016). However, vegetation modelling evidence suggests that feedbacks only provide weak protection for *Larix* forests against evergreen forest taxa invasion. The inference of feedbacks is strongly dependent on the processes that are incorporated and their parameterisation, requiring a much broader empirical base than is currently available for northern Asia. Therefore, we aim to quantify the feedbacks in the coupled high-latitude forest-fire-permafrost-climate system along broad environmental gradients (Kruse et al. 2020, Kruse et al. 2019a,Kruse et al. 2018, Kruse et al. 2016b).
Similar to the 2018 expeditions to Chukotka and Central Yakutia (Kruse et al. 2019b), we aimed at assessing the full aboveground biomass as well as belowground carbon stocks by taking biomass samples from individual trees and shrubs, the surface vegetation and soil samples. Furthermore, we extended UAV-based mapping for the assessment of the 3D-structure of forests for upscaling plot information on larger areas. Mapping data of the forest areas from optical passive and active sensors on drones will allow us to capture optical multispectral orthomosaics, including thermal images and high-resolution 3D point clouds to assess biophysical parameters linked to vegetation state, structure and surface morphology.

Figure 3.4.1: *The vegetation team on top of a mountain in the Verkhoyansk mountain region in August 2022 (left) and at the final expedition dinner in Yakutsk, September 2022 (right). (Stefan Kruse, Birgit Heim, Elisabeth Dietze, Laura Schild, Timon Miesner, Josias Gloy, Barbara von Hippel, Victor Smirnikov, Robert Jackisch, Alexei Kolmogorov*

Methods and Fieldwork summary

Forest plots

We defined the approximate site locations for establishing plots prior to field work, based on Landsat satellite Normalized Difference Vegetation Index (NDVI) trend analyses where we selected regions of change versus no change, and plots within a wide range of NDVI, including checking the selection with a high spatial resolution ESRI satellite background image. The aim was to cover a broad range of representative boreal vegetation types. When arriving at the site location, we defined a plot centre, so that the surrounding minimum of 15 m in all directions would represent a homogeneous vegetation type (Figure 3.4.2). (In one case with a very dense young forest, we chose a smaller plot size). It is important to note that we choose the plot centre to be representative for the wider surrounding, as we dug the soil plots and harvested for tree and ground vegetation biomass outside of the 15 m radius forest plots, to keep the selected forest plots without long term destruction.

Figure 3.4.2: *Left: Example of the 15 m radius layout for a forest plot, here well visible as this was an intensively burnt forest site with all ground vegetation destroyed. Birgit Heim in the plot documenting the microtopography of the intensively burned plot. Right: Example of the 15 m radius layout for a forest plot affected by ground fire: Betula trees show heat-dried brown leaves only - larch trees mostly kept their green needles. (Photos: Stefan Kruse)*

Estimations of projective crown cover and canopy height were made for every species present on the plot. For every tree species, up to 10 individuals were chosen for detailed inventory, and marked with letter cards that would allow us to identify the tree on drone images. The trees were chosen to represent the entire range of height, diameter and vitality present on the plot. The measurements taken for these trees include height, diameter at base (Figure 3.4.3), diameter at breast height, height of crown base, crown diameter and number of cones. A tree core was drilled and taken for every tree that was wide enough to likely survive the procedure, and a sample for genetic analysis was taken from needles/leaves or bark cambium.
Finally, for all trees ($>$ 40 cm) on the plot, i.e. within 15 m of the plot center, we recorded species and height, which was estimated based on the height of the previously measured trees.
Leaf Area Index LAI measurements could be performed within the plots if the illumination conditions were suitable, using a LICOR LAI 2200-C sensor with an unshaded reference measurement outside forest on clearings. Dendrometer sensors for tree growth measurements were installed at selected trees inside the forest plots (Figure 3.4.4), also at selected plots we installed Time Lapse Cameras for long-term monitoring. Outside of the plot, we chose between three and five individuals of every tree and shrub species on the plot, and felled them to take samples for biomass estimation: Three stem disks from different heights and branch samples, along with estimations regarding how often branches of similar size occur in the tree, will allow us to calculate the tree biomass (Figure 3.4.3).

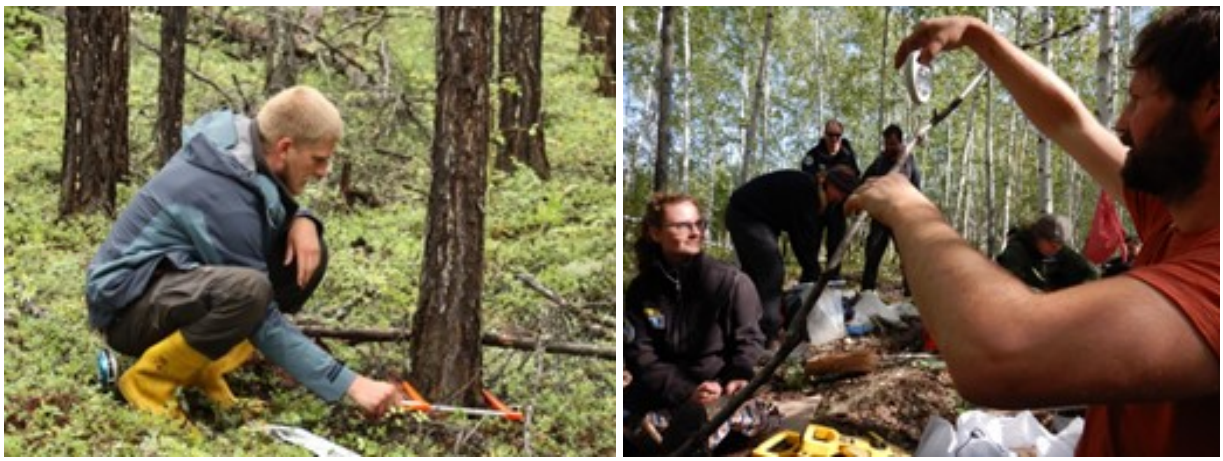

Figure 3.4.3: *Left: Timon Miesner measuring tree basal diameter inside the 15 m radius forest plot. Right: Laura Schild and Stefan Kruse weighting, subsampling and labelling tree biomass samples outside, but close and representative to the selected 15 m radius forest plot. (In background: Barbara von Hippel, Josias Gloy, Robert Jackisch, Elisabeth Dietze). (Photo: Birgit Heim)*

Figure 3.4.4: *Alexei Kolmogorov installing a dendrometer sensor for tree growth measurements on an old larch at a plot in the Verkhoyansk mountain region. (Photo: Stefan Kruse)*

Ground Vegetation

The ground vegetation cover inside the 15 m radius forest plots was assessed according to the following scheme described in (Figure 3.4.5). Care was always taken not to damage the ground vegetation cover of the plots and work as carefully as possible and with as few people as possible inside the plot. First, surface pollen samples were always taken in the centre of the main plot. The projective vegetation cover around the plot centre was recorded in rings of 50 cm width and up to 2 m from the plot centre. The ground vegetation of the selected forest plot was inspected and, depending on the heterogeneity of the overall ground vegetation, divided into subplot categories. If the ground cover was homogenous, only one ground vegetation cover subtype was determined. If the ground vegetation cover was more heterogeneous, a second ground vegetation cover type was established, in case of higher heterogeneity in some cases, also a third ground cover vegetation type was determined. The case that the ground vegetation cover was

homogenous was the standard (VA only). In case of more ground vegetation subtypes represented e.g. dry and moist endmembers and in few cases up to three rather homogeneous vegetation subtypes (namely VA, VB and VC) were obvious. The ground vegetation projective cover in percent was estimated for each of the vegetation subplots on the 15 m radius main plot. To do so, four subplots (2 x 2 m) per vegetation type (the selected VA in case of one homogenous representative vegetation type, or VB and VC with more vegetation types, accordingly) were placed inside and outside of the main plot (Figure 3.4.5). As described before, depending on the heterogeneity of the ground vegetation cover, specimens up to 40 cm in height were included in the assessment of projective cover. The cover of taxa in the moss layer was estimated separately. Specimens of all taxa were collected at least once on each main plot for the preparation of a Herbarium, as well as for samples for genetic analyses. All subplots as well as the plot centre were photographed for documentation.
Additionally, above ground biomass (AGB) was harvested in the subplots outside of the main plot (named VAx, VBx and VCx accordingly) (Figure 3.4.6). This was done on a 50 x 50 cm partition in the 2 x 2 m subplots. Biomass was separated by Taxon and its fresh weight measured in the field using field scales.

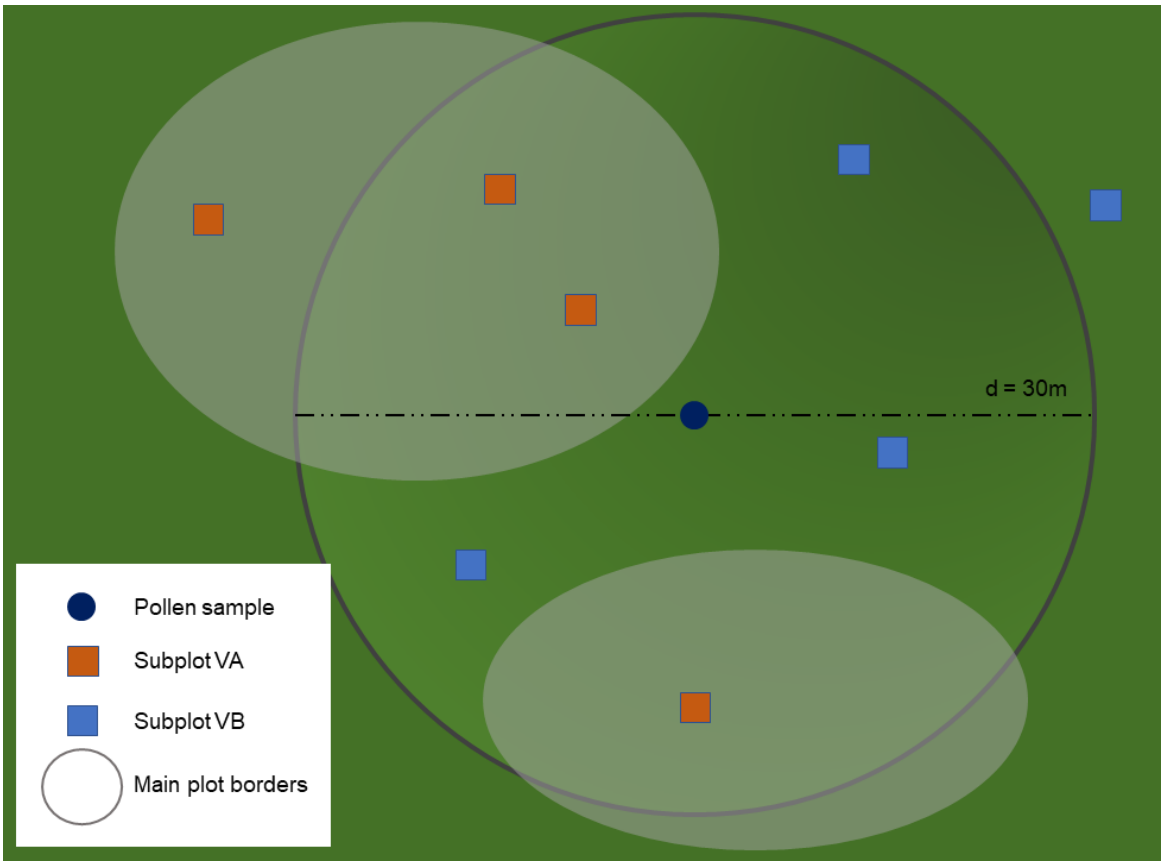

Figure 3.4.5: *Example 15 m radius main plot with the pollen sample in the centre of the forest plot. In this case, two ground cover vegetation subtypes 'VA' (red colours) and 'VB' (blue colours) were determined and accordingly, six subplots inside and two subplots outside the 15 m radius main plot*

Figure 3.4.6: *Sampling of ground vegetation biomass (Laura Schild and Josias Gloy) at the subplots together with the soil pit digging and soil sampling (Barbara von Hippel, Elisabeth Dietze)*

Rhizospheres

Outside of the 15 m-radius plots, the rhizosphere of selected plant taxa, namely *Larix*, *Vaccinium*, *Betula*, *Salix*, *Pinus*, and *Picea* was sampled when present (Figure 3.4.7). We collected leaves/needles, root tips and rhizosphere soil as well as bulk soil. Nitrile gloves were worn and sprayed with ethanol before sampling and in between sampling of different species to avoid contamination. The samples were kept cool in the field and were frozen when returning to the camp when it was possible.

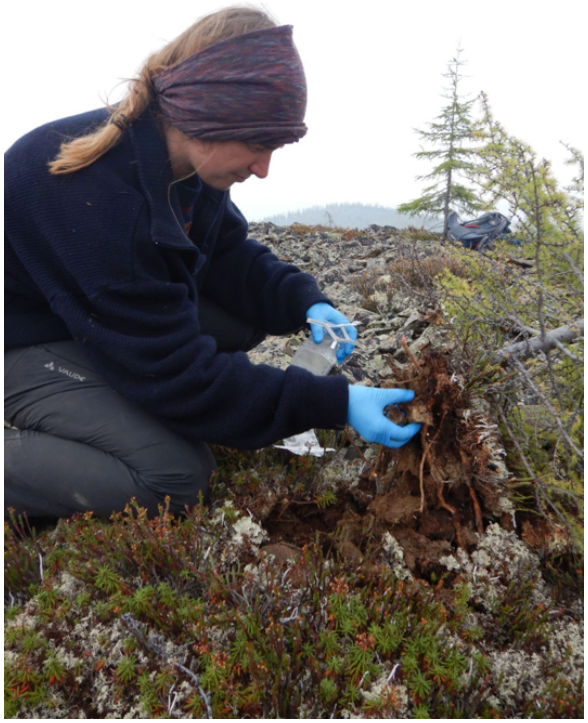

Figure 3.4.7: *Rhizosphere sampling close to forest plots (Barbara von Hippel), in this case Larix rhizospheres, in the mountain region. (Photo: Timon Miesner)*

Soils

To assess the soil conditions that are characteristic to the vegetation, soil profiles were dug for each occurring ground cover vegetation subtype (“VA”, “VB”, “VC”) of the specific forest plots. The soil pits were excavated down to at least 50 cm or to the top of permafrost. In the Verkhoyansk mountain region the active layer depth at the time of the soil profile digging was very shallow, mostly between 20 and 30 cm. In contrast, in the mostly sandy soils that we encountered in the Yakutian lowlands, the active layer depth in August 2021 was mostly deeper than 120 cm and digging the soil profile the permafrost table could mostly not be reached anymore, except for a few sites. Like this, however, conditions were optimal to take good soil cores in the Central Yakutian lowlands (Figure 3.4.8).

Figure 3.4.8: *Soil core sampling close to forest plots (Elisbath Dietze) (Photo: Timon Miesner)*

After excavating the soil profile, we first described the soils, including the thickness of each horizon, soil colour and soil characteristics and a photo was taken. A minimum of three horizon types were defined: the litter horizon (L), organic horizon (O) and mineral horizon (M). Sometimes more than one organic layer occurred in the soil profile and we defined O1, O2, M1, M2, accordingly. Before sampling, the electrical conductivity (EC) as well as the temperature and water content were measured, often in high resolution down the profile using a W.E.T. sensor kit. All horizons were sampled after the following scheme, illustrated in (Figure 3.4.9). First, a biomarker sample (BM) was sampled with gloves and a sterile knife and wrapped in aluminum foil, then a volumetric sample called “cylinder” with a steel case of a volume of 100 cm^3 was sampled (C) and a bulk sample called “plate” (P), which can be used for any other analysis not requiring a defined volume or sterile treatment. All samples were weighted with their fresh weight in the field or in the camp.

Next to the soil pit, the litter horizon and/or top soil was sampled in a sterile tube for environmental DNA analyses. Seven soil cores were retrieved in plastic liners (9 cm diameter) from few sites of different post-fire ages for infiltration experiments. In total, 77 soil pits associated with the vegetation plots were sampled for c. 280° C, P and BM samples, respectively, and 81 DNA samples (Figure 3.4.6).

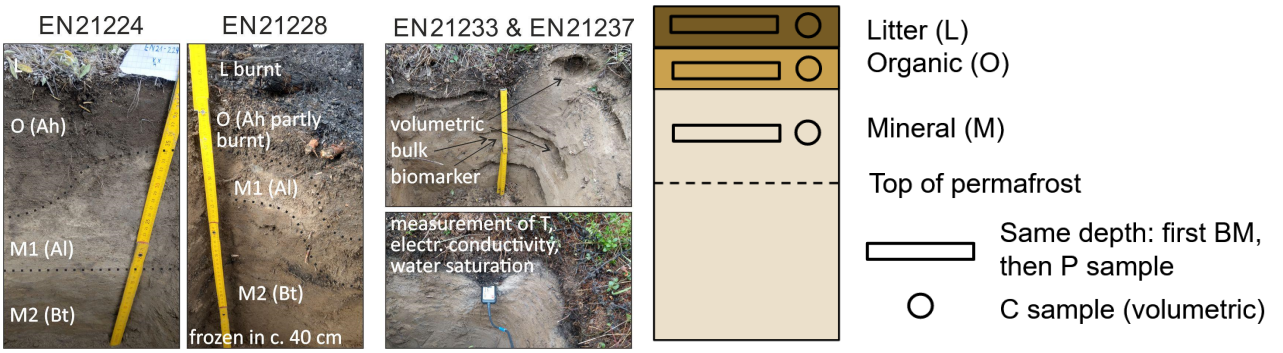

Figure 3.4.9: *Examples of soil profiles illustrating left: the stratigraphic naming convention (analogue soil horizons according to German soil classification) for the EN21224 alas site and EN21228 a larch forest that burnt in summer 2021). Centre: examples for type of sampling (after samples were taken, see text) and soil physical measurements. Right: schematic sampling scheme for biomarker (BM), bulk (P) and cylinder (C) samples*

In addition, we installed temperature and moisture loggers in a majority of the soil profiles and inserted nutrient bags between the horizon boundaries to assess the weathering processes connected to this region and land surface and lithology.

UAV-based mapping of forest

For the drone-based land surface mapping, predominantly of forests, we employed a "DJI M300 RTK" drone, equipped with the Real-Time Kinematic (RTK) module and the corresponding mobile D-RTK antenna (Figure 3.4.10). The drone served as a sensor platform for acquisitions using i) a multispectral MicaSense Altum camera and ii) a light-detection-and-ranging (LiDAR) YellowScan Mapper scanner. The M300 drone has a flight endurance of up to 55 minutes (no payload) and a payload capacity of 2.7 kg which results in realistic flight times of about 30 minutes and the capacity to autonomously map areas of several hectares per flight in high spatial density and resolution. The remote controller "DJI Smart controller enterprise" allowed mission planning and flight trajectory adjustments in the field. We planned the majority of UAV surveys prior to the expedition with adjustments directly on site. Due to flight safety reasons we restricted flight path design to visual line of sight, and with an additional spotter aid in dense forests. In total, we acquired around 170 high-quality UAV surveys for LiDAR and multispectral, each encompassing a total surface area of ~ 151 km². A standard flight transect was planned to cover at least 500 x 100 m, but often we covered 500 x 200 m depending on the local terrain.

Figure 3.4.10: *In the foreground: Josias Gloy and Robert Jackisch operating the DJI M300 RTK (equipped for this acquisition flight with the YellowScan Mapper Lidar) for take off and a mapping flight. In the background: Yakutia 2021 expedition members protocolling. (Photos: Birgit Heim)*

For UAV multispectral imaging, we employed the “MicaSense Altum” multispectral camera (Figure 3.4.11a) including a downwelling light sensor (DLS2) which also works as the GPS georeferencer for multispectral images. With five channels in the visible to near-infrared (475 nm, 560 nm, 668 nm, 717 nm, 842 nm) at 2064 x 1544 pixels and with one additional thermal channel (8–14 μm, 160 x 120 pixels), the camera provides an exceptionally high spatial and a radiometric resolution of 12 bit in RAW format. We calibrated the raw images to reflectance using the advanced “MicaSense downwelling light sensor version 2” (DLS2), that captures ambient illumination and approximates the sun angle. This method is especially useful during changing overcast conditions. Additionally, the illumination conditions were captured using the MicaSense Altum for pre- and post flight with a calibrated reference panel coated with a lambertian material that ensures stable reflectance between 400–850 nm (Figure 3.4.11c).
For UAV LiDAR measurements we used a “YellowScan Mapper” laser scanner which is attached through the DJI Skyport and features an integrated GNSS antenna (Figure 3.4.11b) on top of the M300 drone. Additionally a separate GNSS base station was required to operate in synchronicity with each LiDAR survey in a distance under 30 km in order to perform the necessary Post-Processed Kinematic (PPK) corrections. The laser operates at 905 nm with a 240 kHz pulse frequency and registers two echos in a 81.7° field of view. Resulting vegetation point clouds provide a point density of 500–1500 points/m^3.

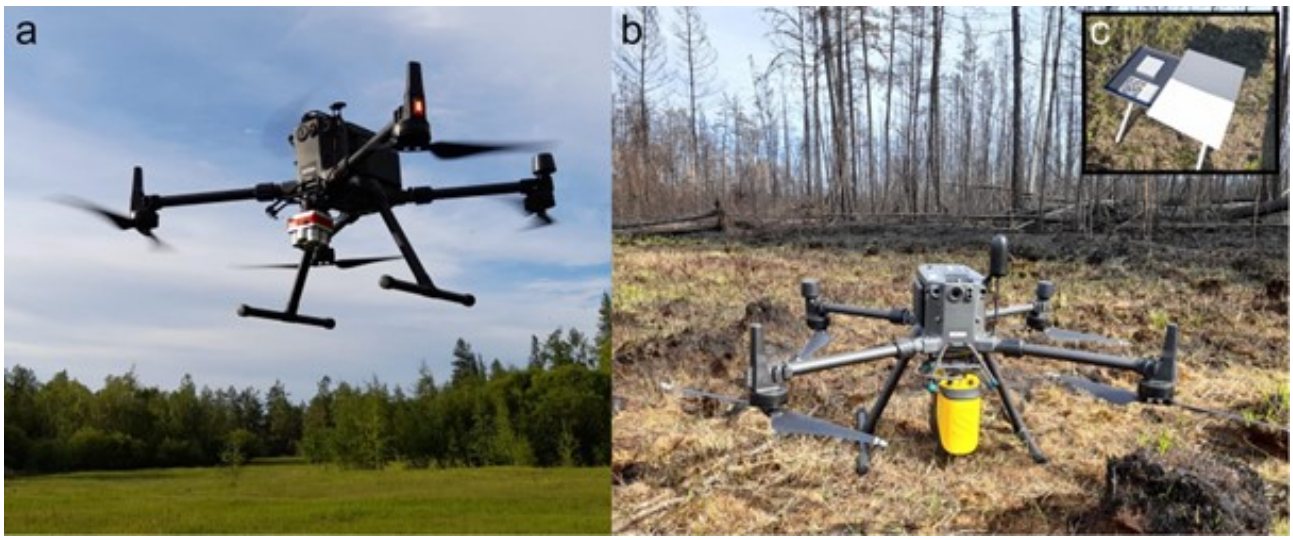

Figure 3.4.11: *Photographs of different UAV survey setups (a) Multispectral camera MicaSense Altum (b) LiDAR scanner YellowScan Mapper (c) Reference ground panel during UAV multispectral survey (Photos: Robert Jackisch)*

Our principal flight settings were based on previous UAV campaign experience by the operators and manufacturer's recommendations. Our UAV LiDAR survey speed was 10 m/s with an altitude of 60-80 m above ground level (agl), and with exceptional altitudes of 100 m agl to ensure sufficient distance between ground obstacles (e.g. vegetation canopy, hilltops). We decided for a LiDAR line overlap of 40–60% per survey that results in line distances of 20–40 m, depending on survey altitude. Total flight time per LiDAR survey usually was significantly shorter than for multispectral because of the larger line distance and the higher flight speed. For the multispectral surveys we programmed a side/forward overlap of 75–85% to achieve high Stereo for Motion (SfM) reconstruction quality. Multispectral flight speed was limited to 5 m/s to suppress motion-blur during image acquisition.

Figure 3.4.12: *Photos on left: setup for downwelling measurements of irradiance and PAR (view on both LICOR sensors (pyranometer and quantum sensor) installed 1 m above ground). Right: UAV survey setup for upwelling measurements of irradiance and PAR (view on both LICOR sensors (pyranometer and quantum sensor) attached to the M300) (Photos: Birgit Heim)*

In addition, we experimentally set up UAV albedo acquisitions: we mapped in parallel on the flight lines the upwelling illumination as i) calibrated irradiance and ii) Photosynthetically active radiation (PAR) applying one LICOR Pyranometer, and one LICOR Quantum Sensor. In parallel, we measured downwelling irradiance and PAR on the ground (Figure 3.4.12).

Preliminary results

In the Oymyakon region of the Verkhoyansk mountain range, *Larix* formed an open mountain forest in predominantly pure stands. The shrub *Pinus pumila* occurred at the upper timberline. We encountered open *Larix* forest stands on mountain slopes on stony screes, poor and thinest soils, and on swampy stands on the valley basin floors. Dense ground vegetation occurs in regions with richer soils on gentle slopes. We also encountered post-fire larch thickets characterised by an extremely high tree density. In the Oymyakon mountain region, the active layer in August 2021 was still shallow (only down to 30 to 50 cm depth) and with low temperature, and was frequently characterised by thin, very stony and poor soil layers only.

The Central Yakutian lowland has more favourable climatic and environmental conditions, such as an active layer depth of more than one, sometimes two metres depth in mid to late August 2021. The larch production on forest plots is much higher, with higher and denser forest stands and thicker vegetation understory. Only on the warmer and drier sandy terraces of the Lena River, *Larix* is replaced by Scots pines (*Pinus sylvestris*).

The field assessments revealed that soils are thicker in the lowlands compared to the mountain region, especially at alas grassland sites that typically show high organic matter accumulation. Litter horizons that include the litter of the last year and older fermented and humified organic matter, often also mosses (and lichens especially on the sandy Lena terrace sites), were thicker in older forests with longer time since the last disturbances (e.g. fires) and in depressions. Thicker litter horizons might also coincide with more mature soils, i.e., more intense colouring of soil horizons due to clay and potential iron oxide dislocation, but that needs further investigation. At some sites in the lowlands, a sharp boundary between the O and M horizons and the homogeneity of the O (humic) horizon suggests past agricultural use of some of the forested sites, as has been described from Soviet times. Future laboratory analyses will help to address questions about, for example, below-ground biomass and carbon storage, nutrient composition, weathering and post-fire pyrogenic carbon cycling.

The application of multispectral orthoimages and LiDAR acquisitions is supporting a combined vegetation and 3-D mapping (Figure 3.4.13). Information of multispectral orthoimages can be used for single tree-level analysis, using for example vegetation indices (e.g. NDVI), but has limitations for below-canopy data, especially in dense forests. Here, the active LiDAR pulses can penetrate the dense canopy and retain information of the understorey and ground surface. One relevant LiDAR product for investigation of forest structure is the canopy height model (CHM) and frequency distributions of tree heights potentially revealing different fire succession . The thermal band of the MicaSense camera retains an uncalibrated signal and we did not calibrate for any ground temperature reference during field work. Therefore the thermal information in °C should be interpreted on a qualitative and not absolute basis. Yet also the qualitative information on temperature is highly valuable, as one can, for example, trace coldest temperature in low dense canopies, in this example on degraded thermokarst mounds (baydzharakhs) (Figure 3.4.14).

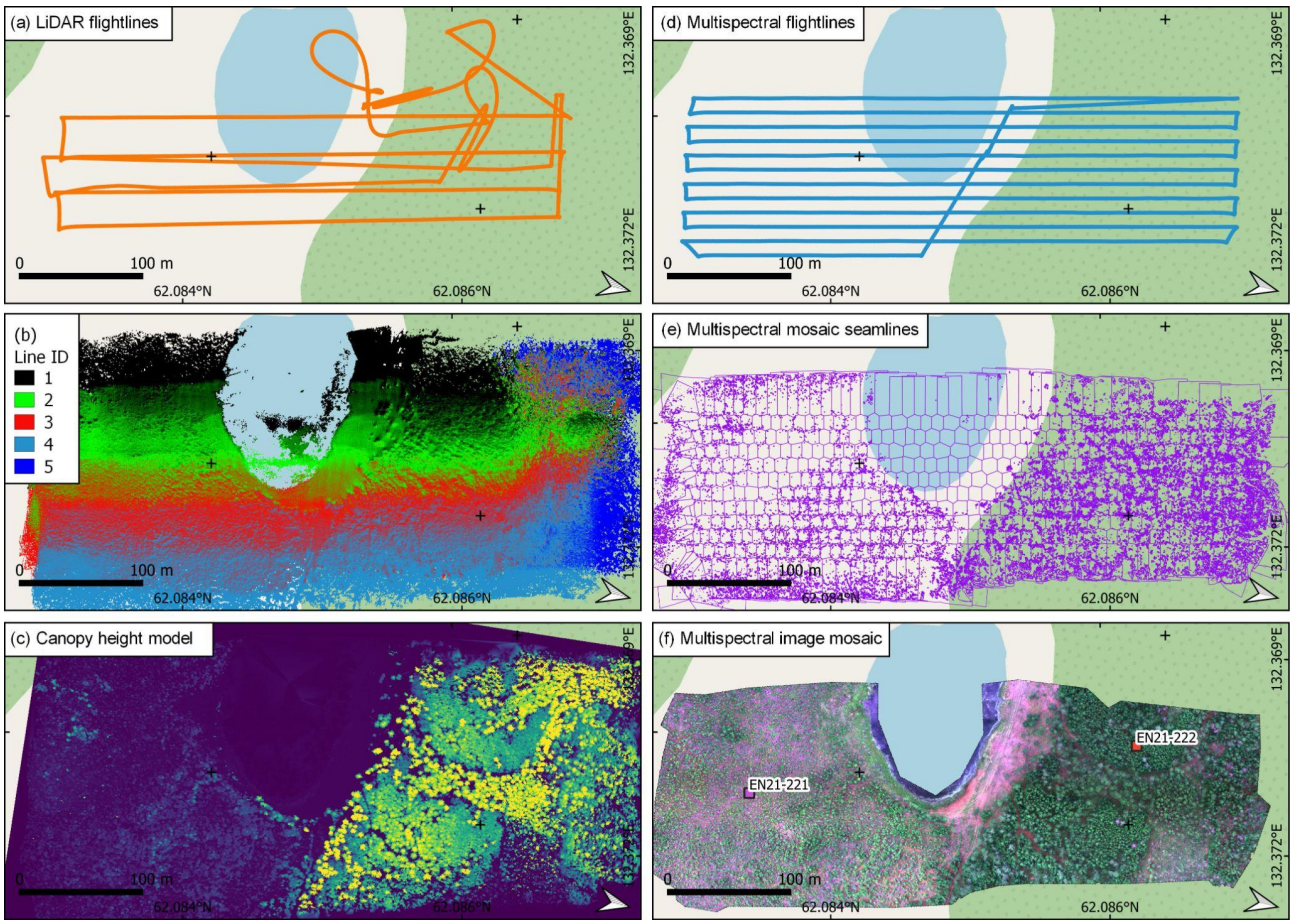

Figure 3.4.13: *Exemplary UAV data acquisition starting from flight lines to data product; Plots EN21-221/222; Acquisition date: 18.08.2021. (a) UAV LiDAR flightlines at 25–30 m distance, (b) LiDAR ground coverage with transect with of ~100 m, (c) LiDAR-based rasterized canopy height model, (d) UAV multispectral flightlines at 10 m distance, (e) Multispectral image mosaic seamlines generated in Agisoft Photoscan, (f) Resulting multispectral image orthomosaic in true-color RGB (camera bands 3, 2, 1) and two GPS points of the enclosed forest plots*

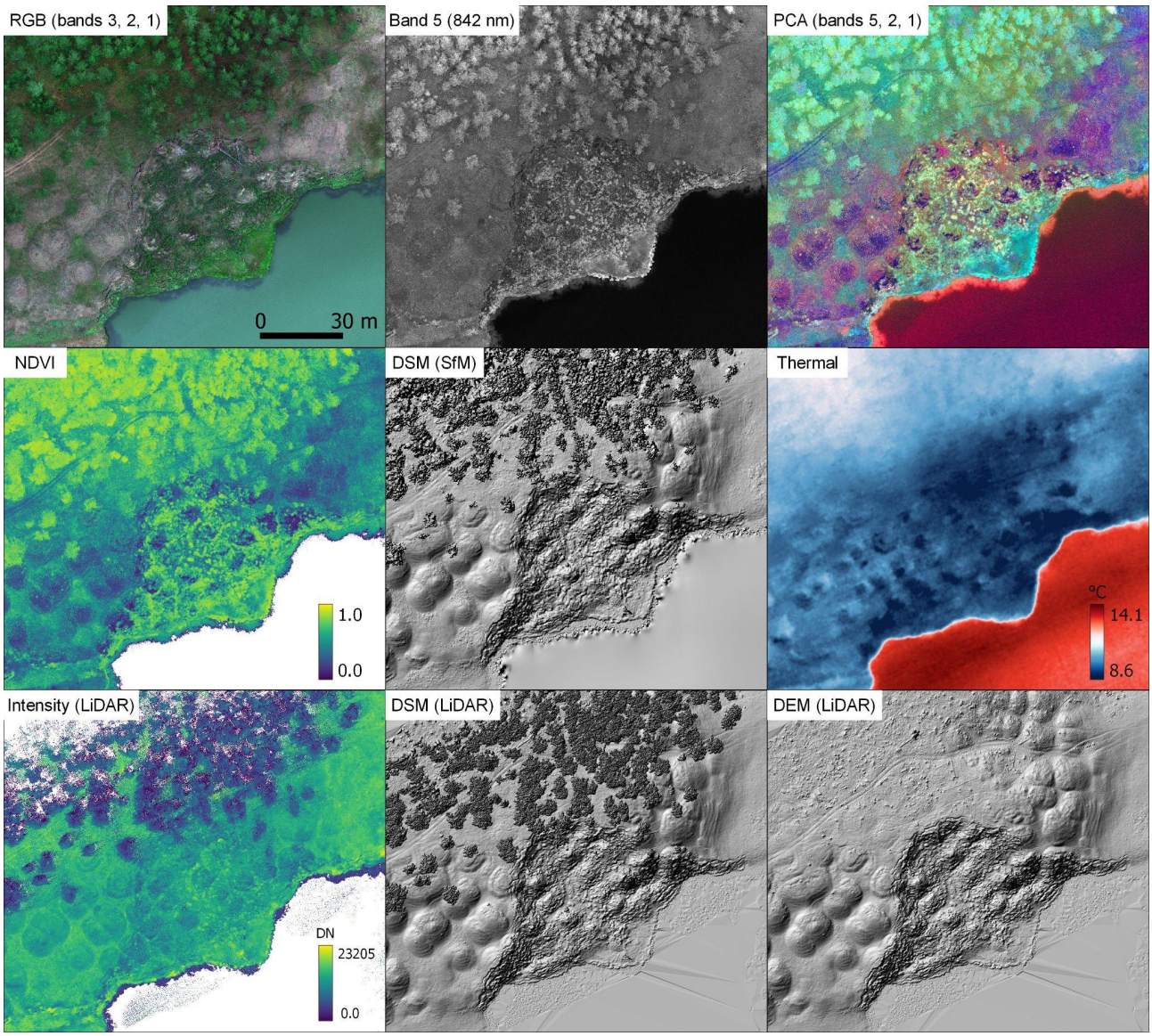

Figure 3.4.14: *An example of available UAV data based on multispectral images and LiDAR scans over the same target, an Alas lake (EN21-419) north of Churapcha. 62.09033° N, 132.35398° E. Some analysis products such as the NDVI and the vegetation-removed DEM are provided to illustrate potential investigation targets related not only to forest but also permafrost feature morphology, (in this example thermokarst mounds (baydzharakhs), a thaw slump and shore microtopography)*

Bibliography

Biskaborn, B. K., D. Bolshiyanov, M. N. Grigoriev, A. Morgenstern, L. A. Pestryakova, L. Tsibizov, and A. Dill (2021a): Russian-German Cooperation: Expeditions to Siberia in 2020. In: Berichte zur Polar- und Meeresforschung = Reports on polar and marine research 756, p. 81. DOI: 10.48433/BzPM_0756_2021.

Biskaborn, B. K., D. Yu. Bolshiyanov, M. N. Grigoriev, A. Morgenstern, L. A. Pestryakova, L. V. Tsibizov, and A. Dill (2021b): Russian-German Cooperation: Expeditions to Siberia in 2020. In Berichte zur Polar- und Meeresforschung. Reports on Polar and Marine Research. In: Alfred-Wegener-Institut, Helmholtz-Zentrum fr Polar- und Meeresforschung 756, pp. 1–81. DOI: 10.48433/BzPM_0756_2021.

Biskaborn, B. K., B. Narancic, K. R. Stoof-Leichsenring, L. A. Pestryakova, P. G. Appleby, G. T. Piliposian, and B. Diekmann (2021c): Effects of climate change and industrialization on Lake Bolshoe Toko, eastern Siberia. In: Journal of Paleolimnology 65, pp. 335–352. DOI: 10.1007/s10933-021-00175-z.

Biskaborn, B. K., L. Nazarova, T. Kröger, L. A. Pestryakova, L. Syrykh, G. Pfalz, U. Herzschuh, and B. Diekmann (2021d): Late Quaternary Climate Reconstruction and Lead-Lag Relationships of Biotic and Sediment-Geochemical Indicators at Lake Bolshoe Toko. In: Frontiers in Earth Science 9.737353, pp. 1–22. DOI: 10.3389/feart.2021.737353.

Biskaborn, B. K., L. Nazarova, L. A. Pestryakova, L. Syrykh, K. Funck, H. Meyer, B. Chapligin, S. Vyse, R. Gorodnichev, E. Zakharov, R. Wang, G. Schwamborn, H. L. Bailey, and B. Diekmann (2019a): Spatial distribution of environmental indicators in surface sediments of Lake Bolshoe Toko, Yakutia, Russia. In: Biogeosciences 16.20, pp. 4023–4049. DOI: 10.5194/bg-16-4023-2019.

Biskaborn, B. K., S. L. Smith, J. Noetzli, H. Matthes, G. Vieira, D. A. Streletskiy, P. Schoeneich, V. E. Romanovsky, A. G. Lewkowicz, A. Abramov, M. Allard, J. Boike, W. L. Cable, H. H. Christiansen, R. Delaloye, B. Diekmann, D. Drozdov, B. Etzelmüller, G. Grosse, M. Guglielmin, T. Ingeman-Nielsen, K. Isaksen, M. Ishikawa, M. Johansson, H. Johannsson, A. Joo, D. Kaverin, A. Kholodov, P. Konstantinov, T. Kröger, C. Lambiel, J.-P. Lanckman, D. Luo, G. Malkova, I. Meiklejohn, N. Moskalenko, M. Oliva, M. Phillips, M. Ramos, A. B. K. Sannel, D. Sergeev, C. Seybold, P. Skryabin, A. Vasiliev, Q. Wu, K. Yoshikawa, M. Zheleznyak, and H. Lantuit (2019b): Permafrost is warming at a global scale. In: Nature Communications 10.264, pp. 1–11. DOI: 10.1038/s41467-018-08240-4.

Boike, J., T. Grau, B. Heim, F. Günther, M. Langer, S. Muster, I. Goutte, and S. Lange (2016): Satellite-derived changes in the permafrost landscape of central Yakutia, 2000–2011: Wetting, drying, and fires. In: Global and Planetary Change 139, pp. 116–127. DOI: 10.1016/j.gloplacha.2016.01.001Get.

Boike, J., J. Nitzbon, K. Anders, M. Grigoriev, D. Bolshiyanov, M. Langer, S. Lange, N. Bornemann, A. Morgenstern, P. Schreiber, C. Wille, S. Chadburn, I. Gouttevin, E. Burke, and L. Kutzbach (2019): A 16-year record (2002–2017) of permafrost, active-layer, and meteorological conditions at the Samoylov Island Arctic permafrost research site, Lena River delta, northern Siberia: an opportunity to validate remote-sensing data and land surface, snow, and permafrost models. In: Earth System Science Data 11.1, pp. 261–299. DOI: 10.5194/essd-11-261-2019.

Bosikov, N. P. (1991): Alaas evolution of Central Yakutia. Yakutsk: Yakutsk Permafrost Institute SD USSR AS.

Bowden, W. B., M. N. Gooseff, A. Balser, A. Green, B. J. Peterson, and J. Bradford (2008): Sediment and nutrient delivery from thermokarst features in the foothills of the North Slope, Alaska: Potential impacts on headwater stream ecosystems. In: Journal of Geophysical Research 113.G2. DOI: 10.1029/2007JG000470.

Camill, P. (2005): Permafrost Thaw Accelerates in Boreal Peatlands During Late-20th Century Climate Warming. In: Clim. Change 68, pp. 135–152. DOI: 10.1007/s10584-005-4785-y.

Crate, S., M. Ulrich, J. O. Habeck, A. R. Desyatkin, R. V. Desyatkin, A. N. Fedorov, T. Hiyama, Y. Iijima, S. Ksenofontov, C. Mészáros, and H. Takakura (2017): Permafrost livelihoods: A transdisciplinary review and analysis of thermokarst-based systems of indigenous land use. In: Anthropocene 18, pp. 89–104. DOI: 10.1016/j.ancene.2017.06.001.

Douglas, T. A., M. R. Turetsky, and C. D. Koven (2020): Increased rainfall stimulates permafrost thaw across a variety of Interior Alaskan boreal ecosystems. In: npj Climate and Atmospheric Science 28.3, pp. 1–7. DOI: 10.1038/s41612-020-0130-4.

Enache, M. and B. Cumming (2007): Charcoal morphotypes in lake sediments from British Columbia (Canada): an assessment of their utility for the reconstruction of past fire and precipitation. In: Journal of Paleolimnology 38, pp. 347–363. DOI: 10.1007/s10933-006-9084-8.

Ershov, E. D. (1982): Termoeroziya dispersnyh porod (Thermal erosion of dispersed sediments). Moscow: Izd-vo MGU, p. 194.

Everdingen, R. O. van (2005): Multi-language glossary of permafrost and related ground-ice terms. Calgary, Canada: The Arctic Institute of North America.

Freeman, C., C. D. Evans, D. T. Monteith, B. Reynolds, and N. Fenner (2001): Export of Organic Carbon from Peat Soils. In: Nature 412, pp. 785–785. DOI: 10.1038/35090628.

Frey, K. E. and L. C. Smith (2005): Amplified carbon release from vast West Siberian peatlands by 2100. In: Geophys. Res. Lett. 32, p. L09401. DOI: 10.1029/2004GL022025.

Fuchs, M., D. Bolshiyanov, M. Grigoriev, A. Morgenstern, L. Pestryakova, L. Tsibizov, and A. Dill (2021a): Russian-German Cooperation: Expeditions to Siberia in 2019. In: Berichte zur Polar- und Meeresforschung = Reports on polar and marine research, Bremerhaven, Alfred Wegener Institute for Polar and Marine Research 749, p. 272. DOI: 10.48433/BzPM_0749_2021.

Fuchs, M., D. Bolshiyanov, M. Grigoriev, A. Morgenstern, L. Pesttryakova, L. Tsibizov, and A. Dill (2021b): Russian-German Cooperation: Expeditions to Siberia in 2019. In Berichte zur Polar- und Meeresforschung. Reports on Polar and Marine Research. In: Alfred-Wegener-Institut, Helmholtz-Zentrum für Polar- und Meeresforschung 749, pp. 1–266. DOI: 10.48433/BzPM_0749_2021.

Geissler, W., P. Dergach, F. Krueger, S. Gukov, C. Haberland, N. Tsukanov, D. Peresypkin, M. Zeckra, S. Petrunin, L. Eponeshnikova, S. Shibaev, B. Baranov, A. Ploetz, A. Krylow, R. Tuktarov, and D. Vollmer (2021): Seismicity of the Laptev Sea Rift. In: Russian-German Cooperation: Expeditions to Siberia in 2019 749, pp. 122–130. DOI: 10.48433/BzPM_0749_2021.

Glückler, R., U. Herzschuh, S. Kruse, A. Andreev, S. A. Vyse, B. Winkler, B. K. Biskaborn, L. Pestryakova, and E. Dietze (2021): Wildfire history of the boreal forest of south-western Yakutia (Siberia) over the last two millennia documented by a lake-sediment charcoal record. In: Biogeosciences 18.13, pp. 4185–4209. DOI: 10.5194/bg-18-4185-2021.

Godin, E., D. Fortier, and S. Coulombe (2014): Effects of thermo-erosion gullying on hydrologic flow networks, discharge and soil loss. In: Environmental Research Letters 9.10, p. 105010. DOI: 10.1088/1748-9326/9/10/105010.

Gooseff, M. N., A. Balser, W. B. Bowden, and J. B. Jones (2009): Effects of Hillslope Thermokarst in Northern Alaska. In: Eos, Transactions American Geophysical Union 90.4, pp. 29–30. DOI: 10.1029/2009EO040001.

Grigor'ev, M. N. (1993): Kriomorfogenez ust'evoj oblasti doliny r. Leny (Cryomorphogenesis of the estuarine region of the Lena River valley). Yakutsk: IMZ SO RAN., p. 176.

Herzschuh, U. (2016): Glacial legacies on interglacial vegetation at the Pliocene-Pleistocene transition in NE Asia. In: Nature Communications 7,11967.

– (2020): Legacy of the Last Glacial on the present-day distribution of deciduous versus evergreen boreal forests. In: Global Ecol Biogeogr 29, pp. 198–206.

Herzschuh, U., L. A. Pestryakova, L. A. Savelieva, L. Heinecke, T. Boehmer, B. K. Biskaborn, A. Andreev, A. Ramisch, A. L. C. Shinneman, and H. J. B. Birks (2013): Siberian larch forests and the ion content of thaw lakes form a geochemically functional entity. In: Nature Communications 4.2408, pp. 1–8. DOI: 10.1038/ncomms3408.

Holmes, R. M., J. W. McClelland, B. J. Peterson, S. E. Tank, E. Bulygina, T. I. Eglinton, V. V. Gordeev, T. Y. Gurtovaya, P. A. Raymond, D. J. Repeta, R. Staples, R. G. Striegl, A. V. Zhulidov, and S. A. Zimov (2012): Seasonal and Annual Fluxes of Nutrients and Organic Matter from Large Rivers to the Arctic Ocean and Surrounding Seas. In: 35 Estuaries and Coasts, pp. 369–382. DOI: 10.1007/s12237-011-9386-6.

Imaev, V., L. Imaeva, O. Smekalin, A. Chipizubov, A. Ovsyuchenko, and I. Kolodeznikov (2018): Neotectonics of the Kharaulakh sector of the Laptev Shelf. In: Russian Geology and Geophysics 59.7, pp. 813–826. DOI: 10.1016/j.rgg.2018.07.007.

Juhls, B., A. Morgenstern, A. Chetverova, A. Eulenburg, J. A. Hölemann, V. Povazhnyi, and P. P. Overduin (2020a): Lena River surface water monitoring near the Samoylov Island Research Station. In: PANGAEA. DOI: 10.1594/PANGAEA.913197.

Juhls, B., C. A. Stedmon, A. Morgenstern, H. Meyer, J. Hölemann, B. Heim, V. Povazhnyi, and P. P. Overduin (2020b): Identifying Drivers of Seasonality in Lena River Biogeochemistry and Dissolved Organic Matter Fluxes. In: Front. Environ. Sci. 8, p. 53. DOI: 10.3389/fenvs.2020.00053.

Kaufman, D. et al. (2020): A global database of Holocene paleotemperature records. In: Scientific Data 7.115, pp. 1–34. DOI: 10.1038/s41597-020-0445-3.

Kruse, S., D. Bolshiyanov, M N. Grigoriev, A. Morgenstern, L. Pestryakova, L. Tsibizov, and A. Udke (2019a): Russian-German Cooperation: Expeditions to Siberia in 2018. In Berichte zur Polar- und Meeresforschung. Reports on Polar and Marine Research. In: Alfred-Wegener-Institut, Helmholtz-Zentrum für Polar- und Meeresforschung 734, pp. 1–257. DOI: 10.2312/BzPM_0734_2019.

– (2019b): Russian-German Cooperation: Expeditions to Siberia in 2018. In: Berichte zur Polar- und Meeresforschung = Reports on polar and marine research, Bremerhaven, Alfred Wegener Institute for Polar and Marine Research 734, p. 257. DOI: 10.2312/BzPM_0734_2019.

– (2019c): Russian-German Cooperation: Expeditions to Siberia in 2018. In Berichte zur Polar- und Meeresforschung. Reports on Polar and Marine Research. In: Alfred-Wegener-Institut, Helmholtz-Zentrum für Polar- und Meeresforschung 734, pp. 1–257. DOI: 10.2312/BzPM_0734_2019.

Kruse, S., D. Bolshiyanov, M.N. Grigoriev, A. Morgensten, L.A. Pestryakova, L. Tsibizov, and A. Udke (2019a): Expedition to Chukotka and Central Yakutia: Modern vegetation studies and lake sediment coring at the Tundra-Taiga-Transition zone in Chukotka and Yakutia. In: Reports on Polar and Marine Research: Russian-German Cooperation: Expeditions to Siberia in 2018, Alfred-Wegener-Institut Helmholtz-Zentrum für Polar- und Meeresforschung 734.

Kruse, S., L.S. Epp, M. Wieczorek, L.A. Pestryakova, K.R. Stoof-Leichsenring, and U. Herzschuh (2018): High gene flow and complex treeline dynamics of Larix Mill. stands on the Taymyr Peninsula (north-central Siberia) revealed by nuclear microsatellites. In: Tree Genetics and Genomes 14(2).

Kruse, S., A. Gerdes, N.J. Kath, L.S. Epp, K.R. Stoof-Leichsenring, L.A. Pestryakova, and U. Herzschuh (2016b): Dispersal distances and migration rates at the arctic treeline in Siberia - a genetic and simulation-based study. In: Biogeosciences 16, pp. 1211–1224.

Kruse, S., A.I. Kolmogorov, L.A. Pestryakova, and U. Herzschuh (2020): Long-lived larch clones may conserve adaptations that could restrict treeline migration in northern Siberia. In: Ecology and Evolution 10(18), pp. 10017–10030.

Kruse, S., K. Stoof-Leichsenring, K.R. Keperveem, P.P. Blender, F. Bolshiyanov, D.Y. Grigoriev, A. Morgenstern, and H. Meyer (2016): Past and present vegetation dynamics at the most eastern extension of the Siberian boreal treeline. Russian-German Cooperation: Expeditions to Siberia in 2016. Reports on Polar and Marine Research. In: Alfred-Wegener-Institut, Helmholtz-Zentrum für Polar- und Meeresforschung, pp. 130–137.

Kruse, S., M. Wieczorek, F. Jeltsch, and U. Herzschuh (2019b): Treeline dynamics in Siberia under changing climates as inferred from an individual-based model for Larix. In: Ecological Modelling 338, pp. 101–121.

Labutin, Yu. V., V.I. Perfil'eva, Yu. Revin, Yu.Yu. Blokhin, A.G. Degtyarev, R.V. Desyatkin, A.A. Egorova, F.N. Kirillov, V.I. Perfil'ev, and E.I. Petrova. (1985): The flora and fauna of the Lena River Delta. Yakutsk: Siberian Branch of the USSR Academy of Sciences (in Russian).

Miesner, T, U. Herzschuh, L.A. Pestryakova, M. Wieczorek, E.S. Zakharov, A.I. Kolmogorov, P.V. Davydova, and S. Kruse (2022): Forest structure and individual tree inventories of north-eastern Siberia along climatic gradients. In: ESSD 152, pp. 1–19.

Neumann, R. B., C. J. Moorberg, J. D. Lundquist, J. C. Turner, M. P. Waldrop, J. W. McFarland, E. S. Euskirchen, C. W. Edgar, and M. R. Turetsky (2019): Warming Effects of Spring Rainfall Increase Methane Emissions From Thawing Permafrost. In: Geophysical Research Letters 46.3, pp. 1393–1401. DOI: 10.1029/2018GL081274.

Nikolin, E. G. and I. A. Yakshina (2017): Invasion of boreal flora elements in Arctic Yakutia (village Tiksi). In: The North Caucasus Ecological Herald (in Russian) 13.3, pp. 36–37.

Overduin, P. P., F. Blender, D. Y. Bolshiyanov, M. N. Grigoriev, A. Morgenstern, and H. Meyer (2017): Russian-German Cooperation: Expeditions to Siberia in 2016. In Berichte zur Polar- und Meeresforschung. Reports on Polar and Marine Research. In: Alfred-Wegener-Institut, Helmholtz-Zentrum für Polar- und Meeresforschung 709, pp. 1–295. DOI: 10.2312/BzPM_0709_2017.

Pospeev, A. (2018): Sovremennaya prakticheskaya elektrorazvedka. Novosibirsk: Akademicheskoe izdatel'stvo Geo.

Potapov, V., A. Kartozia, A. Zaplavnova, and P. Dergach (2021): New studies of the deep geophysical structure in the southern part of the Lena Delta. In: Russian-German Cooperation: Expeditions to Siberia in 2019 749, pp. 122–130. DOI: 10.48433/BzPM_0749_2021.

Schirrmeister, L., L. Pestryakova, A. Schneider, and S. Wetterich (2016): Studies of Polygons in Siberia and Svalbard. In Berichte zur Polar- und Meeresforschung. Reports on Polar and Marine Research. In: Alfred-Wegener-Institut, Helmholtz-Zentrum für Polar- und Meeresforschung. 697, pp. 1–275. DOI: 10.2312/BzPM_0697_2016.

Sharlov, M. (2017): FastSnap Digital Electroprospecting system. User guide. Sigma-Geo LLC, Irkutsk.

Shevtsova, I., B. Heim, S. Kruse, J. Schröder, E.I. Troeva, L.A. Pestryakova, E.S. Zakharov, and U. Herzschuh (2020): Strong shrub expansion in tundra-taiga, tree infilling in taiga and stable tundra in central Chukotka (north-eastern Siberia) between 2000 and 2017. In: Environmental Research Letters 15(8)085006.

Sidorchuk, A. Yu. and A.V. Baranov (1999): Erozionnye processy Central'nogo Yamala (Erosion processes of Central Yamal). Saint Petersburg: RNII kul'turnogo i prirodnogo naslediya, p. 350.

Stedmon, C. A., R. M. W. Amon, A. J. Rinehart, and S. A. Walker (2011): The supply and characteristics of colored dissolved organic matter (CDOM) in the Arctic Ocean: Pan Arctic trends and differences. In: Marine Chemistry 124, pp. 108–118. DOI: 10.1016/J.MARCHEM.2010.12.007.

Thibodeau, B., D. Bauch, H. Kassens, and L. A. Timokhov (2014): Interannual variations in river water content and distribution over the Laptev Sea between 2007 and 2011: The Arctic Dipole connection. In: Geophys. Res. Lett. 41, pp. 7237–7244. DOI: 10.1002/2014GL061814.

Timofeev, D. A. (1981): Terminologiya flyuvial'noj geomorfologii (Terminology of fluvial geomorphology). Moscow: Nauka, p. 268.

Walker, X., J. Baltzer, S. Cumming, N. Day, C. Ebert, S. Goetz, J. Johnstone, S. Potter, B. Rogers, E. Schuur, M. Turetsky, and M. Mack (2019): Increasing wildfires threaten historic carbon sink of boreal forest soils. In: Nature 572, pp. 520–523. DOI: 10.1038/s41586-019-1474-y.

Wieczorek, M., S. Kruse, Kolomogorov L.S, A. Nikolaev, A.N. Heinrich, F. Jeltsch, L.A. Pestryakova, R. Zibulski, and U. Herzschuh (2017a): Dissimilar responses of larch stands in northern Siberia to increasing temperatures – a field and simulation based study. In: Ecology.

Wieczorek, M., T. Miesner, U. Herzschuh, L.A. Pestryakova, E.S. Zakharov, A.I. Kolmogorov, P.V. Davydova, and S. Kruse (2017b): Disturbance-effects on treeline larch-stands in the lower Kolyma River area (NE Siberia). In: Silva Fennica 51 (id 166).

Appendix

A.1 List of participants

Table A.1.1: List of participants in the Expedition Lena 2021 based on Research Station Samoylov Island

No.	Name	Institution	Duration
1	Abramova, Ekaterina	LDR, IPGG	04.05.2021-23.09.2021
2	Alekhina, Irina	AARI	16.07.2021-10.08.2021
3	Beckebanze, Lutz	UHH	04.09.2021-23.09.2021
4	Belimov, Andrey	ARRIAM	16.07.2021-10.08.2021
5	Bornemann, Niko	AWI-P	04.09.2021-23.09.2021
6	Chernova, Elizaveta	SPbU	16.07.2021-10.08.2021
7	Dergach, Petr	IPGG, NSU	10.07.2021-29.07.2021
8	Evgrafova, Svetlana	FI	07.08.2021-10.08.2021
9	Grigoriev, Mikhail	MPI, IPGG	20.08.2021-28.08.2021
10	Kadutskii, Valerii	FI	07.08.2021-28.08.2021
11	Karlov, Denis	ARRIAM	16.07.2021-10.08.2021
12	Kartoziia, Andrei	IPGG, NSU, IGM SB RAS	10.07.2021-29.07.2021
13	Lashchinskiy, Nikolay	IPGG, CSBG	16.07.2021-29.07.2021
14	Lebedeva, Lyudmila	MPI	04.09.2021-11.09.2021
15	Lisovski, Simeon	AWI-P	07.07.2021-16.07.2021
16	Mirbach, Charlotta	UHH	04.09.2021-23.09.2021
17	Morgenstern, Anne	AWI-P	20.08.2021-28.08.2021
18	Novikov, Aleksandr	UK	07.07.2021-29.07.2021
19	Polyakov, Vyacheslav	AARI	20.08.2021-23.09.2021
20	Ponasenko, Svyatoslav	IPGG	10.07.2021-29.07.2021
21	Potapov, Vladimir	IPGG, NSU	10.07.2021-29.07.2021
22	Pravkin, Sergey	AARI	20.08.2021-11.09.2021
23	Shamov, Vladimir	PGI, MPI	04.09.2021-11.09.2021
24	Tarbeeva, Anna	MSU	07.07.2021-16.07.2021 and 04.09.2021-11.09.2021

Table A.1.2: List of participants in the Expedition Yakutia 2021

No.	Name	Institution	Duration
1	Baisheva, Izabella	NEFU, AWI-P	03.08.2021-03.09.2021
2	Biskaborn, Boris	AWI-P	03.08.2021-21.08.2021
3	Davydova, Paraskovya	NEFU	03.08.2021-21.08.2021
4	Dietze, Elisabeth	AWI-P, UG	14.08.2021-03.09.2021
5	Eder, Iris	AWI-P	03.08.2021-03.09.2021
6	Egorov, Aital	NEFU	03.08.2021-03.09.2021
7	Gloy, Josias	AWI-P	03.08.2021-03.09.2021
8	Glückler, Ramesh	AWI-P	03.08.2021-03.09.2021
9	Heim, Birgit	AWI-P	03.08.2021-26.08.2021
10	Herzschuh, Ulrike	AWI-P, UP	03.08.2021-03.09.2021
11	Jackisch, Robert	TU-B, AWI-P	03.08.2021-03.09.2021
12	Kahl, Jan	AWI-P	03.08.2021-21.08.2021
13	Kolmogorov, Alexei	NEFU	03.08.2021-03.09.2021
14	Kruse, Stefan	AWI-P	03.08.2021-03.09.2021
15	Meister, Philip	AWI-P, UP	03.08.2021-21.08.2021
16	Miesner, Timon	AWI-P, TU-B	03.08.2021-03.09.2021
17	Pestryakov, Aleksey	NEFU	03.08.2021-21.08.2021
18	Schild, Laura	AWI-P	03.08.2021-03.09.2021
19	Smirnikov, Victor	NEFU	03.08.2021-03.09.2021
20	Stieg, Amelie	AWI-P	03.08.2021-03.09.2021
21	Syrovatskiy, Igor	NEFU	03.08.2021-21.08.2021
22	Ushnitskaya, Lena	NEFU	03.08.2021-03.09.2021
23	von Hippel, Barbara	AWI-P	03.08.2021-03.09.2021
24	Zakharov, Evgenii	NEFU	03.08.2021-03.09.2021

Table A.1.3: List of participating institutions

Abbr.	Institution
AARI	Arctic and Antarctic Research Institute, St. Petersburg, Russia
ARRIAM	All-Russia Research Institute for Agricultural Microbiology, Saint Petersburg, Russia
AWI-B	Alfred Wegener Institute Helmholtz Centre for Polar and Marine Research, Bremerhaven, Germany
AWI-P	Alfred Wegener Institute Helmholtz Centre for Polar and Marine Research, Potsdam, Germany
CSBG	Central Siberian Botanical Garden, Novosibirsk, Russia
FI	V.N.Sukachev Institute of Forest Siberian Branch of Russian Academy of Sciences, Krasnoyarsk, Russia
GFZ	Helmholtz-Zentrum Potsdam – German Research Center for Geosciences, Potsdam, German
GS RAS	Yakutsk Branch Federal Research Centre Geophysical Survey, Russian Academy of Sciences, Yakutia, Russia
IGM SB RAS	V. S. Sobolev Institute of Geology and Mineralogy, Siberian Branch, Russian Academy of Science, Novosibirsk, Russia
IPGG	Trofimuk Institute of Petroleum-Gas Geology and Geophysics, Siberian Branch, Russian Academy of Sciences, Novosibirsk, Russia
LDR	Lena Delta Reserve, Tiksi, Sakha Republic, Russia
MPI	Melnikov Permafrost Institute, Siberian Branch, Russian Academy of Sciences, Yakutsk, Russia
MSU	Lomonosov Moscow State University, Moscow, Russia
NEFU	Federal State Autonomous Educational Institution of Higher Education “M. K. Ammosov North-Eastern Federal University”, Yakutsk, Russia
NSU	Novosibirsk State University, Novosibirsk, Russia
PGI	Pacific Geographical Institute Far-Eastern Branch, Russian Academy of Sciences, Vladivostok, Russia
SPbU	Saint Petersburg State University, St. Petersburg, Russia
TU-B	Technical University of Berlin, Berlin, Germany
UG	University of Göttingen, Göttingen, Germany
UHH	University of Hamburg, Hamburg, Germany

Abbr.	Institution
UK	Kazan Federal University, Kazan, Russia
UP	University of Potsdam, Potsdam, Germany

A.2 Supplementary material – Expedition Lena 2021

Table A.2.1: Core set of parameters

Parameter	Details	Sample Type / Volume (ml)	Preservation	Storage
Core parameters (always sampled & measured)				
Temperature (in field)	measured during sampling (WTW Cond 340i)		-	-
Electrical conductivity (in field)	measured during sampling (WTW Cond 340i)		-	-
Electrical conductivity (in lab)	Measured on WTW Multilab 540	on rest sample or CDOM sample	-	variable
Dissolved organic carbon (DOC)	filtered, 0.45 μM cellulose acetate (CA)	20 ml	acidified to pH<2 with HCl	cool, dark, glass vial
Colored dissolved organic material (CDOM)	filtered, 0.45 μM cellulose acetate (CA)	100 ml	-	cool, dark, brown glass
Stable isotopes of water	unfiltered	10 ml		cool, polyethylene bottle
Rest sample	unfiltered (for EC (lab), additional parameter or reanalysis if needed)	60 ml		frozen, polyethylene bottle
Nutrients, total	unfiltered	60 ml		frozen, polyethylene bottle
Nutrients, dissolved	filtered, 0.45 μM cellulose acetate (CA)	60 ml		frozen, polyethylene bottle
Additional parameters (not always sampled & measured)				
Major cations	filtered, 0.45 μM cellulose acetate (CA)	on rest sample and CDOM		
Major anions	filtered, 0.45 μM cellulose acetate (CA)	on rest sample and CDOM		
FDOM	filtered, 0.45 μM cellulose acetate (CA)	no FDOM measurements after sample #201 yet.		
D^{14}C-DOC	filtered, 0.45 μM cellulose acetate (CA), beginning on 06.04.2019; sample frequency irregular	250 / 60 ml	acidified to pH<2 with HCl	acid-washed HDPE bottles, frozen

Table A.2.2: List of samples collected to date (as of October 2021) at the Research Station Samoylov Island

ID	Date	Time
1	20.04.2018	21:00
2	24.04.2018	20:30
3	26.04.2018	18:00
4	30.04.2018	12:00
5	04.05.2018	19:00
6	08.05.2018	14:00
7	12.05.2018	10:30
8	16.05.2018	10:00
9	20.05.2018	10:00
10	24.05.2018	12:00
11	28.05.2018	14:00
12	01.06.2018	12:00
13	05.06.2018	13:00
14	09.06.2018	14:00
15	13.06.2018	12:00
18	17.06.2018	12:00
19	21.06.2018	14:00
20	25.06.2018	15:00
21	29.06.2018	11:00
22	03.07.2018	20:00
23	08.07.2018	11:30
24	12.07.2018	8:30
25	16.07.2018	19:00
26	20.07.2018	20:00
27	26.07.2018	19:00
28	30.07.2018	20:05

ID	Date	Time
29	03.08.2018	20:00
30	07.08.2018	21:00
31	11.08.2018	19:00
32	15.08.2018	19:00
33	19.08.2018	19:00
34	23.08.2018	19:00
35	27.08.2018	19:00
36	01.09.2018	19:00
37	05.09.2018	19:00
38	09.09.2018	19:00
39	13.09.2018	19:00
40	17.09.2018	11:00
41	21.09.2018	14:00
42	25.09.2018	10:00
43	29.09.2018	19:00
44	03.10.2018	8:00
45	07.10.2018	19:00
46	11.10.2018	8:00
47	15.10.2018	14:00
48	19.10.2018	14:00
49	24.10.2018	8:00
50	31.10.2018	19:00
51	03.11.2018	12:00
52	07.11.2018	14:00
53	11.11.2018	14:00
54	16.11.2018	16:00

ID	Date	Time
55	20.11.2018	14:00
56	24.11.2018	14:00
57	28.11.2018	11:00
58	02.12.2018	13:00
59	06.12.2018	14:00
60	09.12.2018	15:00
61	14.12.2018	15:00
62	18.12.2018	13:00
63	22.12.2018	13:00
64	26.12.2018	15:00
65	06.01.2019	14:00
66	11.01.2019	14:00
67	18.01.2019	15:10
68	25.01.2019	14:00
69	02.02.2019	16:00
70	07.02.2019	14:00
71	12.02.2019	14:00
72	19.02.2019	15:00
73	25.02.2019	16:00
74	01.03.2019	16:00
75	11.03.2019	14:00
76	19.03.2019	14:00
77	28.03.2019	17:00
78	06.04.2019	13:00
79	11.04.2019	15:00
80	22.04.2019	12:00

ID	Date	Time
81	30.04.2019	15:00
82	06.05.2019	12:00
83	10.05.2019	14:00
84	16.05.2019	14:00
85	20.05.2019	14:00
86	22.05.2019	10:00
87	23.05.2019	14:00
88	24.05.2019	13:00
89	25.05.2019	11:00
90	26.05.2019	15:00
91	27.05.2019	18:00
92	28.05.2019	17:00
93	29.05.2019	18:00
94	30.05.2019	13:00
95	31.05.2019	14:00
96	01.06.2019	10:00
97	02.06.2019	10:00
98	03.06.2019	16:00
99	04.06.2019	15:00
100	05.06.2019	10:00
101	06.06.2019	10:00
102	07.06.2019	14:00
103	08.06.2019	10:00
104	09.06.2019	16:00
105	10.06.2019	14:00
106	11.06.2019	16:00

ID	Date	Time
107	12.06.2019	8:00
108	13.06.2019	21:00
109	14.06.2019	19:00
110	15.06.2019	14:00
111	16.06.2019	10:00
112	17.06.2019	12:00
113	18.06.2019	9:00
114	19.06.2019	18:00
115	20.06.2019	22:00
116	21.06.2019	18:00
117	22.06.2019	10:00
118	23.06.2019	14:00
119	24.06.2019	13:00
120	25.06.2019	12:00
121	26.06.2019	8:00
122	27.06.2019	18:00
123	28.06.2019	13:30
124	29.06.2019	10:00
125	30.06.2019	11:00
126	01.07.2019	14:00
127	02.07.2019	11:00
128	04.07.2019	14:00
129	07.07.2019	16:30
130	10.07.2019	11:00
131	12.07.2019	14:30
132	14.07.2019	15:20

ID	Date	Time
133	16.07.2019	16:30
134	18.07.2019	11:00
135	20.07.2019	10:00
136	22.07.2019	11:30
137	24.07.2019	10:00
138	26.07.2019	10:30
139	28.07.2019	11:00
140	30.07.2019	10:10
141	01.08.2019	10:30
142	03.08.2019	11:20
143	05.08.2019	11:20
144	07.08.2019	9:20
145	09.08.2019	14:40
146	12.08.2019	11:00
147	14.08.2019	21:30
148	16.08.2019	10:30
149	18.08.2019	11:00
150	20.08.2019	10:30
151	22.08.2019	10:40
152	24.08.2019	10:40
153	26.08.2019	9:00
154	28.08.2019	10:30
155	30.08.2019	15:30
156	01.09.2019	17:00
157	03.09.2019	16:00
198	05.09.2019	10:00

ID	Date	Time
199	07.09.2019	10:00
200	09.09.2019	9:00
201	11.09.2019	10:00
202	13.09.2019	6:00
203	15.09.2019	11:00
204	17.09.2019	9:00
205	19.09.2019	12:00
206	21.09.2019	9:00
207	23.09.2019	10:00
208	25.09.2019	8:00
209	27.09.2019	9:00
210	29.09.2019	8:00
211	01.10.2019	8:00
212	03.10.2019	8:00
213	05.10.2019	9:00
214	07.10.2019	8:00
215	09.10.2019	8:00
216	11.10.2019	8:00
217	13.10.2019	8:00
218	15.10.2019	10:00
219	17.10.2019	8:00
220	19.10.2019	9:00
221	21.10.2019	9:00
222	23.10.2019	8:00
223	25.10.2019	9:00
224	27.10.2019	8:00

ID	Date	Time
225	29.10.2019	10:00
226	31.10.2019	10:00
227	02.11.2019	10:00
228	04.11.2019	10:00
229	06.11.2019	11:00
230	08.11.2019	12:00
231	10.11.2019	12:00
232	12.11.2019	11:00
233	14.11.2019	10:00
234	16.11.2019	10:00
235	18.11.2019	12:00
236	20.11.2019	12:00
237	22.11.2019	12:00
238	24.11.2019	12:00
239	26.11.2019	11:00
240	28.11.2019	12:00
241	30.11.2019	12:00
242	02.12.2019	12:00
243	04.12.2019	11:00
244	06.12.2019	12:00
245	08.12.2019	10:00
246	10.12.2019	11:00
247	12.12.2019	10:00
248	14.12.2019	11:00
249	16.12.2019	11:00
250	18.12.2019	11:00

ID	Date	Time
251	20.12.2019	12:00
252	22.12.2019	11:00
253	24.12.2019	12:00
254	26.12.2019	12:00
255	28.12.2019	13:00
256	30.12.2019	13:00
257	01.01.2020	13:00
258	03.01.2020	13:00
259	05.01.2020	12:00
260	07.01.2020	12:00
261	09.01.2020	13:00
262	11.01.2020	12:00
263	14.01.2020	13:00
264	18.01.2020	13:00
265	22.01.2020	13:00
266	26.01.2020	12:00
267	30.01.2020	12:00
268	03.02.2020	12:00
269	07.02.2020	12:00
270	11.02.2020	12:00
271	15.02.2020	13:00
272	19.02.2020	12:00
273	23.02.2020	13:00
274	27.02.2020	13:00
275	01.03.2020	12:00
276	05.03.2020	12:00

ID	Date	Time
277	09.03.2020	13:00
278	13.03.2020	12:00
279	17.03.2020	11:00
280	21.03.2020	11:00
281	25.03.2020	12:00
282	29.03.2020	12:00
283	04.04.2020	12:00
284	11.04.2020	12:00
285	18.04.2020	12:00
286	25.04.2020	12:00
287	02.05.2020	12:00
288	09.05.2020	10:00
289	10.05.2020	9:00
290	11.05.2020	9:00
291	12.05.2020	9:00
292	13.05.2020	8:00
293	14.05.2020	9:00
294	15.05.2020	8:00
295	16.05.2020	8:00
296	17.05.2020	10:00
297	18.05.2020	8:00
298	19.05.2020	9:00
299	20.05.2020	10:00
300	21.05.2020	10:00
301	22.05.2020	10:00
302	23.05.2020	10:00

ID	Date	Time
303	24.05.2020	11:00
304	25.05.2020	10:00
305	26.05.2020	9:00
306	27.05.2020	10:00
307	28.05.2020	9:00
308	29.05.2020	9:00
309	30.05.2020	9:00
310	31.05.2020	9:00
311	01.06.2020	9:00
312	02.06.2020	9:00
313	03.06.2020	9:00
314	04.06.2020	9:00
315	05.06.2020	9:00
316	06.06.2020	9:00
317	07.06.2020	9:00
318	08.06.2020	9:00
319	09.06.2020	12:00
320	10.06.2020	9:00
321	11.06.2020	9:00
322	12.06.2020	9:00
323	13.06.2020	9:00
324	14.06.2020	9:00
325	15.06.2020	9:00
326	17.06.2020	9:00
327	19.06.2020	9:00
328	21.06.2020	9:00

ID	Date	Time
329	23.06.2020	9:00
330	25.06.2020	9:00
331	27.06.2020	9:00
332	29.06.2020	9:00
333	01.07.2020	9:00
334	03.07.2020	9:00
335	05.07.2020	9:00
336	07.07.2020	9:00
337	09.07.2020	9:00
338	11.07.2020	9:00
339	13.07.2020	9:00
340	15.07.2020	9:00
341	17.07.2020	15:00
342	19.07.2020	11:00
343	21.07.2020	17:00
344	23.07.2020	20:00
345	25.07.2020	9:00
346	27.07.2020	9:00
347	29.07.2020	9:00
348	31.07.2020	9:00
349	01.08.2020	9:00
350	04.08.2020	9:00
351	06.08.2020	9:00
352	08.08.2020	9:00
353	10.08.2020	9:00
354	12.08.2020	9:00

ID	Date	Time
355	14.08.2020	9:00
356	16.08.2020	9:00
357	18.08.2020	9:00
358	20.08.2020	9:00
359	22.08.2020	8:00
360	24.08.2020	9:00
361	26.08.2020	9:00
362	28.08.2020	12:00
363	30.08.2020	10:00
364	01.09.2020	9:00
365	03.09.2020	9:00
366	05.09.2020	9:00
367	07.09.2020	9:00
368	09.09.2020	9:00
369	11.09.2020	9:00
370	13.09.2020	9:00
371	15.09.2020	9:00
372	17.09.2020	9:00
373	19.09.2020	9:00
374	21.09.2020	9:00
375	23.09.2020	9:00
376	25.09.2020	9:00
377	27.09.2020	9:00
378	29.09.2020	9:00
379	01.10.2020	9:00
380	03.10.2020	9:00

ID	Date	Time
381	05.10.2020	9:00
382	07.10.2020	9:00
383	09.10.2020	9:00
384	11.10.2020	9:00
385	13.10.2020	9:00
386	15.10.2020	9:00
387	17.10.2020	9:00
388	19.10.2020	9:00
389	21.10.2020	9:00
390	23.10.2020	9:00
391	25.10.2020	10:00
392	27.10.2020	10:00
393	29.10.2020	9:00
394	31.10.2020	9:00
395	07.11.2020	10:00
396	14.11.2020	11:00
397	21.11.2020	10:00
398	28.11.2020	11:00
399	05.12.2020	13:00
400	12.12.2020	12:00
401	13.12.2020	20:00
402	26.12.2020	16:00
403	02.01.2021	12:00
404	09.01.2021	12:00
405	16.01.2021	12:00
406	23.01.2021	12:00

ID	Date	Time
407	30.01.2021	12:00
408	06.02.2021	11:00
409	13.02.2021	12:00
410	20.02.2021	12:00
411	27.02.2021	18:00
412	06.03.2021	13:00
413	13.03.2021	10:00
414	20.03.2021	11:00
415	27.03.2021	11:00
416	03.04.2021	11:00
417	10.04.2021	12:00
418	17.04.2021	11:00
419	24.04.2021	12:00
420	01.05.2021	11:00
421	08.05.2021	17:00
422	10.05.2021	14:00
423	11.05.2021	17:00
424	12.05.2021	13:00
425	13.05.2021	14:00
426	14.05.2021	14:00
427	15.05.2021	10:00
428	16.05.2021	11:00
429	17.05.2021	12:00
430	18.05.2021	16:00
431	19.05.2021	10:00
432	20.05.2021	15:00

ID	Date	Time
433	21.05.2021	10:00
434	22.05.2021	12:00
435	23.05.2021	10:00
436	24.05.2021	9:00
437	25.05.2021	9:00
438	26.05.2021	11:00
439	27.05.2021	11:00
440	28.05.2021	10:00
441	29.05.2021	10:00
442	30.05.2021	8:00
443	31.05.2021	8:00
444	01.06.2021	8:00
445	02.06.2021	8:00
446	03.06.2021	8:00
447	04.06.2021	8:00
448	05.06.2021	8:00
449	06.06.2021	8:00
450	07.06.2021	11:00
451	08.06.2021	16:00
452	09.06.2021	11:00
453	10.06.2021	11:00
454	11.06.2021	8:00
455	12.06.2021	8:00
456	13.06.2021	11:00
457	14.06.2021	8:00
458	15.06.2021	8:00

ID	Date	Time
459	17.06.2021	9:00
460	19.06.2021	9:00
461	21.06.2021	8:00
462	23.06.2021	8:00
463	25.06.2021	8:00
464	27.06.2021	8:00
465	29.06.2021	8:00
466	01.07.2021	8:00
467	03.07.2021	8:00
468	05.07.2021	8:00
469	07.07.2021	13:00
470	09.07.2021	8:00
471	11.07.2021	8:00

ID	Date	Time
472	13.07.2021	8:00
473	15.07.2021	8:00
474	17.07.2021	8:00
475	19.07.2021	8:00
476	21.07.2021	8:00
477	23.07.2021	8:00
478	25.07.2021	8:00
479	27.07.2021	16:00
480	29.07.2021	11:00
484	07.08.2021	16:30
485	08.08.2021	17:00
486	21.08.2021	18:00
487	23.08.2021	15:00

Table A.2.3: List of samples collected in the central Lena catchment to date (as of October 2021)

Sample ID	Date	Location	Water Level (cm)	Filtration Date	Acidification Date	comment	Lat (DecDeg)	Lon (DecDeg)
LA	2020-06-05	Lena-Tabaga					61.8019	129.6810
LB	2020-06-25	Lena-Tabaga					61.8019	129.6810
LC	2020-07-05	Lena-Tabaga					61.8019	129.6810
LD	2020-07-15	Lena-Tabaga					61.8019	129.6810
LE	2020-07-25	Lena-Tabaga					61.8019	129.6810
L01	2020-10-20	Lena-Tabaga	210	2021-03-26	2021-04-06		61.8019	129.6810
L02	2020-10-31	Lena-Tabaga	171	2021-03-26	2021-04-06		61.8019	129.6810
L03	2020-11-10	Lena-Tabaga	213	2021-03-26	2021-04-06		61.8019	129.6810
L04	2020-11-30	Lena-Tabaga	196	2021-03-26	2021-04-06		61.8019	129.6810
L05	2020-12-10	Lena-Tabaga	148	2021-03-26	2021-04-06		61.8019	129.6810
L06	2020-12-31	Lena-Tabaga	198	2021-03-26	2021-04-06		61.8019	129.6810
L07	2021-01-10	Lena-Tabaga	189	2021-03-26	2021-04-06		61.8019	129.6810
L08	2021-01-31	Lena-Tabaga	128	2021-03-26	2021-04-06		61.8019	129.6810
L09	2021-02-10	Lena-Tabaga	106	2021-03-26	2021-04-06		61.8019	129.6810
L10	2021-03-15	Lena-Tabaga	68	2021-03-31	2021-04-06		61.8019	129.6810
L11	2021-03-31	Lena-Tabaga	59	2021-03-31	2021-04-06		61.8019	129.6810

Sample ID	Date	Location	Water Level (cm)	Filtration Date	Acidification Date	comment	Lat (DecDeg)	Lon (DecDeg)
L12	2021-03-24	Olekma – Troitsk		2021-03-29	2021-04-06		60.3517	120.6955
L13	2021-03-24	Lena – Olekmisk farwater		2021-03-29	2021-04-06		60.3585	120.4422
L14	2021-03-26	Buotama – mouth		2021-03-29	2021-04-06		61.2562	128.7690
L15	2021-03-26	Sinyaya – mouth		2021-03-29	2021-04-06		61.1302	126.8531
L16	2021-04-02	Aldan – Eldikan		2021-04-08	2021-04-08	only 5 bottles. Orange bottle is filled with filtered water	60.7720	135.1415
L17	2021-04-26	Shestakovka – naled (aufeis)		2021-04-30	2021-04-30		61.9457	129.3247
L18	2021-04-06	Maya Riv		2021-04-30	2021-04-30		60.3950	134.6141
L19	2021-04-06	Amga Riv – ice road		2021-04-30	2021-04-30		60.9474	132.2808
L20	2021-04-15	Lena-Tabaga	59	2021-05-02	2021-05-02		61.8019	129.6810
L21	2021-04-30	Lena-Tabaga	68	2021-05-02	2021-05-02		61.8019	129.6810
L22	2021-05-03	Shestakovka – Khamyrdagys-takh		2021-05-13	2021-05-13		61.9286	129.5431
L23	2021-05-04	Shestakovka – Khamyrdagys-takh		2021-05-08	2021-05-08		61.9286	129.5431

Sample ID	Date	Location	Water Level (cm)	Filtration Date	Acidification Date	comment	Lat (DecDeg)	Lon (DecDeg)
L24	2021-05-05	Shestakovka – Khamyrdagys-takh		2021-05-13	2021-05-13		61.9286	129.5431
L25	2021-05-06	Shestakovka – Khamyrdagys-takh		2021-05-09	2021-05-09	very difficult to filter. 4 filters used	61.9286	129.5431
L26	2021-05-07	Shestakovka – Khamyrdagys-takh		2021-05-09	2021-05-09	very difficult to filter. 4 filters used	61.9286	129.5431
L27	2021-05-08	Shestakovka – Khamyrdagys-takh		2021-05-13	2021-05-13		61.9286	129.5431
L28	2021-05-10	Shestakovka – Khamyrdagys-takh		2021-05-13	2021-05-13		61.9286	129.5431
L29	2021-05-13	Shestakovka – Khamyrdagys-takh		2021-05-21	2021-05-21		61.9286	129.5431
L30	2021-05-19	Kemkeme Riv		2021-05-21	2021-05-21		62.0468	128.9288
L31	2021-05-20	Shestakovka – Khamyrdagys-takh		2021-05-21	2021-05-21		61.9286	129.5431

Sample ID	Date	Location	Water Level (cm)	Filtration Date	Acidification Date	comment	Lat (DecDeg)	Lon (DecDeg)
L32	2021-05-28	Shestakovka – Khamyrdagys-takh		07.06.2021	07.06.2021		61.9286	129.5431
L33	2021-06-03	Shestakovka – Khamyrdagys-takh		07.06.2021	07.06.2021		61.9286	129.5431
L34	2021-06-18	Khamyrdagystakh		16.08.2021	16.08.2021		61.9286	129.5431
L35	2021-08-12	Khamyrdagystakh		16.08.2021	16.08.2021		61.9286	129.5431
L36	2021-08-26	Khamyrdagystakh		27.08.2021	27.08.2021		61.9286	129.5431
L37	2021-05-15	Tabaga	422	27.08.2021	27.08.2021		61.8019	129.6810
L38	2021-05-31	Tabaga	416	27.08.2021	27.08.2021		61.8019	129.6810
L39	2021-06-15	Tabaga	724	27.08.2021	27.08.2021		61.8019	129.6810
L40	2021-06-30	Tabaga	639	27.08.2021	27.08.2021	No rest sample bottle	61.8019	129.6810
L41	2021-07-15	Tabaga	436	27.08.2021	27.08.2021		61.8019	129.6810
L42	2021-07-31	Tabaga	375	27.08.2021	27.08.2021		61.8019	129.6810
L43	2021-06-10	Tabaga	619	27.08.2021	27.08.2021		61.8019	129.6810

Table A.2.4: Estimate of the number of nests/individuals from bird species seen on Samoylov Island during the field expedition in July 2021 (individuals seen with binoculars in a distance > 50 m from the island shore are excluded)

Species	**Scientific**	**Russian**	**Numbers***	**Breeding**
Black throated diver	*Gavia arctica*	Чернозобая гагара	3	X
Bewick's swan	*Cygnus columbianus*	Американский лебедь	>10	
White-fronted geese	*Anser albifrons*	Белолобый гусь	>10	
Long-tailed duck	*Clangula hyemalis*	Морянка	4	X
Rough-legged bussard	*Buteo lagopus*	Мохноногий канюк	2	
Peregrine falcon	*Falco peregrino*	Сапсан	1	
Willow grouse	*Lagopus lagopus*	Белая куропатка	1	X
Ringed plover	*Charadrius hiaticula*	Галстучник	6	X
Red phalarope	*Phalaropus scolopaceus*	Плосконосый плавунчик	>20	X
Common snipe	*Gallinago gallinago*	Бекас	3	X
Little stint	*Calidris minutus*	Результаты поиска	>20	X
Temminck's stint	*Calidris temminckii*	Белохвостый песочник	>100	X
Pectoral Sandpiper	*Calidris melanotos*	Дутыш	>20	X
Sharp-tailed sandpiper	*Calidris acuminata*	Острохвостый песочник	>20	X
Dunlin	*Calidris alpina*	Чернозобик	>50	X
Ruff	*Philomachus pugnax*	Турухтан	>30	X
Long-tailed Skua	*Stercorarius longicaudus*	Длиннохвостый поморник	2	
Pomerine Skua	*Stercorarius pomarinus*	Средний поморник	2	
Herring Gull	*Larus argentatus*	Серебристая чайка	1	X
Glaucous Gull	*Larus hyperboreus*	Бургомистр	>5	
Arctic tern	*Sterna paradisaea*	Полярная крачка	>5	X
White wagtail	*Motacilla alba*	Белая трясогузка	>20	X

*If nest or chocks have been seen Breeding =X, and the numbers refer to nest, otherwise to observed individuals.

Species	Scientific	Russian	Numbers*	Breeding
Red-throated pipit	*Anthus cervinus*	Краснозобый конёк	>50	X
Bluethroat	*Luscinia svecica*	Варакушка	1	X
Fieldfare	*Turdus pilaris*	Рябинник	1	
Little bunting	*Emberiza pusilla*	Овсянка-крошка	>5	X
Lapland longspur	*Calcarius lapponicus*	Лапландский подорожник	>50	X
Snow bunting	*Plectrophenax nivalis*	Пуночка	>30	X
Hoary redpoll	*Carduelis hornemanni*	Тундряная чечётка	>30	X
Common raven	*Corvus corax*	Ворон	2	
White-fronted geese	*Anser albifrons*	Белолобый гусь	2	X
Long-tailed duck	*Clangula hyemalis*	Морянка	2	X
Peregrine falcon	*Falco peregrino*	Сапсан	1	X
Willow grouse	*Lagopus lagopus*	Белая куропатка	1	X
Temminck's stint	*Calidris temminckii*	Белохвостый песочник	>20	X
Golden plover	*Pluvialis apricaria*	Золотистая ржанка	3	X
Long-tailed Skua	*Stercorarius longicaudus*	Длиннохвостый поморник	2	X
White wagtail	*Motacilla alba*	Белая трясогузка	>2	X
Red-throated pipit	*Anthus cervinus*	Краснозобый конёк	>10	X
Lapland longspur	*Calcarius lapponicus*	Лапландский подорожник	>10	X
Snow bunting	*Plectrophenax nivalis*	Пуночка	>5	X
Northern wheatear	*Oenanthe oenanthe*	Обыкновенная каменка	1	X

*If nest or chocks have been seen Breeding =X, and the numbers refer to nest, otherwise to observed individuals.

Table A.2.5: Estimate of the number of nests/individuals from bird species seen on south-eastern Kurungnakh Island during the field expedition in July 2021 (individuals seen with binoculars in a distance >50 m from the island shore are excluded)

Species	**Scientific**	**Russian**	**Numbers***	**Breeding**
White-fronted geese	*Anser albifrons*	Белолобый гусь	2	x
Long-tailed duck	*Clangula hyemalis*	Морянка	2	x
Peregrine falcon	*Falco peregrino*	Сапсан	1	x
Willow grouse	*Lagopus lagopus*	Белая куропатка	1	x
Temminck's stint	*Calidris temminckii*	Белохвостый песочник	>20	x
Golden plover	*Pluvialis apricaria*	Золотистая ржанка	3	x
Long-tailed Skua	*Stercorarius longicaudus*	Длиннохвостый поморник	2	x
White wagtail	*Motacilla alba*	Белая трясогузка	>2	x
Red-throated pipit	*Anthus cervinus*	Краснозобый конёк	>10	x
Lapland longspur	*Calcarius lapponicus*	Лапландский подорожник	>10	x
Snow bunting	*Plectrophenax nivalis*	Пуночка	>5	x
Northern wheatear	*Oenanthe oenanthe*	Обыкновенная каменка	1	x

*If nest or chocks have been seen Breeding =x, and the numbers refer to nest, otherwise to observed individuals.

Table A.2.6: List of legume species and number of symbiotic nodules collected during the Lena Delta Expedition 2021

Sampling date	Plant species	Sampling location	Number of nodules
14.07.2021	*Oxytropis nigrescens*	Tiksi, road to Lake Sevastian-Kuele	28
14.07.2021	*Oxytropis adamsiana*	Tiksi, road to Lake Sevastian-Kuele	35
14.07.2021	*Astragalus alpinus*	Tiksi, road to Lake Sevastian-Kuele	27
14.07.2021	*Astragalus umbellatus*	Tiksi, road to Lake Sevastian-Kuele	80
14.07.2021	*Oxytropis mertensiana*	Tiksi, road to Lake Sevastian-Kuele	65
14.07.2021	*Astragalus norvegicus*	Tiksi, road to Lake Sevastian-Kuele	44
15.07.2021	*Astragalus tugarinovii*	Southwestern shore of Lake Sevastian-Kuele	25
15.07.2021	*Oxytropis nigrescens*	Southwestern shore of Lake Sevastian-Kuele	14
15.07.2021	*Oxytropis taimyrensis*	Southwestern shore of Lake Sevastian-Kuele	48
15.07.2021	*Oxytropis adamsiana*	Southwestern shore of Lake Sevastian-Kuele	33
15.07.2021	*Hedysarum arcticum*	Southwestern shore of Lake Sevastian-Kuele	29
17.07.2021	*Oxytropis adamsiana*	Samoylov Island, at the terrace	17
17.07.2021	*Astragalus alpinus*	Samoylov Island, at the terrace	35
17.07.2021	*Hedysarum arcticum*	Samoylov Island, at the terrace	39
18.07.2021	*Oxytropis nigrescens*	Samoylov Island, northeast terrace	21
17.07.2021	*Astragalus norvegicus*	Samoylov Island, at the terrace	25
18.07.2021	*Astragalus umbellatus*	Samoylov Island, northeast terrace	15
18.07.2021	*Lathyrus palustris*	Samoylov Island, floodplain	28
18.07.2021	*Vicia cracca*	Samoylov Island, floodplain	35
24.07.2021	*Lathyrus palustris*	Samoylov Island, a floodplain in the north of the island off the coast	23
28.07.2021	*Astragalus norvegicus*	America Haya, bank by the stream, right side	13
28.07.2021	*Hedysarum arcticum*	America Haya, bank by the stream, right side	14
29.07.2021	*Oxytropis*	Khabarov weather station	33

Sampling date	Plant species	Sampling location	Number of nodules
22.07.2021	*Astragalus frigidus*	Tit-Ary Island, on the slope of the terrace	36
22.07.2021	*Astragalus norvegicus*	Right bank of the Lena River, floodplain of the Chinke River	14
22.07.2021	*Astragalus frigidus*	Right bank of the Lena River, sandy slope near the floodplain of the Chinke River	22
22.07.2021	*Oxytropis sordida*	Khabarov weather station	28
24.07.2021	*Astragalus tugarinovii*	Kurungnakh Island	16
28.07.2021	*Hedysarum arcticum*	America-Haya, southern slope of the mountain, left bank of the river	23
28.07.2021	*Astragalus umbellatus*	America-Haya, southern slope of the mountain, river floodplain	21
14.08.2021	*Vicia cracca*	Tiksi, road to the port, right side	23
14.08.2021	*Lathyrus palustris*	Tiksi, road to the port, right side	19

Table A.2.7: List of key thermal erosion forms and dates of the repeated aerial surveys

No.	Name	Coordinates N latitude E longitude	Coordinates	Aug. 2019	Sept. 2020	July 2021	Sept. 2021
“Khabarovo” key site							
1.	Meteorologichesky gully	72°23’40” 126°49’10”	N 72.39444 E 126.81944	+	+	+	
2.	Meteorologichesky gully (left)	72°23’46” 126°49’00”	N 72.39611 E 126.81667	+	+	+	
3.	Neskuchny gully	72°23’22” 126°49’52”	N 72.38944 E 126.83111	+	+		
4.	Rill №1	72°23’32” 126°51’27”	N 72.39222 E 126.85750		+	+	+
5.	Rill №2	72°23’49” 126°51’05”	N 72.39694 E 126.85139				+
6.	Arbuznaya Rill	72°23’58” 126°49’04”	N 72.39944 E 126.81778				+
“Kurungnakh” key site							
7.	Gully №2 left	72°20’02” 126°16’40”	N 72.33389 E 126.27778				+
8.	Gully №2 right	72°19’54” 126°16’40”	N 72.33167 E 126.27778				+
9.	Gully №3	72°19’18” 126°15’44”	N 72.32167 E 126.26222			+	
10.	Gully №4	72°19’39” 126°16’15”	N 72.32750 E 126.27083			+	+
11.	Activny Gully (left)	72°22’27” 126°14’18”	N 72.37417 E 126.23833				+
12.	Activny Gully (right)	72°22’18” 126°14’24”	N 72.37167 E 126.24000				+
13.	Levaya rill	72°19’43” 126°02’28”	N 72.32861 E 126.04111			+	
14.	Pravaya Rill	72°19’44”9724”’ 126°02’03”5711”’	N 72.32916 E 126.03433			+	
“Tiksi” key site							
15.	Tiksi Gully	71°37’54” 128°52’43”	N 71.63167 E 128.87861			+	+

A.3 Supplementary material – Expedition to Central Yakutia

Table A.3.1: RU-Land 2021 Yakutia: List of long and short sediment cores, surface sediment samples, and water CTD profiles

Site ID	Longitude E	Latitude N	Date	Lake name	Water Depth (m)	Description Sample/Activity	Gear
EN21101	141.0462	63.3420	09.08.2021	Ulu	17.3	2 short cores and 1 long core (10m)	UWITEC Gravity corer 90 mm and Usinger and Niederreiter Hybrid 90mm Piston system
EN21102	141.0461	63.3419	12.08.2021	Ulu	17.4	Parallel long core to EN21101with 1 m overlap, drilled until 7 m (stored in freezer)	UWITEC Usinger and Niederreiter Hybrid 90mm Piston system
EN21103	141.0461	63.3419	13.08.2021	Ulu	17.4	2nd parallel long core to EN21101 with 1 m overlap, drilled until 11m	UWITEC Usinger and Niederreiter Hybrid 90mm Piston system
EN21105	141.0519	63.3467	14.08.2021	Ulu	21	Surface sediment sample (0-1 cm)	sediment grabber
EN21106	141.0387	63.3409	14.08.2021	Ulu	25	Surface sediment sample (0-1 cm)	sediment grabber
EN21107	141.0320	63.3376	14.08.2021	Ulu	3	Surface sediment sample (0-1 cm)	sediment grabber
EN21108	141.0361	63.3339	14.08.2021	Ulu	12	Surface sediment sample (0-1 cm)	sediment grabber
EN21109	141.0304	63.3427	14.08.2021	Ulu	23	Surface sediment sample (0-1 cm)	sediment grabber
EN21110	141.0270	63.3492	14.08.2021	Ulu	11	Surface sediment sample (0-1 cm)	sediment grabber
EN21111	141.0141	63.3464	14.08.2021	Ulu	4.5	Surface sediment sample (0-1 cm)	sediment grabber
EN21112	141.0134	63.3506	14.08.2021	Ulu	5.5	5.5 m water profile	water sampler small
EN21112	141.0134	63.3506	14.08.2021	Ulu	5.5	Surface sediment sample (0-1 cm)	sediment grabber
EN21113	141.0214	63.3447	14.08.2021	Ulu	21	Surface sediment sample (0-1 cm)	sediment grabber
EN21114	141.0407	63.3366	14.08.2021	Ulu	17	Surface sediment sample (0-1 cm)	sediment grabber
EN21115	141.0528	63.3347	14.08.2021	Ulu	16	Surface sediment sample (0-1 cm)	sediment grabber
EN21116	141.0570	63.3366	14.08.2021	Ulu	9	9 m water profile	water sampler small
EN21117	141.0727	63.3384	14.08.2021	Ulu	43	Surface sediment sample (0-1 cm)	sediment grabber
EN21118	141.0820	63.3331	14.08.2021	Ulu	30	Surface sediment sample (0-1 cm)	sediment grabber
EN21119	141.0754	63.3355	14.08.2021	Ulu	29	Surface sediment sample (0-1 cm)	sediment grabber
EN21120	141.0790	63.3372	14.08.2021	Ulu	11	Surface sediment sample (0-1 cm)	sediment grabber

Site ID	Longitude E	Latitude N	Date	Lake name	Water Depth (m)	Description Sample/Activity	Gear
EN21121	141.0702	63.3318	14.08.2021	Ulu	12	Surface sediment sample (0-1 cm)	sediment grabber
EN21122	141.0628	63.3330	15.08.2021	Ulu	18	Surface sediment sample (0-1 cm)	sediment grabber
EN21123	141.0620	63.3414	15.08.2021	Ulu	18	Surface sediment sample (0-1 cm)	sediment grabber
EN21124	141.0527	63.3416	15.08.2021	Ulu	18.5	Surface sediment sample (0-1 cm)	sediment grabber
EN21124	141.0527	63.3416	15.08.2021	Ulu	18.5	18.5 m water profile	water sampler small
EN21125	141.0407	63.3321	15.08.2021	Ulu	20	Surface sediment sample (0-1 cm)	sediment grabber
EN21126	141.0394	63.3453	15.08.2021	Ulu		Surface sediment sample (0-1 cm)	sediment grabber
EN21127	141.0241	63.3412	15.08.2021	Ulu	7	Surface sediment sample (0-1 cm)	sediment grabber
EN21128	141.0241	63.3412	15.08.2021	Ulu	21	UWITEC Hybrid 90mm Piston system (Usinger) until 174 cm, covering full and intact Holocene	Usinger
EN21128	141.0241	63.3412	15.08.2021	Ulu	21	Surface sediment sample (0-1 cm)	sediment grabber
EN21129	141.0436	63.3328	15.08.2021	Ulu		Surface sediment sample (0-1 cm)	sediment grabber
EN21130	141.0366	63.3410	15.08.2021	Ulu		Surface sediment sample (0-1 cm)	sediment grabber
EN21131	141.0301	63.3485	15.08.2021	Ulu		Surface sediment sample (0-1 cm)	sediment grabber
EN21132	141.0424	63.3468	15.08.2021	Ulu		Surface sediment sample (0-1 cm)	sediment grabber
EN21133	141.0550	63.3425	15.08.2021	Ulu		Surface sediment sample (0-1 cm)	sediment grabber
EN21134	141.0750	63.3354	15.08.2021	Ulu		Surface sediment sample (0-1 cm)	sediment grabber
EN21135	141.0603	63.3314	15.08.2021	Ulu		Surface sediment sample (0-1 cm)	sediment grabber
EN21136	141.0687	63.3362	16.08.2021	Ulu		Conductivity-Temperature-Depth profile	CTD
EN21137	141.0678	63.3363	16.08.2021	Ulu		Conductivity-Temperature-Depth profile	CTD
EN21138	141.0625	63.3406	16.08.2021	Ulu		Conductivity-Temperature-Depth profile	CTD
EN21139	141.0561	63.3396	16.08.2021	Ulu		Conductivity-Temperature-Depth profile	CTD

Site ID	Longitude E	Latitude N	Date	Lake name	Water Depth (m)	Description Sample/Activity	Gear
EN21140	141.0456	63.3403	16.08.2021	Ulu		Conductivity-Temperature-Depth profile	CTD
EN21141	141.0396	63.3409	16.08.2021	Ulu		Conductivity-Temperature-Depth profile	CTD
EN21142	141.0327	63.3415	16.08.2021	Ulu		Conductivity-Temperature-Depth profile	CTD
EN21143	141.0257	63.3433	16.08.2021	Ulu		Conductivity-Temperature-Depth profile	CTD
EN21144	141.0221	63.3447	16.08.2021	Ulu		Conductivity-Temperature-Depth profile	CTD
EN21145	141.0176	63.3472	16.08.2021	Ulu		Conductivity-Temperature-Depth profile	CTD
EN21146	141.0592	63.3291	17.08.2021	Ulu		water sample for isotopes	sample vial
EN21150			15.08.2021	Ulu	1.7	Surface sediment sample (0-1 cm)	
EN21151			15.08.2021	Ulu	0.6	Surface sediment sample (0-1 cm)	
EN21152			15.08.2021	Ulu	6.2	Surface sediment sample (0-1 cm)	
EN21153			15.08.2021	Ulu	3.5	Surface sediment sample (0-1 cm)	
EN21158			15.08.2021	Ulu		surface water sample	
EN21160	129.6937	62.0198	21.08.2021	Saysary	4.5	4.5 m water profile	water sampler small
EN21160	129.6937	62.0198	21.08.2021	Saysary	4.5	Short Core (38 cm)	Gravity corer 90mm
EN21160	129.6937	62.0198	21.08.2021	Saysary	4.5	Long Core (260 cm)	Gravity corer 90mm
EN21161	129.6944	62.0197	21.08.2021	Saysary	5	Long Core (260 cm)	UWITEC 60mm Piston Coring
EN21161	129.6944	62.0197	21.08.2021	Saysary		Surface sediment sample (0-1 cm)	sediment grabber
EN21164	129.6932	62.0203	23.08.2021	Saysary		Surface sediment sample (0-1 cm)	sediment grabber
EN21165	129.6911	62.0192	23.08.2021	Saysary		Surface sediment sample (0-1 cm)	sediment grabber
EN21166	129.6941	62.0184	23.08.2021	Saysary		Surface sediment sample (0-1 cm)	sediment grabber
EN21167	129.6972	62.0193	23.08.2021	Saysary		Surface sediment sample (0-1 cm)	sediment grabber
EN21168	129.6977	62.0206	23.08.2021	Saysary		Surface sediment sample (0-1 cm)	sediment grabber

Table A.3.2: RU-Land_2021_Yakutia: List of sampled lakes, lake and landscape characteristics

Site ID	Longitude E	Latitude N	Elevation (m a.s.l)	Date	Lake name	Water body type	Depth (m)	District	Landform	Landscape setting
EN21401	63.3366	141.0570	946	14.08.2021	Ulu	glacial lake	43	Oymyakonsky District	mountain range	large glacial lake, close to national highway, open larch forest and open grassland
EN21402	63.3270	141.0843	989.38	08.08.2021		glacial lake	12.6	Oymyakonsky District	mountain range	glacial lake close to national highway, in open larch forest
EN21403	63.3201	141.0799	1036.04	08.08.2021		glacial lake	14.1	Oymyakonsky District	mountain range	small glacial lake, in open larch forest
EN21404	63.3294	141.1181	999.81	09.08.2021		glacial lake	11.3	Oymyakonsky District	mountain range	small glacial lake, in open larch forest
EN21405	63.4389	140.3983	1260.36	10.08.2021		glacial lake	33.8	Oymyakonsky District	mountain range	lake in mountain tundra catchment, close to national highway
EN21406	63.3100	141.0720	1141.85	11.08.2021		glacial lake	6.7	Oymyakonsky District	mountain range	small lake in open larch forest
EN21407	63.3102	141.0634	1130.36	11.08.2021		glacial lake	14.3	Oymyakonsky District	mountain range	glacial lake, in open larch forest
EN21408	63.3878	140.5752	1253.71	12.08.2021		glacial lake	8.9	Oymyakonsky District	mountain range	glacial lake in cirque catchment in open larch forest
EN21409	63.3918	140.5811	1223	12.08.2021		glacial lake	5.5	Oymyakonsky District	mountain range	glacial lake in cirque catchment in open larch forest
EN21410	63.2304	142.9573	788.99	13.08.2021		lake	7.4	Oymyakonsky District	mountain range	lake in grassland catchment , close to national highway
EN21411	63.2217	142.8945	798.8	13.08.2021		lake	7.8	Oymyakonsky District	mountain range	lake in grassland catchment , close to national highway
EN21412	63.2189	139.5503	1308.85	14.08.2021		lake	3.2	Tomponsky District	mountain range	lake in mountain tundra catchment, close to national highway

Site ID	Longitude E	Latitude N	Elevation (m a.s.l)	Date	Lake name	Water body type	Depth (m)	District	Landform	Landscape setting
EN21413	63.2280	139.5759	1309.7	14.08.2021		lake	4.1	Tomponsky District	mountain range	lake in mountain tundra catchment, close to national highway
EN21414	63.3286	141.1654	962.26	15.08.2021		glacial lake	5.2	Oymyakonsky District	mountain range	glacial lake in small catchment in open larch forest
EN21415	63.3324	141.1591	952.72	15.08.2021		glacial lake	5.2	Oymyakonsky District	mountain range	glacial lake in small catchment in open larch forest
EN21416	62.0846	132.3706	306.97	18.08.2021		thermokarst lake	1.3	Churapchinsky District	plain	alaas lake close to old fire scar
EN21417	62.0800	132.3637	299.59	18.08.2021	Imitte	thermokarst lake	1.7	Churapchinsky District	plain	alaas lake close to old fire scar
EN21418	62.0822	132.3473	300.41	18.08.2021		thermokarst lake	4.8	Churapchinsky District	plain	Tyympy-stage thermokarst lake in dense larch forest
EN21419	62.0877	132.3534	289.27	18.08.2021	Lankyly	thermokarst lake	3.4	Churapchinsky District	plain	large shallow flow-through thermokart lake
EN21420	62.0388	132.3943	170.73	19.08.2021		thermokarst lake	1.6	Churapchinsky District	plain	two former alaas lakes joined together, thermokarst mounds (baydzharakhs)
EN21421	62.0141	132.4127	160.09	19.08.2021	Nidzhili	thermokarst lake	1.7	Churapchinsky District	plain	large alaas lake close to village, thermokarst mounds (baydzharakhs)
EN21422	62.0350	132.3634	172.44	19.08.2021		thermokarst lake	2.1	Churapchinsky District	plain	alaas lake
EN21423	62.3872	133.7447	190.05	20.08.2021		thermokarst lake	3.1	Tattinsky District	plain	freshly burnt larch forest in catchment
EN21424	62.3299	133.6651	278.1	20.08.2021	Esebit-Talata	thermokarst lake	4.9	Tattinsky District	plain	freshly burnt larch forest in catchment
EN21425	62.1693	130.9102	200.53	22.08.2021	Batygytta	thermokarst lake	1.5	Megino-Kangalassky District	plain	large elongated thermokarst lake in hilly terrain

Site ID	Longitude E	Latitude N	Elevation (m a.s.l)	Date	Lake name	Water body type	Depth (m)	District	Landform	Landscape setting
EN21426	62.1808	130.8822	216.93	22.08.2021		thermokarst lake	8.4	Megino-Kangalassky District	plain	elongated thermokarst lake in hilly terrain
EN21426-2	62.1773	130.8796	209	22.08.2021		thermokarst lake		Megino-Kangalassky District	plain	small elongated thermokarst lake in hilly terrain
EN21427	62.1434	130.9355	200.99	22.08.2021	Aryylaakh	thermokarst lake	2.4	Megino-Kangalassky District	plain	large thermokarst lake close to settlement and National Highway
EN21428	62.2815	130.3724	164.01	23.08.2021	Taas-kyel the 1st	thermokarst lake	19.3	Megino-Kangalassky District	plain	alaas lake in open mixed forest catchment
EN21429	62.2631	130.3397	133.21	23.08.2021	Arga-Kyubediki	thermokarst lake	5.6	Megino-Kangalassky District	plain	alaas lake in open mixed forest catchment
EN21430	62.3105	130.3333	142	23.08.2021	Elyuktey	thermokarst lake		Megino-Kangalassky District	plain	alaas lake in open mixed forest catchment
EN21431	62.1293	130.8697	235.39	24.08.2021		thermokarst lake	2.1	Megino-Kangalassky District	plain	irregularly shaped alaas lake in forest catchment
EN21432	62.1357	130.8860	230.16	24.08.2021		thermokarst lake	2.1	Megino-Kangalassky District	plain	alaas lake in forest catchment
EN21433	62.1381	130.8705	228.98	24.08.2021		thermokarst lake	7	Megino-Kangalassky District	plain	alaas lake in forest catchment
EN21434	62.1454	130.8669	203.31	24.08.2021		thermokarst lake	2.1	Megino-Kangalassky District	plain	alaas lake in forest catchment
EN21435	62.3575	130.6139	133.67	25.08.2021	Ochchuguy-Matta	thermokarst lake	3.1	Megino-Kangalassky District	plain	large alaas lake close to settlement
EN21436	62.3508	130.3528	125.08	25.08.2021		thermokarst lake	2.4	Megino-Kangalassky District	plain	alaas lake in forest catchment

Site ID	Longitude E	Latitude N	Elevation (m a.s.l)	Date	Lake name	Water body type	Depth (m)	District	Landform	Landscape setting
EN21437	62.3431	130.3742	127.32	25.08.2021		thermokarst lake	0.5	Megino-Kangalassky District	plain	alaas lake in forest catchment
EN21438	62.1554	130.6390	133.47	26.08.2021		thermokarst lake	1.8	Megino-Kangalassky District	plain	alaas lake close to agricultural field
EN21439	62.1644	130.6614	137.06	26.08.2021	Nal	thermokarst lake	6.9	Megino-Kangalassky District	plain	large irregularly shaped alaas lake, close to large settlement and national highway, with high anthropogenic influence
EN21440	62.2004	130.6501	133.76	26.08.2021	Arga Ebe	thermokarst lake	1	Megino-Kangalassky District	plain	alaas lake, close to national highways, with high anthropogenic influence
EN21441	62.2070	130.7146	140.82	26.08.2021	Segeley	thermokarst lake	2.4	Megino-Kangalassky District	plain	large irregularly shaped alaas lake, close to large settlement and national highway, with high anthropogenic influence
EN21442	61.7858	130.5020	172.1	28.08.2021		thermokarst lake	2	Megino-Kangalassky District	plain	alaas lake in multi-lake alaas basin
EN21443	61.7864	130.4892	167.75	28.08.2021		thermokarst lake	1.5	Megino-Kangalassky District	plain	irregularly shaped alaas lake in multi-lake alaas basin
EN21444	61.7799	130.4932	172.96	28.08.2021		thermokarst lake	1.9	Megino-Kangalassky District	plain	alaas lake in grass covered alaas in forest catchment

Site ID	Longitude E	Latitude N	Elevation (m a.s.l)	Date	Lake name	Water body type	Depth (m)	District	Landform	Landscape setting
EN21445	61.7676	130.4949	171.82	28.08.2021		thermokarst lake	1	Megino-Kangalassky District	plain	alaas lake in grass covered alaas in forest catchment
EN21446	61.7648	130.4599	224	28.08.2021		thermokarst lake	2	Megino-Kangalassky District	plain	irregularly shaped alaas lake in grass covered alaas in forest catchment
EN21447	61.7655	130.4684	223	28.08.2021		thermokarst lake	2.8	Megino-Kangalassky District	plain	irregularly shaped alaas lake in in grass covered alaas in forest catchment
EN21448	61.7461	130.5330	202.37	29.08.2021		thermokarst lake	2	Megino-Kangalassky District	plain	Tyympy-like thermokarst lake in forest catchment
EN21449	61.7471	130.5389	202.07	29.08.2021		thermokarst lake	1.6	Megino-Kangalassky District	plain	alaas lake in multi-lake alaas basin
EN21450	61.7376	130.5249	247.69	29.08.2021		thermokarst lake	3.9	Megino-Kangalassky District	plain	alaas lake (2 joined former alaas lakes) in forest catchment
EN21451	61.7398	130.5256	234	29.08.2021		thermokarst lake		Megino-Kangalassky District	plain	Tyympy-stage thermokarst lake in forest catchment
EN21452	61.7604	130.5507	245.75	29.08.2021		thermokarst lake	2.8	Megino-Kangalassky District	plain	irregularly shaped alaas lake in grass covered alaas in forest catchment
EN21453	61.8996	130.4902	146.25	30.08.2021		thermokarst lake	2.8	Megino-Kangalassky District	plain	irregularly shaped alaas lake in grass covered alaas
EN21454	61.8965	130.4273	144	30.08.2021		thermokarst lake	1.2	Megino-Kangalassky District	plain	alaas lake in grass covered alaas in forest catchment
EN21455	61.9025	130.4117	143.88	30.08.2021		thermokarst lake	1	Megino-Kangalassky District	plain	alaas lake, with pingo

Site ID	Longitude E	Latitude N	Elevation (m a.s.l)	Date	Lake name	Water body type	Depth (m)	District	Landform	Landscape setting
EN21456	61.8856	130.4483	154	30.08.2021		thermokarst lake		Megino-Kangalassky District	plain	alaas lake, with pingo
EN21457	61.7334	130.2533	114.6	31.08.2021	Maya	thermokarst lake	0.7	Megino-Kangalassky District	plain	large irregularly shaped alaas lake, close to large settlement and national highway, with high anthropogenic influence
EN21458	61.7322	130.2601	126.21	31.08.2021		thermokarst lake	4.1	Megino-Kangalassky District	plain	Tyympy-stage thermokarst lake, within settlement, high anthropogenic influence
EN21459	61.7781	130.3753	136	31.08.2021	Byokyo	thermokarst lake		Megino-Kangalassky District	plain	alaas lake, close to large settlement and national highway, with high anthropogenic influence
EN21462	61.7175	130.4814	173.36	01.09.2021		thermokarst lake	1.7	Megino-Kangalassky District	plain	alaas lake in forest catchment
EN21463	61.7449	130.5035	173.36	01.09.2021		thermokarst lake	2.8	Megino-Kangalassky District	plain	irregularly shaped alaas lake in forest catchment
EN21464	61.7556	130.4919	226.09	01.09.2021		thermokarst lake	5.6	Megino-Kangalassky District	plain	irregularly shaped alaas lake, thermokarst mounds (baydzharakhs)
EN21465	61.7542	130.4924	231	02.09.2021		thermokarst lake		Megino-Kangalassky District	plain	small alaas lake in multi-lake catchment

Site ID	Longitude E	Latitude N	Elevation (m a.s.l)	Date	Lake name	Water body type	Depth (m)	District	Landform	Landscape setting
EN21466	61.7536	130.4920	230	02.09.2021		thermokarst lake		Megino-Kangalassky District	plain	small alaas lake in multi-lake catchment
EN21467	61.7623	130.4848	187.46	02.09.2021		thermokarst lake	3.2	Megino-Kangalassky District	plain	Tyympy-stage thermokarst lake in forest catchment

Table A.3.3: RU-Land_2021_Yakutia: List of sampled vegetation plots, vegetation and landscape characteristics

Site ID	Longitude E	Latitude N	Elevation (m a.s.l.)	Date	District	Landform	Landscape
EN21201	139.5437	63.2178	1280	06.08.2021	Tomonsky District	mountain range	Tundra in mountain valley
EN21202	141.0746	63.3252	993	08.08.2021	Oymyakonsky District	mountain range	Larch forest in mountain region
EN21203	140.4125	63.4301	1136	09.08.2021	Oymyakonsky District	mountain range	Forest tundra in mountain region
EN21204	140.4028	63.4425	1202	10.08.2021	Oymyakonsky District	mountain range	Larch forest in mountain region
EN21205	140.4069	63.4386	1219	10.08.2021	Oymyakonsky District	mountain range	Larch forest in mountain region
EN21206	141.0707	63.3438	1120	11.08.2021	Oymyakonsky District	mountain range	Forest patch on mountain plateau
EN21207	141.0698	63.3444	1098	11.08.2021	Oymyakonsky District	mountain range	Gravel slopes in mountain region
EN21208	141.0683	63.3453	1105	11.08.2021	Oymyakonsky District	mountain range	Gravel slopes in mountain region
EN21209	140.5541	63.3985	1315	12.08.2021	Oymyakonsky District	mountain range	Larch forest in mountain region
EN21210	140.5593	63.3977	1388	12.08.2021	Oymyakonsky District	mountain range	Regosol on mountain top
EN21211	140.5536	63.4006	1243	12.08.2021	Oymyakonsky District	mountain range	Larch forest in mountain region
EN21212	142.9624	63.2326	814	13.08.2021	Oymyakonsky District	mountain range	Larch forest in mountain region
EN21213	142.9638	63.2304	835	13.08.2021	Oymyakonsky District	mountain range	Larch forest in mountain region
EN21214	142.9577	63.2326	763	13.08.2021	Oymyakonsky District	mountain range	Larch forest in mountain region
EN21215	139.5409	63.2107	1444	14.08.2021	Tomonsky District	mountain range	Larch forest in mountain region
EN21216	139.5417	63.2123	1407	14.08.2021	Tomonsky District	mountain range	Tundra on gravel in mountain region
EN21217	140.5976	63.4387	1037	15.08.2021	Oymyakonsky District	mountain range	Burned vegetation in mountain valley

Site ID	Longitude E	Latitude N	Elevation (m a.s.l.)	Date	District	Landform	Landscape
EN21218	140.5795	63.4283	1041	15.08.2021	Oymyakonsky District	mountain range	Tundra in mountain valley close to River Aufeis
EN21219	140.5883	63.4256	1040	15.08.2021	Oymyakonsky District	mountain range	Forest in mountain valley
EN21220	132.3668	62.0798	180	18.08.2021	Churapchinsky District	plain	Maedow in Alas
EN21221	132.3726	62.0832	197	18.08.2021	Churapchinsky District	plain	Burned vegetation in permafrost lowland region
EN21222	132.3708	62.0860	222	18.08.2021	Churapchinsky District	plain	Larch forest in permafrost lowland region
EN21223	132.3706	62.0872	216	18.08.2021	Churapchinsky District	plain	Larch forest in permafrost lowland region
EN21224	132.3885	62.0428	206	19.08.2021	Churapchinsky District	plain	Alas grassland in permafrost lowland region
EN21225	132.3912	62.0442	215	19.08.2021	Churapchinsky District	plain	Larch forest in permafrost lowland region
EN21226	132.3891	62.0456	193	19.08.2021	Churapchinsky District	plain	Larch forest in permafrost lowland region
EN21227	132.3963	62.0405	225	19.08.2021	Churapchinsky District	plain	Alas grassland in permafrost lowland region
EN21228	133.7490	62.3850	208	20.08.2021	Tattinsky District	plain	Burned vegetation in permafrost lowland region
EN21229	133.7507	62.3845	200	20.08.2021	Tattinsky District	plain	Burned vegetation in permafrost lowland region
EN21230	133.6880	62.3345	181	20.08.2021	Tattinsky District	plain	Burned vegetation in permafrost lowland region
EN21231	133.6841	62.3347	175	20.08.2021	Tattinsky District	plain	Burned vegetation in permafrost lowland region
EN21232	130.9112	62.1722	188	22.08.2021	Megino-Kangalassky District	plain	Mixed forest in permafrost lowland region
EN21233	130.9039	62.1696	189	22.08.2021	Megino-Kangalassky District	plain	Larch forest in permafrost lowland region
EN21234	130.3776	62.2870	139	23.08.2021	Megino-Kangalassky District	plain	Pine forest in permafrost lowland region

Site ID	Longitude E	Latitude N	Elevation (m a.s.l.)	Date	District	Landform	Landscape
EN21235	130.3766	62.2756	155	23.08.2021	Megino-Kangalassky District	plain	Pine forest in permafrost lowland region
EN21236	130.3279	62.2622	152	23.08.2021	Megino-Kangalassky District	plain	Pine forest in permafrost lowland region
EN21237	130.8748	62.1301	182	24.08.2021	Megino-Kangalassky District	plain	Larch forest in permafrost lowland region
EN21238	130.8735	62.1335	193	24.08.2021	Megino-Kangalassky District	plain	Larch forest in permafrost lowland region
EN21239	130.1160	62.3161	94	25.08.2021	Megino-Kangalassky District	plain	Spruce forest in permafrost lowland region
EN21240	130.1514	62.3534	119	25.08.2021	Megino-Kangalassky District	plain	Spruce forest in permafrost lowland region
EN21241	130.6518	62.1484	137	26.08.2021	Megino-Kangalassky District	plain	Forest succession on abandonned field in permafrost lowland region
EN21242	130.6536	62.1484	141	26.08.2021	Megino-Kangalassky District	plain	Forest succession on abandonned field in permafrost lowland region
EN21243	130.6540	62.1494	143	26.08.2021	Megino-Kangalassky District	plain	Cereal field in Alas in permafrost lowland region
EN21244	130.6596	62.1569	128	26.08.2021	Megino-Kangalassky District	plain	Forest succession on abandonned settlement in permafrost lowland region
EN21245	130.4849	61.7844	208	28.08.2021	Megino-Kangalassky District	plain	Mixed forest in permafrost lowland region
EN21246	130.4925	61.7831	201	28.08.2021	Megino-Kangalassky District	plain	Mixed forest in permafrost lowland region
EN21247	130.5000	61.7798	218	28.08.2021	Megino-Kangalassky District	plain	Grassland in permafrost lowland region
EN21248	130.5303	61.7479	226	29.08.2021	Megino-Kangalassky District	plain	Forest succession on abandonned settlement
EN21249	130.5307	61.7457	225	29.08.2021	Megino-Kangalassky District	plain	Forest succession on abandonned settlement
EN21250	130.5326	61.7457	231	29.08.2021	Megino-Kangalassky District	plain	Birch forest in permafrost lowland region
EN21251	130.5286	61.7401	221	29.08.2021	Megino-Kangalassky District	plain	Larch forest in permafrost lowland region

Site ID	Longitude E	Latitude N	Elevation (m a.s.l.)	Date	District	Landform	Landscape
EN21252	130.4824	61.8972	138	30.08.2021	Megino-Kangalassky District	plain	Burned vegetation
EN21253	130.4848	61.8950	126	30.08.2021	Megino-Kangalassky District	plain	Larch forest in permafrost lowland region
EN21254	130.4888	61.8948	131	30.08.2021	Megino-Kangalassky District	plain	Larch forest in permafrost lowland region
EN21255	130.3867	61.7691	177	31.08.2021	Megino-Kangalassky District	plain	Larch forest in permafrost lowland region
EN21256	130.8388	61.7664	130	31.08.2021	Megino-Kangalassky District	plain	Mixed forest in permafrost lowland region
EN21257	130.3915	61.7705	176	31.08.2021	Megino-Kangalassky District	plain	Grassland in Alas in permafrost lowland region
EN21258	130.4234	61.8992	146	01.09.2021	Megino-Kangalassky District	plain	Larch forest in permafrost lowland region
EN21259	130.5005	61.9013	140	01.09.2021	Megino-Kangalassky District	plain	Larch forest in permafrost lowland region
EN21260	130.4797	61.7639	226	02.09.2021	Megino-Kangalassky District	plain	Larch forest in permafrost lowland region
EN21261	130.4577	61.7668	210	03.09.2021	Megino-Kangalassky District	plain	Larch forest in permafrost lowland region

Die **Berichte zur Polar- und Meeresforschung** (ISSN 1866-3192) werden beginnend mit dem Band 569 (2008) als Open-Access-Publikation herausgegeben. Ein Verzeichnis aller Bände einschließlich der Druckausgaben (ISSN 1618-3193, Band 377-568, von 2000 bis 2008) sowie der früheren **Berichte zur Polarforschung** (ISSN 0176-5027, Band 1–376, von 1981 bis 2000) befindet sich im electronic Publication Information Center **(ePIC)** des Alfred-Wegener-Instituts, Helmholtz-Zentrum für Polar- und Meeresforschung (AWI); see https://epic.awi.de. Durch Auswahl “Reports on Polar- and Marine Research“ (via “browse”/”type”) wird eine Liste der Publikationen, sortiert nach Bandnummer, innerhalb der absteigenden chronologischen Reihenfolge der Jahrgänge mit Verweis auf das jeweilige pdf-Symbol zum Herunterladen angezeigt.

The **Reports on Polar and Marine Research** (ISSN 1866-3192) are available as open access publications since 2008. A table of all volumes including the printed issues (ISSN 1618-3193, Vol. 377-568, from 2000 until 2008), as well as the earlier **Reports on Polar Research** (ISSN 0176-5027, Vol. 1–376, from 1981 until 2000) is provided by the electronic Publication Information Center **(ePIC)** of the Alfred Wegener Institute, Helmholtz Centre for Polar and Marine Research (AWI); see URL https://epic.awi.de. To generate a list of all Reports, use the URL http://epic.awi.de and select “browse”/”type” to browse ”Reports on Polar and Marine Research”. A chronological list in declining order will be presented, and pdf-icons displayed for downloading.

Zuletzt erschienene Ausgaben:

Recently published issues:

772 (2023) Russian-German Cooperation: Expeditions to Siberia in 2021, edited by Anne Morgenstern, Birgit Heim, Luidmila A. Pestryakova, Dmitry Yu. Bolshiyanov, Mikhail N. Grigoriev, Dmitry Ayunov, Antonia Dill, and Iuliia Jünger

771 (2023) The Expedition PS132 of the Research Vessel POLARSTERN to the Atlantic Ocean in 2022, edited by Karen H. Wiltshire and Angelika Dummermuth with contributions of the participants

770 (2023) The Expedition PS131 of the Research Vessel POLARSTERN to the Fram Strait in 2022, edited by Torsten Kanzow with contributions of the participants

769 (2023) The Expedition TRITON2021 of the Hendes Dansk Majestæt Skib TRITON to the Atlantic Ocean in 2021, edited by Rebecca McPherson, Carina Engicht and Torsten Kanzow

768 (2022) Mit Erich von Drygalski in die Ostantarktis – Paul Björvigs Tagebuch von der ersten deutschen Südpolarexpedition 1901-1903. Aus dem Norwegischen übersetzt von Volkert Gazert und herausgegeben von Cornelia Lüdecke

767 (2022) Expeditions to Antarctica: ANT-Land 2021/22 Neumayer Station III, Kohnen Station, Flight Operations and Field Campaigns, edited by Christine Wesche and Julia Regnery with contributions of the participants

766 (2022) The Expedition West-Alaska 2016 of the ERC group PETA-CARB to permafrost regions in western Alaska in 2016, edited by Josefine Lenz, Matthias Fuchs, Ingmar Nitze, Jens Strauss, Guido Grosse

765 (2022) The Expeditions PS130/1 and PS130/2 of the Research Vessel *Polarstern* to the Atlantic Ocean in 2022, edited by Simon Dreutter and Claudia Hanfland with contributions of the participants

764 (2022) The Expedition PS128 of the Research Vessel *Polarstern* to the Weddell Sea, Lazarew Sea, Riiser-Larsen Sea, Cosmonaut Sea, and Cooperation Sea in 2022, edited by Ralf Tiedemann and Juliane Müller with contributions of the participants

ALFRED-WEGENER-INSTITUT
HELMHOLTZ-ZENTRUM FÜR POLAR-
UND MEERESFORSCHUNG

BREMERHAVEN

Am Handelshafen 12
27570 Bremerhaven
Telefon 0471 4831-0
Telefax 0471 4831-1149
www.awi.de

HELMHOLTZ